R. & M. No. 2622
(10,766)
A.R.C. Technical Report

MINISTRY OF SUPPLY

AERONAUTICAL RESEARCH COUNCIL
REPORTS AND MEMORANDA

The Aerodynamic Characteristics of Flaps

By

A. D. YOUNG, M.A.

LONDON: HER MAJESTY'S STATIONERY OFFICE
1953
FIFTEEN SHILLINGS NET

The Aerodynamic Characteristics of Flaps

By

A. D. YOUNG, M.A.

COMMUNICATED BY THE PRINCIPAL DIRECTOR OF SCIENTIFIC RESEARCH (AIR),
MINISTRY OF SUPPLY

*Reports and Memoranda No. 2622**

February, 1947

Summary.—This report collects and summarises the results of work that has been done both in this and other countries on the aerodynamic characteristics of flaps prior to and during the period of the war. The report has both a philosophical and practical aim, *viz.*, to demonstrate, as far as possible, such underlying unity as exists in the behaviour of the large variety of flaps that have been developed and investigated, and hence to present charts and tables which will enable designers to predict with acceptable accuracy the characteristics of any particular flap arrangement.

In section 2 a brief description of the various flaps considered is given, and these are also illustrated in Fig. 1. Section 3 is devoted to a discussion of the definitions of the lift, drag and pitching moment increments, based on the normal and on the effective (extended or reduced) wing chords. Section 4 deals in some detail with split and plain flaps, whilst section 5 is devoted to the simple slotted flaps of the Handley Page and N.A.C.A. types. A large variety of flaps classified as high-lift flaps are considered in section 6, these include Fowler flaps, double Fowler flaps, N.A.C.A. single and double-slotted flaps, single and double Blackburn flaps, Blackburn flaps with flap leading-edge slots, Blackburn flaps with inset slots, Blackburn flaps with deflected shrouds and Venetian-blind flaps. The main characteristics of these high-lift flaps are also summarised in Table 2. The effect of wing-body interference on the drag and lift increments of split and slotted flaps is discussed in section 7, whilst section 8 summarises the aerodynamic effects of wing leading-edge slots. The effect of flaps on induced drag is dealt with in section 9. A discussion of the characteristics of nose flaps, with particular reference to the type developed and tested by Kruger in Germany is given in section 10. A brief discussion on brake flaps is given in section 11, whilst the allied subject of dive recovery flaps is examined in section 12. Because of its topical interest, such information as is available on the characteristics of flaps on swept-back wings is summarised in section 13. Section 14 is devoted to a summary of the main formulae and conclusions developed in the report.

The bibliography at the end was compiled with the object of providing as representative a list as possible of the main reports and papers to which a reader might wish to refer for more detailed information.

* R.A.E. Report Aero. 2185, received 6th August, 1947.

Notation

A	Aspect ratio
a	Lift-curve slope
a_0, a_6	Lift-curve slopes corresponding to aspect ratios equal to infinity and six, respectively
b	Wing span
b_f	Flap span
c	Local wing chord
c_f	Flap chord
$\bar{c}$	Mean wing chord
c_N	Chord of nose flap
c'	Effective wing chord (*see* Fig. 4)
C_L, C_m	Lift and pitching moment coefficients, respectively, based on c
C_L', C_m'	Lift and pitching moment coefficients, respectively, based on c'
ΔC_L, ΔC_m	Increments in lift and pitching moment coefficients, respectively, due to a flap at $\alpha - \alpha_0 = 10$ deg
$\Delta C_L'$, $\Delta C_m'$	Increments in lift and pitching moment coefficients, respectively, based on c', at $\alpha - \alpha_0 = 10$ deg, for a full-span flap on a wing of aspect ratio $= 6$
C_{D0}, C_{Di}	Profile drag coefficient and induced drag coefficient, respectively
ΔC_{D0}	Profile drag coefficient increment due to a flap at $\alpha - \alpha_0 = 6$ deg
ΔC_{Lf}	Increment in C_L due to a flap when full span and in the trailing edge position on a wing of aspect ratio $= 6$
ΔC_{mr}, $\Delta C_{m'r}$	Increment in C_m, C_m' due to a flap when full span on a rectangular wing
C_{m0}	Pitching moment at zero lift
ΔC_{m0}	Increment in C_{m0} due to a flap
ΔC_{BD}, ΔC_{BL}, ΔC_{BM} and ΔC_{Be}	Increments due to brake flaps (*see* section 11)
$C_{L\,max}$	Maximum lift coefficient
$\Delta C_{L\,max}$	Increment in $C_{L\,max}$ due to a flap or slat

$\Delta C_{m\,(st)}$	Increment in value of C_m at the stall, due to a slat
$\Delta(dC_m/dC_L)_{0\cdot 8\,C_{L\,max}}$	Increment in gradient dC_m/dC_L measured at $C_L = 0{\cdot}8\,C_{L\,max}$ due to a slat
$F(A)$	Function representing variation of lift-curve slope with aspect ratio (*see* Fig. 3)
K	Function required to determine induced drag of flapped wings (*see* Figs. 18, 19, 20)
s_f'	$b_f(c_f + t_i)$
t_i	Normal distance from wing surface to chord line in plane of flap hinge
t	Maximum wing thickness
s_T	Tail semi-span
y_i	Distance of inboard end of flap from centre-line of aircraft
α	Wing incidence
α_0	Incidence for zero lift
β	Flap angle
γ	Angle of sweepback
Γ	Tan γ
$\delta_1, \delta_2, \delta_3$	Functions required to determine the profile drag coefficient increment of a flap (Figs. 10, 11, 12)
$\lambda_1, \lambda_2, \lambda_3, \lambda_{22}$	Functions required to determine the lift coefficient increment of a flap (Figs. 5, 6, 7, 8, 9)
μ_1, μ_2, μ_3	Functions required to determine the pitching moment coefficient increments of a flap (Figs. 13, 14, 27)
ε	Downwash

Suffices 1 and 2 refer to the first and second flaps, respectively, of a flap combination, suffix w refers to the wing alone.

1. *Introduction*.—The invention of the flap dates back to the very early days of aeronautics. It may be said to have been born with the aileron when the latter was first used to replace wing warping as a means of providing lateral control. From then on, the possibilities of the flap as a device for increasing lift or drag must have been apparent to many. As early as 1914 quite extensive model tests were made at the National Physical Laboratory by Nayler and others[6] on a number of aerofoils equipped with a form of large chord plain flap, and plain flaps were used on a number of types of aeroplanes during the first World War. Since then, various forms of flaps have been developed and tested all over the world, ranging in complexity from the simple split flap to large chord high lift flaps of two or more components. A detailed historical summary of the early developments of flaps will be found in Ref. 5.

The flap only became a device of practical importance, however, in the early 1930's. Very rapid advances had by then been made in the aerodynamic efficiency and cleanness of aircraft, accompanied by rapid increase in wing loadings. In consequence, gliding angles had decreased, and landing and take-off speeds had increased, until landing and take-off difficulties threatened to offset the advantages of further aerodynamic improvements. The flap was then adopted as the obvious solution, as it provided both lift to reduce the stalling speed and drag to increase the gliding angle. For take-off, the advantage of the extra lift due to the flap had to be weighed against the disadvantages of the drag, but it soon became clear that even with the simple split flap there was something to be gained at take-off when a moderate setting of the flap was used. The development of the slotted flap was then stimulated since it promised a relatively small drag increase at moderate settings for take-off, with a drag increase that could be made comparable to that of a split flap at large settings for landing.

The demands of the Fleet Air Arm, with its stringent landing and take-off conditions, have hastened the development of flaps giving large lift increments. To distinguish such flaps from the more normal and less ambitious varieties, they will be referred to as high-lift flaps. In recent years many forms of high-lift flaps have been produced, some of which are in current use. They all involve some degree of effective wing-area extension and, in consequence, a certain amount of mechanical complication and extra weight, which must be taken into account in estimating their value for any particular design. The more ambitious of these flaps promise maximum lift coefficients of the order of 4·0, and in combination with wing leading-edge slats lift coefficients of the order of 4·5 are possible[3].

During recent years much of the data accumulated in research laboratories all over the world on flaps of various kinds has been sifted and analysed (*see*, for example, Refs. 3, 4, 39, 60). Enough order has been extracted from these data to make it possible to predict with reasonable accuracy the aerodynamic characteristics of flaps, at least of the simpler kind. The main purpose of this report is to collect in a convenient form the results of such analyses, and, in addition, to cover a few aspects of the subject that have so far not been adequately dealt with.

With the acquisition of war-time German research data it has become clear that sweepback may offer considerable advantages for high-speed designs. It is, therefore, desirable that some reference to the characteristics of flaps on sweptback wings should be made in a review of this kind. Unfortunately, the available data are neither systematic nor comprehensive enough to enable adequately reliable quantitative rules to be deduced from them. The discussion given in section 13 is offered as an interim summary of these data, with the reservation that future research may render the conclusions out of date and possibly incorrect. Apart from this section, the report is confined entirely to flaps on wings without sweepback.

2. *Brief Descriptions of Types of Flaps Considered*.—2.1. *Plain Flaps*.—If a portion of the rear of a wing is simply hinged, then that portion is defined as a plain flap (*see* Fig. 1a). The plain flap is the starting point for all forms of control, and its aerodynamic characteristics will therefore be dealt with very fully, at least for angular movements up to about 20 deg, in the monographs dealing with controls. It is not, therefore, proposed to consider plain flaps in any great detail over that range of angular movement in this monograph.

The effectiveness of the flap derives from the fact that on rotation it changes the camber of the section and so permits of a change of circulation and therefore, of lift at a given incidence. The change in chordwise loading produced by a positive setting of the flap is of the type illustrated in Fig. 2b, having a maximum near the wing leading edge and a secondary peak at the flap hinge but falling to zero at the flap trailing edge[29].

2.2. *Split Flaps*.—The term split flap is normally understood to mean a flap that is formed by splitting the wing trailing edge in a roughly chordwise direction back to a hinge, about which the lower portion of the wing trailing edge can rotate, the upper portion remaining fixed (*see* Fig. 1b). The definition has tended to become generalised to cover any flap that is hinged on or in contact with the wing under surface and whose operation does not alter the wing upper surface. Thus split flaps may lie forward of the trailing-edge position, as is frequently required for dive brakes or flaps on sweptback wings, or their line of contact with the wing may slide back as they open, as for Zap-type flaps (*see* Fig. 1b). Unless otherwise stated, however, when reference is made to split flaps in this report, the simple trailing-edge type will be understood.

Split flaps boost the circulation when operated, by increasing the suction behind them and therefore at the wing trailing edge, and alleviating the adverse pressure gradient on the wing upper surface. The resulting change in the chordwise loading distribution is not unlike that for plain flaps except for the discontinuity in pressure across the split flap and a rather greater suction at the trailing edge.

2.3. *Slotted Flaps*.—When a portion of the rear of a wing can be rotated to leave a well-defined slot between it and the rest of the wing, then it is referred to as a slotted flap. It may be simply hinged just below its nose, as in the case of the Handley Page type of slotted flap (*see* Fig. 1c) or it may be operated with a link or track mechanism, as in the case of the N.A.C.A. (Fig. 1d), Blackburn (Fig. 1e) and Fowler (Fig. 1f, 1g) types of flaps. All slotted flaps have a certain amount of backward movement when operated.

The lift increments of slotted flaps result from three main factors. The first is the effective change of camber produced by setting down the flap, as with plain flaps. The second is due to the flow through the slot re-energising the boundary layer, when the slot is well designed, and so delaying flow separation from the flap. The third is the increase of effective lifting surface due to the rearward movement of the flap. In the case of the simple Handley Page type of flap, the hinge is not very much below the flap nose and the rearward extension is small, the contribution to the lift increment associated with this extension is then comparatively unimportant. On the other hand, in the case of the Fowler flap, the rearward extension is considerable, being about the length of the flap chord, and the corresponding contribution to the lift increment is very important. The Blackburn type of flap is, in this respect, half way between the Handley Page and Fowler types of flap. It moves about an effective hinge centre set well below the flap nose, and when fully extended provides a considerable extension of lifting area.

As noted above, the effect of the slot in helping to delay flow separation from the flap and so boosting circulation depends very critically on the design of the slot. Details of efficient slot designs cannot be given here ; they are to a considerable extent a function of the wing section and flap angle, and reference should be made to the separate reports giving the results of tests of different slot shapes (*see*, for example, Refs. 54 to 57, 60, 62, 63, 66 to 70, 74, 76 to 78). The more important dimensions that have been found to lead to successful slot shapes are indicated in Fig. 1. All that can be said here is that breakaway in the slot must be avoided, and so the slot must converge steadily from the lower to the upper surface. Further, the flow from the slot must merge smoothly into the flow round the wing and flap ; hence, an appreciable length of lip or shroud to the upper surface of the slot is an advantage. In general, it should be possible to fit a smooth curve connecting the wing and flap contours.

It is important to realise that if the slot is not efficient it may be worse than no slot at all, as the flow through it may then stimulate rather than suppress flow breakaway over the flap. It is this tendency of a well-designed slot to suppress flow breakaway over the flap that gives the slotted flap its characteristic of low drag at small or moderate flap angles.

Since the optimum slot shape is a function of flap angle, the shape for the Handley Page simply-hinged flap is usually designed to be at its best for moderate to large flap angles (*i.e.*, 40 to 60 deg). The N.A.C.A. slotted flap, however, was developed, on the basis of a series of fairly exhaustive tests, to have, as far as the practical requirements of a track permitted, the optimum shape at all flap settings. The N.A.C.A. type of flap, therefore, provides rather more lift than the Handley Page type at small to moderate flap angles. The flap paths adopted are given in Table 1.

A typical chordwise loading distribution with a slotted flap is shown in Fig. 2a[29]. It will be seen to be similar to that due to a split or plain flap except that there is a much greater intensity of loading on the flap itself when the flap is slotted (for fuller details of loading distributions on flapped wings *see* Ref. 29).

2.4. *Multiple Flaps.*—2.4.1. *N.A.C.A. double-slotted flaps*[54, 58, 62].—By providing a second slotted flap to the rear of a first a more efficient flap system is obtained, since the effective camber change is attained more smoothly and a further extension of lifting area is provided. N.A.C.A. double-slotted flaps of different sizes are illustrated in Fig. 1h, 1i. Just as for the single-slotted flaps, these were arranged to move on tracks in such a way that the slots were the optimum shapes as far as possible, at all flap angles. Details of the flap paths are given in Table 1.

2.4.2. *Double Fowler flap*[76].—The double Fowler flap is illustrated in Fig. 1j. The front flap is a large chord slotted flap of normal design, the rear flap is a Fowler flap, which when retracted is housed in the lower surface of the front flap.

2.4.3. *Blackburn split and slotted flap*[68, 71].—The Blackburn split and slotted flap is illustrated in Fig. 1k. The split flap hinges about the leading edge of the slotted flap and is of the same chord length. It forms the lower face of the slotted flap when retracted, and the two are geared together by a linkage.

2.4.4. *Slotted flap with slat*[69, 70].—Following on reports of preliminary tests in France, some investigations have been made by Blackburn Aircraft Ltd. of a slotted flap with a slat arranged ahead of the flap in the slot. In the retracted position the flap and slat must fit snugly into the wing. A typical arrangement tested is illustrated in Fig. 1l.

2.4.5. *Slotted flap with inset slots*[69, 70].—A variant on the same theme is the provision of fixed inset slots in the flap. A typical arrangement as tested at Blackburn Aircraft Ltd. is illustrated in Fig. 1m.

2.4.6. *Slotted flap with deflected shroud*[69].—Blackburn Aircraft Ltd. have also tested the possibilities of gearing part of the rear of the upper lip or shroud of the slot to deflect downwards with the flap, and so helping to smooth the change in effective camber. This arrangement is illustrated in Fig. 1n.

2.4.7. *N.A.C.A. Venetian-blind flaps*[77, 78].—Taking the idea of multiple slotted flaps still further we have the N.A.C.A. Venetian-blind flap, illustrated in Fig. 1o. Here a Fowler flap is replaced by a series of small flaps which separate as the flap opens leaving slots between them. In the arrangement illustrated there are four component flaps.

3. *Definitions of Increments and of Effective* (*extended or reduced*) *Wing Chords.*—3.1. *Lift Coefficient Increment.*—It is well known that model measurements of $C_{L\,\max}$ of wings are profoundly influenced by the test conditions, *e.g.*, scale effect, tunnel turbulence, model finish, and model size in relation to tunnel size. These effects have so far defied adequate analysis. Increments in $C_{L\,\max}$ due to flaps are also subject to these extraneous effects. It has been found, however, that increments in lift coefficient due to flaps at a given incidence below the stall are almost independent of such effects; and for trailing-edge flaps that do not extend the chord appreciably, the increments are almost independent of incidence over a wide range of incidence.*

* This fact is linked with the basis of most theoretical work on simple trailing-edge flaps, which assumes that the effect of the flap on lift is equivalent to a constant change of incidence. This change is a function only of the flap chord and setting and is independent of wing incidence.

We are mainly interested in the available lift coefficient increments at take-off and landing, and it has, therefore, been decided[3, 4, 60] to adopt the increment at an incidence of 10 deg above the no-lift angles to define the lift coefficient increment of a flap, as this incidence is representative of the range of incidence in which we are interested. The increment is generally written ΔC_L. It may be noted that an analysis by Stewart[92] of some flight measurements of $C_{L\,max}$ on various flapped wings suggests that the lift coefficient increment ΔC_L is a good guide to the magnitude of the full scale increment in $C_{L\,max}$.

The lift coefficient increment due to a flap is a function of the aspect ratio of the wing. This point will be dealt with in more detail later, but it may be noted here that for a flap that does not extend the wing chord, the increment varies with aspect ratio in exactly the same way as does the lift-curve slope of the wing alone. A curve representing this variation, derived by Levacic in an unpublished analysis of the latest available experimental data, is shown in Fig. 3 as the function $F(A)/F(6)$. For convenience, the aspect ratio of 6·0 is taken as standard, unless otherwise stated, quoted values of lift coefficient increments refer to this aspect ratio.

For a full-span flap, experiments show that the lift coefficient increment is practically independent of taper ratio[3].

3.2. *Profile Drag Coefficent Increment.*—The increment in profile drag coefficient due to a flap at a given incidence is rather more influenced by test conditions than is the lift coefficient increment. Nevertheless, the influence of test conditions and wing incidence is still sufficiently small over a wide range of incidence for us to accept the increment at a standard incidence as a reliable measure of the profile drag characteristics of a flap. Since our main interest is centred on the effect of the flap drag on take-off the standard incidence has been taken to be 6 deg above the no-lift angle[3, 4]. This increment is written as ΔC_{D0}.

The profile drag increment of a flap is assumed to be independent of aspect ratio.

3.3. *Pitching Moment Coefficient Increment.*—The pitching moment coefficient increment of a wing due to a flap at a given incidence is always closely correlated with the lift coefficient increment. Like the latter it is practically independent of test conditions and, if the flap does not extend the wing chord, it is independent of wing incidence. As in the case of the lift coefficient increment, the standard incidence has been taken as 10 deg above the no-lift angle[3]. In two important respects the pitching moment coefficient increment differs from the lift coefficient increment, firstly, theory[12] shows it to be independent of aspect ratio and secondly for a full-span flap it is a function of taper ratio.

The pitching moment coefficient increment is written as ΔC_m and, unless otherwise stated, is referred to the wing quarter-chord point.*

3.4. *Extended (or Reduced) Chords.*—In correlating results obtained with flaps that extend the chord with those for flaps which do not, we must introduce the concept of effective or extended chord or area[3, 60].

The definition of the extended chord c' for a full-span flap is illustrated in Fig. 4a. If the flap is rotated about the point of intersection of the wing and flap chord lines until the two chord lines coincide, then the distance from the leading edge of the wing to the trailing edge of the flap in this position is defined as the extended chord.† For a double flap the definition follows along analogous lines Fig. 4b. The rear flap is first assumed to rotate about the point of intersection of the rear flap chord line with the front flap chord line until the two lines coincide, and then both flaps are rotated about the point of intersection of the front flap chord line and the wing chord line until these two chord lines coincide. The distance from the wing leading edge to the new position of the trailing edge is defined as the extended chord.

* There is, of course, an effect on the pitching moment of a complete aeroplane with flaps, due to the change of downwash at the tailplane accompanying the change in wing loading caused by the flaps. This effect is not considered here, but attention may be drawn to the work contained in Refs. 93 to 95.

† The chord line of a flap is the line that is fixed in the flap and is coincident with the wing chord line when the flap is fully retracted.

In the case of a split flap set forward of the usual trailing edge position, the same process is applied to determine the effective (in this case, reduced) chord, *see* Fig. 4c.

3.5. *Increments Based on Effective Chords.*—3.5.1. *Lift coefficient increment.*—3.5.1.1. *Full-span flaps.*—It is reasonable to expect that if we base the lift and pitching moment coefficient increments on the extended or effective chords and not on the actual wing chords, then it should be possible to bring results obtained with flaps that extend the chord to conform with results on flaps that do not alter the chord. In particular, we may expect the increments based on the extended chord to be independent of incidence. This follows from the fact that the basic geometry of effective wing plus flap does not differ from that of an ordinary wing and flap arrangement. In the case of a split flap lying ahead of the trailing edge position, and which, therefore, reduces the effective chord, the same expectation holds, although the reasoning underlying it is somewhat different and more crude. A split flap on the under surface of a wing can very roughly be said to increase the pressure ahead of it on the under surface of the wing by a constant amount, and to decrease the pressure both behind it and on the upper surface of the wing by a constant amount. It follows that behind the flap the change produced by it in the loading on the under surface tends to be neutralised by the change in the loading on the upper surface, and the increments in lift and pitching moment derive almost entirely from the change in loading produced ahead of the flap. Hence, it may be argued that as far as these overall increments are concerned, the flap behaves as if it were a trailing-edge flap on a wing of chord equal to the reduced chord. This argument is approximate and cannot be taken too far; it will clearly be inapplicable if the ratio of the flap chord to the distance from the flap hinge to wing trailing edge is less than some minimum value. However, for flaps hinged not farther forward than about $0{\cdot}5c$ from the leading edge and of chord not less than about $0{\cdot}1c$, experiment indicates that it is acceptable[132].

The lift coefficient based on the effective chord c' is given by

$$C_L' = C_L \frac{c}{c'},$$

and hence the lift coefficient increment based on the effective chord is

$$\Delta C_L' = C_L \frac{c}{c'} - C_{Lw}, \qquad (1)$$

where C_{Lw} is the lift coefficient of the plain wing.

But $$\Delta C_L = C_L - C_{Lw},$$

and hence $$\Delta C_L' = \Delta C_L \frac{c}{c'} - C_{Lw}\left(1 - \frac{c}{c'}\right). \qquad (2)$$

We can write this equation alternatively as

$$\Delta C_L = \Delta C_L' \frac{c'}{c} + C_{Lw}\left(\frac{c'}{c} - 1\right). \qquad (3)$$

As already remarked, it is convenient, in developing charts from which lift coefficient increments can be estimated, to consider the increments for a standard aspect ratio of 6·0. Hence we require formulae for converting either a measured lift increment ΔC_L for any aspect ratio to an increment $\Delta C_L'$ corresponding to an aspect ratio of 6·0, or conversely for converting from an increment $\Delta C_L'$ at the standard aspect ratio to an increment ΔC_L at any aspect ratio.

Referred to the standard aspect ratio and effective chord

$$C_L' = C_L \frac{c}{c'} \frac{F(6)}{F(A)}, \qquad (4)$$

where A is the aspect ratio of the wing considered, and $F(A)/F(6)$ is the ratio of slopes of the lift curves at the aspect ratios A and 6, and is shown in Fig. 3 as a function of aspect ratio.

The increment $\Delta C_L'$ is then

$$\Delta C_L' = C_L' - C_{Lw} \frac{F(6)}{F(A)}$$

$$= \frac{F(6)}{F(A)} \left[C_L \frac{c}{c'} - C_{Lw} \right].$$

C_{Lw} is the lift coefficient of the plain wing at aspect ratio A.

The increment ΔC_L is given by

and hence $\Delta C_L = C_L - C_{Lw}$,

$$\Delta C_L' = \frac{F(6)}{F(A)} \left[\Delta C_L \frac{c}{c'} - C_{Lw} \left(1 - \frac{c}{c'} \right) \right]. \quad \ldots \quad (5)$$

Alternatively $\Delta C_L = \Delta C_L' \frac{c'}{c} \frac{F(A)}{F(6)} + C_{Lw} \left(\frac{c'}{c} - 1 \right). \quad \ldots \quad (6)$

It follows that if we can develop a general process for predicting $\Delta C_L'$ we should then be able to determine ΔC_L for the general case of an extending chord flap on a wing of any aspect ratio.*

It may be noted that, unlike $\Delta C_L'$, ΔC_L is dependent on incidence for a flap that extends or reduces the chord, since part of ΔC_L is due to the effective change of chord and is proportional to wing incidence (*i.e.*, the term containing C_{Lw} in equation (6)). From equation (6)

$$\frac{d}{d\alpha} (\Delta C_L) = a_w \left(\frac{c'}{c} - 1 \right), \quad \ldots \quad (7)$$

where a_w is the lift-curve slope of the wing alone. It follows that

$$a = a_w \frac{c'}{c}, \quad \ldots \quad (8)$$

where a is the lift-curve slope of the wing plus flap.

3.5.1.2. *Part-span flaps.*—Our usual problem is to derive ΔC_L for a part-span flap given $\Delta C_L'$ for a full-span flap. The simplest procedure is first to derive ΔC_L as if the flaps were full-span and then to apply a factor for converting the lift increment to that for part-span flaps. This factor, which is discussed in rather more detail in section 4.1.2, is here denoted by $\lambda_3(b_f/b)$, where b_f is the flap span and b is the wing span. It is represented for various taper ratios by the curves of Fig. 9. These curves are based on theory[16, 4] checked with experimental results.

We have then

$$\Delta C_L \text{ (part-span flaps)} = \lambda_3(b_f/b)\, \Delta C_L \text{ (full-span flaps)}. \quad \ldots \quad (9)$$

3.5.2. *Pitching moment increments.*—3.5.2.1. *Full-span flaps (rectangular wing).*—Taking moments about the extended chord quarter-chord point and reducing the moments to coefficient form in terms of the extended chord, we easily find that

$$C_m' = C_m \left(\frac{c}{c'} \right)^2 + \frac{C_L}{4} \left(1 - \frac{c}{c'} \right) \frac{c}{c'}, \quad \ldots \quad (10)$$

where C_m and C_L are the pitching moment coefficients and lift coefficients referred to the basic wing chord and quarter-chord point.

But $\Delta C_m' = C_m' - C_{mw}$,

where $C_{mw} = C_m$ of the wing with flap retracted.

* Strictly, account should have been taken in the above of the change of effective aspect ratio with the operation of a flap that extends the chord. The effect is, however, generally small, and in the analysis of a considerable amount of empirical data it has been found more convenient to ignore it.

Hence $$\Delta C_m' = \Delta C_m \left(\frac{c}{c'}\right)^2 + \frac{C_L}{4}\frac{c}{c'}\left(1 - \frac{c}{c'}\right) - C_{mw}\left[1 - \left(\frac{c}{c'}\right)^2\right]. \quad \ldots \quad \ldots \quad (11)$$

Or $$\Delta C_m = \Delta C_m' \left(\frac{c'}{c}\right)^2 - \frac{C_L}{4}\frac{c'}{c}\left(\frac{c'}{c} - 1\right) + C_{mw}\left[\left(\frac{c'}{c}\right)^2 - 1\right] \quad \ldots \quad \ldots \quad (12)$$

Hence, if we have measured ΔC_m, C_L and C_{mw} we can calculate $\Delta C_m'$, or, alternatively, having estimated ΔC_L (and hence C_L), $\Delta C_m'$ and knowing C_{mw} we can estimate ΔC_m.

The pitching moment coefficient increments $\Delta C_m'$ are, according to the lifting-line theory, independent of aspect ratio, but this may not be strictly true for very small aspect ratios.

Since the full-span pitching moment coefficient increments are dependent on taper ratio, it is convenient to refer to the increments for a rectangular wing as standard and they will be denoted by ΔC_{mr} and $\Delta C_m'{}_r$.

3.5.2.2. *Part-span flaps.*—As with the lift coefficient increments, the simplest procedure for estimating ΔC_m for part-span flaps, given an estimate of $\Delta C_m'{}_r$ for full-span flaps, is first to estimate ΔC_{mr} for full-span flaps as above, and then to apply a conversion factor, which is a function of the flap span and taper ratio. The function is shown in Fig. 14 as $\mu_2(b_f/b)$, its derivation is discussed in more detail in section 4.3.2. Thus

$$\Delta C_m \text{ (part-span flap)} = \mu_2(b_f/b)\ \Delta C_{mr} \text{ (full-span flaps)}. \quad \ldots \quad \ldots \quad (13)$$

4. *Split and Plain Flaps.*—4.1. *Lift Coefficient Increments.*—4.1.1. *Full-span flaps.*—Thin aerofoil theory shows that for a plain hinged flap

$$\Delta C_L = a_w \lambda_1(c_f/c)\ \beta \quad \ldots \quad (14)$$

where a_w is the lift-curve slope of the wing, c_f is the flap chord, $\lambda_1(c_f/c)$ is the function shown in Fig. 5 and β is the flap angle. It was, therefore, argued by Young and Hufton[4] that in the analysis of experimental data on flaps we could start by assuming

$$\Delta C_L = \frac{F(A)}{F(6)}\ \lambda_1(c_f/c)\ \lambda_2(\beta), \quad \ldots \quad (15)$$

where $F(A)$ is the function relating the wing lift-curve slope and the aspect ratio (Fig. 3) and $\lambda_2(\beta)$ is a function to be determined from the experimental data and which would presumably vary from one kind of flap to another.

More generally, for flaps that extend the chord, we should have

$$\Delta C_L' = \frac{F(A)}{F(6)}\ \lambda_1(c_f/c')\ \lambda_2(\beta),$$

and since we have agreed to quote $\Delta C_L'$ always for the standard aspect ratio of 6

$$\Delta C_L' = \lambda_1(c_f/c)\ \lambda_2(\beta). \quad \ldots \quad (16)$$

An analysis of a considerable amount of available data on split flaps has established the curves shown in Fig. 6, with a scatter of within $\pm$ 10 per cent. It will be seen that the effectiveness of split flaps increases rapidly with wing thickness. Presumably, with increase of wing thickness the boundary layer on the wing thickens and tends to break away over the rear of the wing. This tendency is suppressed by the increased suction and more favourable pressure gradient at the trailing edge produced by the flap. With other types of flap that form part of the wing upper surface (including slotted flaps), there is an opposing effect due to the sharp cambering of the wing upper surface in the region of the flap hinge, and in general these two effects then largely balance, the net effect of varying wing thickness being small.

For flaps that extend the chord, such as Zap or Gouge flaps*, or flaps that reduce the effective chord, such as flaps lying ahead of the normal trailing-edge position, we apply equation (6) to determine ΔC_L, having first determined $\Delta C_L'$ by means of equation (16) above.

* The Gouge flap is rather like the Blackburn flap (Fig. 1c) but with no slot between the flap and wing.

Analysis of some experimental data has shown that the corresponding increments for plain flaps on wings of thickness of about 12 per cent are not appreciably different from those for split flaps on wings of that thickness. If the argument above is accepted, we may expect that the increments for plain flaps will not show the variation with wing thickness shown by split flaps. Therefore, it is suggested that the curve of Fig. 6 for $\lambda_2(\beta)$ for a wing thickness of 12 per cent be used for plain flaps on wings of all thicknesses within the usual range.

4.1.2. *Part-span flaps.*—From calculations of Hollingdale[16] one can derive the theoretical ratio of the lift coefficient increment of a part-span flap of any type to the corresponding increment for a full-span flap. This ratio is shown as a function of flap span for various taper ratios in Fig. 9, and is denoted by $\lambda_3(b_f/b)$. An analysis of experimental data[4] has shown reasonable agreement between experiment and these theoretical curves. Hence, for part-span flaps

$$\Delta C_L' = \lambda_1(c_f/c')\ \lambda_2(\beta)\ \lambda_3(b_f/b)\,. \qquad (17)$$

It may be noted that, where a flap has a central cut-out so that the spanwise positions of its inboard and outboard ends are at $b_{f1}/2$ and $b_{f2}/2$ from the centre-line, respectively, then the part-span correction factor is

$$\lambda_3(b_{f2}/b) - \lambda_3(b_{f1}/b)\,.$$

It must be emphasised that the factor λ_3 applies to all types of flaps.

4.2. *Profile Drag Coefficient Increments.*—4.2.1. *Full-span flaps.*—Proceeding on much the same lines as in the analysis of lift coefficient increments, Young and Hufton[4] assumed that

$$\Delta C_{D0} = \delta_1(c_f/c)\ .\ \delta_2(\beta)\,, \qquad (18)$$

where δ_2 and δ_2 are functions that were determined from experimental data. The resulting curves for trailing edge split flaps are shown in Fig. 10a and b.

It will be noted that for these flaps the profile drag increment is roughly $1{\cdot}1 \sin^2\beta$ in terms of the area of the flap. For a discussion of the profile drag increments of split flaps ahead of the trailing edge (*see* section 11).

The data of Ref. 39 indicate that the profile drag increments of plain flaps on wings of thickness of about 12 per cent are not quite so large as the corresponding increments of split flaps, and they are reasonably fitted by the function for $\delta_2(\beta)$ for plain flaps shown on Fig. 10b. For the reasons explained above we may expect little variation of these increments with wing thickness, and it is suggested that the function shown be generally used for plain flaps.

For flaps of the Zap or Gouge type in their fully extended position the increment should be readily calculable from the plain flap case if allowance is made for the chord extension.

4.2.2. *Part-span flaps.*—General considerations confirmed by experimental data led Young and Hufton[4] to conclude that the drag increment of a part-span flap of any type is proportional to the area of the flapped part of the wing. Hence, to determine the increment for a part-span flap we must multiply the increment for a full-span flap by the ratio of the flapped wing area to the total wing area. The latter ratio, denoted by $\delta_3(b_f/b)$, is shown in Fig. 12 as a function of flap span for wings of various taper ratios. Thus, for a part-span flap

$$\Delta C_{D0} = \delta_1(c_f/c)\ .\ \delta_2(\beta)\ .\ \delta_3(b_f/b)\,. \qquad (19)$$

If there is a flap cut-out with the inboard and outboard ends given by the spanwise ordinates $b_{f1}/2$ and $b_{f2}/2$, respectively, then

$$\Delta C_{D0} = \delta_1(c_f/c)\ \delta_2(\beta)\ [\delta_3(b_{f2}/b) - \delta_3(b_{f1}/b)]\,. \qquad (20)$$

4.3. *Pitching Moment Increments.*—4.3.1. *Full-span flaps.*—From an unpublished analysis of the pitching moment increments of plain and split flaps by Haile the curves of Fig. 13 have been deduced showing the ratio

$$\mu_1 = -\Delta C_{m'r}'/\Delta C_L'$$

as a function of flap-chord/wing-chord (effective) for various thickness/chord ratios. $\Delta C_L'$ is here estimated for an aspect ratio of 6·0. Hence, having obtained an estimate of $\Delta C_L'$, we can estimate $\Delta C_{m'r}$ from

$$\Delta C_{m'r} = - \mu_1 \Delta C_L'. \qquad (21)$$

For flaps that alter the effective chord, as for split flaps ahead of the normal trailing edge position, we must then apply equation (12) to obtain ΔC_{mr}. This method is found to be very satisfactory if the flap hinge is not forward of about 0·5c behind the leading edge ; ahead of that position the concept of reduced chord breaks down.

It is of interest to note that for moderate to large flap chords (*i.e.*, c_f/c' from 0·2 to 0·4) the value of μ_1 is roughly 0·25, *i.e.*, the extra lift due to a flap acts at about the mid-point of the extended chord.

4.3.2. *Part-span flaps.*—If it is assumed (as in Ref. 132) that the chordwise loading of each spanwise element of the flapped part of the wing is the same as if it were in two-dimensional flow, and that on the unflapped part of the wing any change in loading is located on the quarter-chord line, then it is easy to show that the ratio of the pitching moment coefficient increment to that for a full-span flap on a rectangular wing is given by the factor $\mu_2(b_f/b)$, where

$$\mu_2(b_f/b) = \frac{\int_{-b_f/2}^{b_f/2} c^2\, ds}{\bar{c}^2} \text{ (over flapped part of wing)} ; \qquad (22)$$

where c is the local chord, and $\bar{c}$ is the mean chord.

An unpublished analysis of experimental data by Haile shows satisfactory agreement with this factor. The factor is given graphically as a function of flap span to wing span for various taper ratios in Fig. 14.

5. *Simple Slotted Flaps (Handley Page and N.A.C.A.).*—5.1. *Lift Coefficient Increments.*—The analysis for slotted flaps was developed by Young and Hufton[4] on exactly the same lines as for split flaps. Therefore, we have

$$\Delta C_L' = \lambda_1(c_f/c')\, \lambda_2(\beta)\, \lambda_3(b_f/b),$$

where the functions λ_1 and λ_3 are the same for all types of flaps and are given in Figs. 5, 9. The empirical function $\lambda_2(\beta)$ is shown in Fig. 7b for the Handley Page type of slotted flap and in Fig. 7a for the N.A.C.A. type of slotted flap. As would be expected from the discussion of section 4.1.1 the slotted flaps do not show a marked influence of wing thickness. Further, as noted in section 2.3, the N.A.C.A. type of flap is appreciably more effective than the Handley Page type for small to moderate flap angles, but its superiority becomes less marked at the larger flap angles.

5.2. *Drag Coefficient Increments.*—The analysis of experimental data was again based, as for split and slotted flaps, on the formula

$$\Delta C_{D0} = \delta_1(c_f/c) \,.\, \delta_2(\beta) \,.\, \delta_3(b_f/b),$$

where the function $\delta_3(b_f/b)$ is the same for all types of flaps (Fig. 12). For both the N.A.C.A. and Handley Page types of slotted flaps the functions $\delta_1(c_f/c)$ and $\delta_2(\beta)$ were found to be the same, they are shown in Fig. 11. It is of interest to note that for slotted flaps the drag coefficient increment expressed in terms of the flap area is about $0{\cdot}5 \sin^2 \beta$.

Fig. 15a shows a plot of the profile drag coefficient increment against the lift coefficient increment for N.A.C.A. slotted flaps of 0·1c, 0·26c and 0·4c chord on wings of NACA 23012, and 23021 section. It will be seen that, from the point of view of economy of drag for a given lift increment, there is little to choose between the three flap chords for values of ΔC_L less than about 0·7. On the thicker wing there appears to be something to be gained in using an 0·4c flap rather than an 0·26c flap. It will be noted that for flap angles increasing beyond about 40 deg there is little increase in lift but a very rapid increase in drag.

5.3. *Pitching Moment Coefficient Increments.*—The analysis of the pitching moment coefficient increments made by Young[3] for N.A.C.A. type of slotted flaps of chord ranging from 0·1c to 0·26c showed that on a wing of 12 per cent thickness

$$\Delta C_{mr}/\Delta C_L \simeq -0{\cdot}33$$

and $$\mu_1 = \Delta C_{m'r}'/\Delta C_L' \simeq -0{\cdot}29\,,$$

where ΔC_L and $\Delta C_L'$ refer to aspect ratio of 6.0.

For flaps of larger chord (0·26c to 0·4c)

$$\Delta C_{mr}/\Delta C_L \simeq -0{\cdot}31$$

and $$\mu_1 = \Delta C_{m'r}'/\Delta C_L' \simeq -0{\cdot}26^5.$$

It will be seen that the figures for $\Delta C_{m'r}'/\Delta C_L'$ are not very different from the figures one would deduce from Fig. 13 for split and plain flaps.

As before, for part-span flaps we apply the factor $\mu_2(b_f/b)$ given in Fig. 14 to the value of ΔC_{mr} determined by means of the above ratios for a full-span flap on a rectangular wing.

6. *High Lift Flaps.*—6.1. *General.*—The remaining flaps to be considered may be classified as high-lift flaps. They are the Fowler flap, Fowler plus split flap, double Fowler flap, N.A.C.A. double-slotted flaps, Blackburn slotted flap, Blackburn slotted plus split flap, Blackburn slotted flap plus flap leading-edge slat, Blackburn slotted flap with inset slots, Blackburn slotted flap with deflected shroud, and Venetian-blind flap. An analysis of the experimental data for most of these flaps was made by Young in Ref. 3. Table 2 summarises the major characteristics of these flaps. The table includes representative values of measured lift, drag and pitching moment coefficient increments, increments in $C_{L\,\max}$ and increments in the slope of the C_m vs. C_L curve at $C_L = 0{\cdot}8C_{L\,\max}$. The latter is given to provide an indication of the measured effect of the flap on the stability of the wing at lift coefficients appropriate to the approach glide. Further, the corresponding values of the lift and pitching moment coefficient increments based on the extended chord (C_L' and $\Delta C_{m'r}'$) are tabulated as well as the estimated values of $\Delta C_L'$ (the method of estimation for the more complicated flaps is discussed in the following section). Finally, the values of the ratios $\Delta C_{mr}/\Delta C_L$ and $\Delta C_{m'r}'/\Delta C_L'$ are also given in the table. It must be emphasised that the amount of available data on which the table is based varies considerably from flap to flap; for the flaps with flap leading-edge slats or inset slots and the Venetian-blind flaps there are little more than single series of test results available.

The table refers to full-span flaps; for part-span flaps the increments must be multiplied by the appropriate factors (*see* Figs. 9, 12, 14) which apply to all types of flaps.

For the single and double Fowler, N.A.C.A. and Blackburn flaps, curves are given in Figs. 15, 16, 17 showing the drag coefficient increments plotted against the lift coefficient increments. This provides a guide as to what is paid in drag in each case to obtain a given lift increment. However, in comparing the drag increments of the various flaps, the differences should be seen in relation to the induced drag. In each case a curve for the induced drag increment is included for comparison, this increment has been estimated on the assumption that the basic C_L of the wing alone is 0·5.

The Youngman flap[91, 110], as fitted to the Barracuda, has not been considered separately here, since in its high-lift position it does not differ aerodynamically from the Fowler flap.*

6.2. *Some Details of the Method of Estimating $\Delta C_L'$.*—For the single N.A.C.A. slotted flaps, and the Fowler and the Blackburn flaps in the fully extended positions, the curve $\lambda_2(\beta)$ of the N.A.C.A. slotted flaps (Fig. 7a) was used, as explained in section 4.1.1. For the Fowler flaps in

* The distinctive feature of the Youngman flap is its link method of operation, which is arranged to provide it with a take-off position (moderate lift, low drag), a landing position (high lift) and a braking position (high drag, little change in lift and trim).

partially retracted positions, the slots are ineffective and the flaps are virtually extending chord split flaps, and hence the curves $\lambda_2(\beta)$ for split flaps (Fig. 6) were used. The Blackburn flaps rotate about an effective hinge, like the Handley Page slotted flaps, and consequently the slots are not at their optimum effectiveness for intermediate flap positions, hence for these positions the Handley Page flap curve (Fig. 7b) was used.

The data of the tests of the various double flaps were analysed as follows. The value of $\Delta C_L'$ for the front or main flap, denoted as $\Delta C_L{}'_1$, was obtained from Figs. 5, 6, 7, using equation (16) in the form

$$\Delta C_L{}'_1 = \lambda_1(c_f/c')\,\lambda_2(\beta_1), \quad \ldots \quad (23)$$

where c_{f1} is the front flap chord, c' is the extended chord, and β_1 is the front flap angle. This increment was then subtracted from the total measured value of $\Delta C_L'$, and the difference, denoted by $\Delta C_L{}'_2$, was attributed to the rear flap. Theoretically (*see* R. & M. 1171[11]), this should be the same function of the ratio of the rear flap chord (c_{f2}) to the extended chord (c) and of the rear flap angle (β_2) as $\Delta C_L{}'_1$ is of c_{f1}/c' and β_1. The process adopted was to assume that

$$\Delta C_L{}'_2 = \lambda_1(c_f/c')\,\lambda_{22}(\beta_2), \quad \ldots \quad (24)$$

using the experimental values of $\Delta C_L{}'_2$ to obtain empirically the function $\lambda_{22}(\beta_2)$. It was found that the resulting values fitted reasonably closely to a single curve for all types of rear or auxiliary flaps, and this curve is shown in Fig. 8. Hence, to obtain $\Delta C_L'$ for any given combination of flaps, we obtain $\Delta C_L{}'_1$ from equation (23) and $\Delta C_L{}'_2$ from equation (24) and the total estimated value of $\Delta C_L'$ is then

$$\Delta C_L' = \Delta C_L{}'_1 + \Delta C_L{}'_2.$$

The agreement between the estimated and measured values of $\Delta C_L'$ for double flaps shown in Table 2 is a guide to the general applicability of the curve derived for $\lambda_{22}(\beta_2)$ to all types of flaps.

Further details on the estimation of $\Delta C_L'$ for the other types of flaps considered will be given in the following sections dealing with the flaps.

6.3. *Fowler Flaps.*—6.3.1. *Single Fowler flaps* (*Figs.* 1*f*, 1*g*).—Because of its large chord extension the Fowler flap is one of the most effective of all flaps for producing lift. We have two main sources to draw on for information on Fowler flaps, *viz.*, tests done by the N.A.C.A.[72 to 74] and tests done at the R.A.E.[76]. The more important results of both series of tests are included in Table 2. As will be seen from Figs. 1*f*, 1*g* the housing of the flap in the N.A.C.A. tests was cut square to the wing lower surface, whereas in the R.A.E. tests the housing was as far as possible faired. Consequently, in the latter tests rather higher lift coefficient increments and considerably smaller drag coefficient increments were measured than in the former tests. This is brought out very clearly in Fig. 16 when the profile drag coefficient increments are plotted against the lift coefficient increments. The 0·4*c* Fowler flap as tested at the R.A.E. is in fact the most economical in drag of all the flaps examined for lift coefficient increments less than about 2·0.

Like the N.A.C.A. slotted flap there is little to gain in lift by increasing the flap angle beyond about 40 deg.

As remarked above, when not fully extended, the Fowler flap acts much as an extending chord split flap ; the difference between the flap partially and fully extended is brought out by a comparison of the dotted and full curves of Fig. 16.

From the columns in Table 2 giving the values of $\Delta C_{mr}/\Delta C_L$ it will be seen that these values are consistently high. A mean of a large number of values* examined is about $-0{\cdot}43$, with a scatter of within $\pm$ 10 per cent. The large pitching moment increment associated with a given lift coefficient increment obtained with this type of flap constitutes its most serious disadvantage. When we examine the values of $\Delta C_m{}'_r/\Delta C_L'$ we see that they cluster around a mean value of $-0{\cdot}27$, which is in fair agreement with the corresponding value for split and plain flaps given in

* Table 2 only shows a representative few of the cases considered.

Fig. 13. This fact, as well as the close agreement shown, between the estimated and measured values of $\Delta C_L'$, illustrates the consistency of the results obtained with widely dissimilar flaps when analysed on the basis of effective chord.

6.3.2. *Fowler plus split flap.*—The results of the R.A.E. tests of a 0·4*c* Fowler flap combined with a 0·1*c* split flap[76] are given in Table 2 and are also included in Fig. 16. The split flap was hinged to the lower surface of the Fowler flap in the trailing edge position. It will be seen that with the optimum setting (35 deg for the Fowler, 45 deg for the split flap) the split flap helps to raise the maximum lift coefficient increment from about 2·0 to 2·4 for a surprisingly small cost in profile drag. The ratio $-\Delta C_{mr}/\Delta C_L$ is high and is much the same as for the single Fowler flap.

6.3.3. *Double Fowler flap* (*Fig.* 1*j*).—The front flap of the double Fowler as tested at the R.A.E. is virtually a 0·4*c* slotted flap of the N.A.C.A. type, and it is the rear flap which provides the essential Fowler characteristic by extending backwards from its housing in the front flap to a distance practically equal to its own chord length. The lift coefficient increment attained by this combination is the highest of all the flaps examined[76], being about 2·65. The drag coefficient increment is small; but like that of the Fowler or Fowler plus split flap the value of $-(\Delta C_{mr}/\Delta C_L)$ is high.

Again we may note that for both the Fowler plus split flap and the double Fowler the value of $-(\Delta C_m{'}_r/\Delta C_L')$ is about 0·23. For a split or plain flap of the same effective chord ratio on a wing of the same thickness this ratio would be about 0·24 (*see* Fig. 13).

It is interesting to note that the optimum setting is about 15 deg for the front flap and about 42 deg for the Fowler flap. It is, in fact, usual to find that for double flaps, where the rear flap extends the chord quite considerably, the optimum front flap angle is relatively small.

6.4. *N.A.C.A. Slotted Flaps.*—6.4.1. *N.A.C.A. single-slotted flaps* (*Fig.* 1*d*).—These have been dealt with in section 5, but for completeness some representative data have been included in Table 2.

6.4.2. *N.A.C.A. double-slotted flaps* (*Fig.* 1*h*, 1*i*).—Comprehensive tests have been made in America of two sets of double-slotted flaps, a relatively small chord combination, *viz.*, 0·26*c* and 0·1*c*, and a large chord combination, 0·4*c* and 0·26*c*. The latter was tested on wings of NACA 23012, 23021 and 23030[62] section, the former on wings of NACA 23012 section[58]. The relative movements of the flaps when operated are given in Table 1, they are in fact the same as those adopted for the single flaps. In Fig. 15b, 15c the drag coefficient increments are plotted against the lift coefficient increments. The optimum flap angles for maximum lift increment combined with a relatively small drag increment vary slightly with wing section and with flap chords, but they are in the region of 30 deg to 40 deg for both flaps. With higher flap angles little lift is lost but there is a rapid increase of drag.

The average values of $\Delta C_{mr}/\Delta C_L$ and $\Delta C_m{'}_r/\Delta C_L'$ are summarised in the following table :—

	$\frac{\Delta C_{mr}}{\Delta C_L}$	$\frac{\Delta C_m{'}_r}{\Delta C_L'}$
0·26*c*, 0·1*c* flap (NACA 23012)	−0·33⁵	−0·29
0·4*c*, 0·26*c* flap (NACA 23012)	−0·34	−0·26⁵
0·4*c*, 0·26*c* flap (NACA 23021)	−0·37	−0·29
0·4*c*, 0·26*c* flap (NACA 23030)	−0·59	−0·43

As with the Fowler flaps, the values of $\Delta C_m{'}_r/\Delta C_L'$ on the 12 per cent thick wing are in fair agreement with the corresponding values for split flaps given in Fig. 13. However, the double-slotted flaps show a surprising increase of $\Delta C_m{'}_r/\Delta C_L'$ with wing thickness. This increase occurs mainly at the higher values of $\Delta C_L'$, and in fact the relation between $\Delta C_m{'}_r$ and $\Delta C_L'$ tends to depart from linearity as the wing thickness increases. Probably, the difference between the type of chordwise lift distribution obtained with slotted flaps and the type obtained with split flaps becomes more accentuated with wing thickness. With the former rather more of the lift increment is concentrated at the flap hinge than with the latter and so a rather larger value of $-\Delta C_{m'r}$ for a given $\Delta C_L'$ may be expected, especially on thick wings. However, the difference does not appear to be serious for wings within the normal practical range of thickness, *viz.*, 0·1*c* to 0·2*c*.

6.5. *Blackburn Flaps.*—6.5.1. *Single Blackburn flaps* (*Fig.* 1*e*).—The Blackburn arrangement is rather more effective than the N.A.C.A. arrangement in exploiting the possibilities of the large chord flap, presumably because of the longer shroud and somewhat larger chord extension. From the data listed in Table 2 it will be seen that the flaps tested on the 23018J section[66] were not so effective as those tested on the 0018/12 and 0018 sections[67]. These latter flaps were a later development in which the slot design was improved and the chordwise extension somewhat increased. It is not surprising to note, therefore, that estimates of $\Delta C_L'$ for intermediate flap angles for the flap on the 23018J section gave better agreement with experiment when based on the Handley Page flap curve for $\lambda_2(\beta)$ than when based on the N.A.C.A. flap curve, whilst the opposite was true for the flap on the NACA 0018 section.*

Fig. 17 shows the increments ΔC_{D0} plotted against ΔC_L for various flap chords ranging from 0·3*c* to 0·6*c* on the 23018J section, and for the flap chord of 0·5*c* on the NACA 0018 section. The marked superiority of the latter flap over the corresponding one on the 23018J section is again apparent. For lift increments above 1·0 the drag increments of Blackburn flaps are in general rather higher than those of the other flaps.

The optimum angle for the Blackburn flap is about 50 deg, which is much the same as for the Handley Page slotted flap.

It will be seen from Table 2 that the pitching moment coefficient increment for a given lift coefficient is relatively low. The mean value of a large number of observations of $\Delta C_{mr}/\Delta C_L$ is about $-0{\cdot}27$, the corresponding mean value of $\Delta C_{m'r}/\Delta C_L'$ is about $-0{\cdot}20$. This latter value is not, however, inconsistent with the curves for $\Delta C_{m'r}/\Delta C_L'$ for plain or split flaps given in Fig. 13, when allowance is made for the large chord of the flap and the fact that nearly all the tests were made on wings of thickness equal to about 18 per cent.

6.5.2. *Blackburn split and slotted flap* (*Fig.* 1*k*).—The Blackburn split and slotted flap has considerable possibilities where both high lift and variable drag are required[68, 71]. Fig. 17b shows the drag increment plotted against the lift increment, and it will be apparent that there is a large range of drag for a given lift made possible by varying the split flap angle keeping the slotted flap angle fixed. Like the single Blackburn flap the double flap involves a relatively small pitching moment increment for a given lift increment, the mean value of $\Delta C_{mr}/\Delta C_L$ is about $-0{\cdot}29$ and the mean value of $\Delta C_{m'r}/\Delta C_L'$ is about $-0{\cdot}24$.

6.5.3. *Blackburn flap with flap leading-edge slat* (*Fig.* 1*l*).—Amongst the many high-lift devices tested by Blackburn Aircraft Ltd. is one for which the flap is equipped with a leading-edge slat[69, 70]. Such an arrangement has obvious mechanical complications, and the slat and flap must be designed to fit snugly when retracted into the wing. However, when properly designed it can be very effective, as it provides both extra chordwise extension and improves the flow over the flap, bringing the point of separation nearer the trailing edge. This latter effect is very important, as can be gauged from the fact that thin aerofoil theory, which assumes no flow breakaway, predicts much higher lift increments at the larger flap angles than is attained in practice. This is brought out in Figs. 6, 7, where the theoretical curves for $\lambda_2(\beta)$ are shown dotted for comparison with the experimental curves. This suggests that there is, therefore, a considerable lift increment still to be gained by suppressing or delaying the flow breakaway from the flap.

* Later tests for which the flap nose was rounded rather more than in the case of the flaps discussed in Refs. 66, 67, showed the flap characteristics to be less sensitive to the slot dimensions and to small deviations of the flap from the optimum setting.

Blackburn Aircraft Ltd. have tested leading-edge slats on 0·4c and 0·5c chord flaps. The main data for the two most promising arrangements are given in Table 2. For the 0·4c flap it was found advisable to use a relatively large slat to get a marked improvement of lift. The estimated value of $\Delta C_L'$ in Table 2 was arrived at by treating the flap plus slat as a single-slotted flap with the leading edge at the nose of the slat, thus, the estimate includes the effect of chord and flap extension due to the slat, but not the effect of flow improvement over the flap. A comparison of the estimated and measured values of $\Delta C_L'$ for the 0·4c flap shows that in this case there could have been no appreciable flow improvement. In the case of the 0·5c flap, however, the leading-edge slat, although small, produced a marked increase in the lift increment, a considerable portion of which must have been due to the resulting improvement of flow over the flap. It is of interest to note that because of this improvement the drag increment for the optimum setting is relatively small. The value of $\Delta C_{mr}/\Delta C_L$ is about $-0{\cdot}35$, but $\Delta C_{m\ r}'/\Delta C_L'$ is in the usual low range for Blackburn flaps, *viz.*, $-0{\cdot}19$ to $-0{\cdot}24$.

6.5.4. *Blackburn flap with inset slots* (*Fig.* 1*m*).—An obviously related device, that was also tested by Blackburn Aircraft Ltd., is that of a flap with fixed inset slots[69, 70]. If the slots are efficiently designed, then, like the flap leading-edge slat, they produce a general improvement of the flow over the flap. The important data for the optimum cases tested are given in Table 2. The cleaning up effect of the slot on the flow over the flap is indicated by the fact that in each case the measured value of $\Delta C_L'$ is considerably greater than the estimated value, whilst the value of ΔC_{D0} is small for the ΔC_L obtained. The values of $-(\Delta C_{mr}/\Delta C_L)$ are 0·29 and 0·35 for the wing with 0·4c and 0·5c flaps respectively, but $-(\Delta C_{m\ r}'/\Delta C_L')$ varies between the limits 0·225 and 0·25.

The simplicity of this device is largely offset by the fact that unless the slot or slots are sealed when the flap is retracted, they will cause a serious increase of drag. The tests indicated that for a slot to function properly it must be cut at a fairly small angle (about 20 deg) to the flap chord. Hence the opening on the upper surface must occur well back, and it will be very difficult to increase the shroud sufficiently to seal the slot.

6.5.5. *Blackburn flap with deflected shroud* (*Fig.* 1*n*).—One of the most effective devices tested by Blackburn Aircraft Ltd. consists of a slotted flap with a slightly longer shroud than usual, and part of the shroud is hinged and arranged to deflect downwards with the flap[69]. The shroud thus smooths over the effective change of camber involved in putting the flap down, and in fact the combination of deflected shroud and flap acts as a double flap. The main data are given in Table 2. The lift coefficient increment attained (2·26) is only slightly less than that attained with either inset slots or a flap leading edge slat, and it probably presents less serious disadvantages than these other devices.

Treating it as a double-slotted flap the estimated value of $\Delta C_L'$ is almost in exact agreement with the measured value. If we regard it as a plain front flap and a rear slotted flap the estimated value of $\Delta C_L'$ is appreciably less than the measured value. This is not surprising, since the slot is near enough to the shroud hinge to dominate the flow there. The pitching moment coefficient increments are relatively small, $\Delta C_{mr}/\Delta C_L$ is $-0{\cdot}3$, whilst $\Delta C_{m\ r}'/\Delta C_L'$ is $-0{\cdot}18$.

6.6. *Venetian-blind Flaps* (*Fig.* 1*o*).—Venetian-blind flaps have at various times aroused a certain amount of interest, since, if their slots function properly, their lift increments should approach the theoretical plain flap values. The results of such tests as have been made, however, have been rather disappointing[77, 78]. Representative data are included in Table 2. The main conclusions of these tests are :—

(1) The optimum spacing of the slat components appears to be one slat-chord length and there is no advantage in using a large number of small slats rather than a small number of large slats.

(2) With the arrangements illustrated in Fig. 1o, the optimum position occurs for the system set at an angle of 60 deg, the individual slats being set at an angle of 40 deg. The lift coefficient increment is then higher and the drag coefficient increment is lower than for the corresponding Fowler flap (*see* Table 2). The main advantage of the slotting derives from the fact that it enables the optimum angle of the flap as a whole to be higher than that of the unslotted flap. The measured and estimated values of $\Delta C_L'$ are in fact, in good agreement.

(3) Slat arrangements can be found for which the slat angles differ from each other, giving even higher lift increments than the one illustrated, but generally these involve a considerably greater drag increment.

(4) The pitching moment increments are high, $-(\Delta C_{mr}/\Delta C_L)$ being of the order of 0·5, whilst $-(\Delta C_m{}'_r/\Delta C_L')$ varies from 0·27 to 0·31.

6.7. *Some Concluding Remarks on High-Lift Flaps.*—It will be clear from the foregoing and a comparison of the columns in Table 2 that the method given in sections 4 and 6.2 for estimating $\Delta C_L'$ and hence ΔC_L is very satisfactory for almost all types of high-lift flaps, except for cases where a particular device is used for cleaning up the flow over the flap itself, as, for example, where the flap has a leading-edge slat or inset slots. Some discretion is necessary in estimating $\Delta C_L'$ where the flap is not fully extended, when it must be decided whether any slots are functioning badly, moderately, or with optimum effectiveness. As already anticipated in section 6.2, in the first case it is best to use the split or plain-flap curves for $\lambda_2(\beta)$ (Fig. 6) depending on the arrangement; in the second case the Handley Page slotted-flap curve is recommended (Fig. 7b) and in the third case the N.A.C.A. slotted-flap curve should be used (Fig. 7a).

The tabulated values of $\Delta C_m{}'_r/\Delta C_L'$ suggest that there is a fair consistency between all types of flaps and that a rough estimate of $\Delta C_m{}'_r$ can be obtained, after calculating $\Delta C_L'$, by assuming $\Delta C_m{}'_r/\Delta C_L' = -0{\cdot}25$. From this estimate of $\Delta C_m{}'_r$ the value of ΔC_{mr} can be calculated using equation (12). Exceptions to this rough rule occur for N.A.C.A. slotted flaps on wings of thickness greater than about 21 per cent. We might go further and note that for each type of flap on wing sections of thin to moderate thickness the ratio $\Delta C_{mr}/\Delta C_L$ is roughly constant and independent of flap chord and angle and of whether the flap is single or double. Mean values for this ratio for the main types of flap are as follows:—

Plain and split flaps	—0·25
Slotted flaps (Handley Page and N.A.C.A.) ..	—0·33
Blackburn flaps	—0·29
Power flaps..	—0·43

No simple unifying rules can be given for estimating ΔC_{D0}, as this is largely the result of an increase in form drag produced by the flap and hence is very sensitive to slot design. A study of the values given in Table 2 should, however, provide a good guide to the probable value of ΔC_{D0} in any particular case.

7. *Wing-body Interference.*—An analysis of such data as there are available from both model and full-scale tests on the effect of wing body interference on the effect of flaps was made by Young and Hufton[4]. This analysis indicates that, as far as the drag increments are concerned, the effect is favourable for split flaps and unfavourable for slotted flaps. In the latter case, the effect may be partially exaggerated by the difficulty in flight on a full-scale aeroplane of ensuring the correct slot shape free from serious distortion effects under load. Rough rules suggested by the analysis, are that for split flaps

$$\Delta C_{D0} \text{ (with interference)} = 0{\cdot}85\ \Delta C_{D0} \text{ (without interference)}$$

and for slotted flaps

$$\Delta C_{D0} \text{ (with interference)} = 1{\cdot}4\ \Delta C_{D0} \text{ (without interference)}.$$

The analysis did not indicate any marked systematic interference effects on lift coefficient increments ; in general, the effect was negligible, although in a few cases it was appreciable.

8. *Flaps Combined with Wing Leading-edge Slats.*—Some of the high-lift flaps discussed above have been tested in combination with wing leading-edge slats,[68,73].

The data are scanty but an analysis has been made by Young in Ref. 3 and the main conclusions suggest the following relations for full-span slats of chord lengths within the range 0·15c to 0·3c set at about 40 deg to the wing chord line :—

(i) $\Delta C_{L\ \max} = 3{\cdot}3\ \dfrac{\text{slat chord}}{\text{wing chord}}$, approx.,

(ii) $\Delta C_{m\,(\text{st.})} = 0{\cdot}9\ \dfrac{\text{slat chord}}{\text{wing chord}}$, approx.,

(iii) $\Delta\alpha_{(\text{st.})} = 10$ deg ($\pm$ 3 deg),

(iv) $\Delta\left(\dfrac{dC_m}{dC_L}\right)_{0\cdot 8\,C_{L\max}} = 0{\cdot}15\ (\pm\ 0{\cdot}07^5)$,

where $\Delta C_{m(\text{st.})}$ is the change in pitching moment coefficient at the stall produced by the slat, and $\Delta\alpha_{(\text{st.})}$ is the change in stalling angle produced by the slat. These increments are additive to those produced by the flap.

9. *Effect of Flaps on Induced Drag.*—In considering the effect of flaps on drag we have so far only considered the effect on profile drag, but flaps may have an important effect on induced drag. This latter effect has been considered theoretically by Young in Ref. 96, where the induced drags of elliptic wings with flaps of various span and various cut-outs have been determined. It is shown that the induced drag can be put in the form

$$C_{Di} = \frac{C_L^2}{\pi A} + \frac{K(\Delta C_L)^2}{\pi A} \quad \ldots \quad (25)$$

where C_L is the total lift coefficient of wing plus flap, ΔC_L is the lift coefficient increment due to the flap, and K is a function of the flap span and cut-out and of the ratio of the aspect ratio (A) to the two-dimensional lift-curve slope of wing (a_0). The function K is reproduced in Figs. 18, 19, 20; these figures correspond to $A/a_0 = \frac{2}{3}$, 1·0 and 2·0 (*i.e.*, A = 4, 6, 12 approximately), respectively.

It will be seen that the above formula for C_{Di} takes the form of the usual elliptic loading term ($C_L^2/\pi A$) plus a term which arises from the departure of the loading of the flapped wing from the elliptic ; it is clear that the latter term can be very important. For a given net flap span this term appears to be least for a cut-out of about 0·1 wing span. It is suggested that where the plan form of the unflapped wing departs appreciably from the elliptic the first term in the above expression for C_{Di} should be replaced by $(C_L^2/\pi A)(1 + \tau)$ where τ is the appropriate correction factor for non-elliptic plan form given by Glauert in Ref. 12.

Similar calculations made for flaps that extend the chord[96] showed that, when the induced drag was expressed in the form of equation (25) above, the chord extension made a negligible difference to the factor K.

10. *Nose Flaps.*—Thin high-speed wing sections with fairly small nose radii of curvature tend to have low maximum lift coefficients, because of the tendency to flow breakaway induced by the sharp wing nose at incidence. It has been suggested that the nose flap might overcome this difficulty. Two forms of nose flap have been developed, one suggested and tested in Germany by Kruger[97,98,100], the other has been suggested in this country.*

* Recent evidence[99] indicates that the Germans were interested in the second form as well as the first,

Kruger's nose flap is illustrated in Fig. 21a. It is hinged at the wing leading edge and rotates out from under the wing and in its optimum position it is set at an angle of about 130 deg to the wing chord. As with a wing leading-edge slat, it does not have a marked effect at incidences below the stalling incidence of the plain wing, but it prolongs the lift curve and delays the stall for several degrees. In effect, it transfers the stagnation point of the wing to the rounded leading edge of the nose flap, and hence, instead of having to pass round the sharp leading edge of the wing at high incidences, the flow is presented with the easier problem of negotiating the flap upper surface and the small discontinuity of curvature at the flap wing junction.

Fig. 21 summarises some of the more important results obtained with this type of flap. The effectiveness of the flap decreases rapidly with increase of wing nose radius of curvature (ϱ). As will be seen from Fig. 21d, for a value of $(\varrho/c)/(t/c)^2$ greater than about 1·0, the flap reduces the lift. Fig. 21b shows the effect of varying the flap angle, the wing section tested is a high speed one with a fairly sharp nose. It will be seen that there is a marked deterioration of effectiveness for flap angles less than the optimum, and it is evident that as the flap is brought into operation rather peculiar and sudden changes of lift and trim must occur. The effect of varying the flap chord at the optimum angular setting on this wing section is illustrated in Fig. 21c. Some representative curves of lift, drag and pitching moment for this section with and without a $0{\cdot}2c$ split flap set at 60 deg and nose flaps of various chords are shown in Fig. 22.

The alternative arrangement involves simply hinging the front portion of the wing making, in effect, a plain leading edge flap (*see* Fig. 21a). This idea is not new (such a flap was tested in 1920 by Harris and Bradfield)[9] but it may have applications to modern high-speed aircraft. It operates in much the same way as Kruger's nose flap, but it may be expected to be much less sensitive to nose radius. It has the advantage that the change in camber, and hence the changes in lift, drag and pitching moment that accompany setting down the flap would take place in an even manner and not in the sudden large jumps associated with the Kruger nose flap. Further, a variety of settings can be used up to the optimum, so that it may be used, if coupled with the trailing edge flap, to provide an adjustable camber to the wing under the pilot's control, suitable camber being chosen for take-off, climb and landing. Some recent preliminary tests have been made at the R.A.E. of a leading-edge flap about $0{\cdot}2c$ in chord on a $7\frac{1}{2}$ per cent thick bi-convex section ; with the flap set down about 30 deg the increase in $C_{L\,\max}$ was about 0·4. Combined with a plain trailing-edge flap of about $0{\cdot}25c$ in chord the $C_{L\,\max}$ attained was 1·9, as compared with the $C_{L\,\max}$ of the plain wing of 0·65.

Both types of leading-edge flap have the disadvantage that their installation would probably eliminate all possibility of achieving far back transition and hence low drag.

11. *Brake Flaps*.—11.1. *General*.—Arising out of the improvements in aerodynamic design and cleanness, that have been made during the last decade, has grown the need for brake flaps for certain types of aircraft. The main applications of brake flaps that developed during the war were to dive bombers, torpedo dropping and to high-speed fighters (particularly night fighters). A further application which has received consideration is to the reduction of the landing run of aircraft.

The brake flap generally takes the form of a flap of relatively small span and chord, and in operation it is frequently set at right angles to the wing surface, although sometimes smaller angles are used. It may be plain or perforated, and it may be attached to the upper or lower surface of the wing ; sometimes flaps on both surfaces in combination are used. Occasionally, the landing flap of a wing has been designed to include a setting at which it can be used as a brake flap. Alternative suggestions include the fitting of brake flaps to the fuselages of aircraft, or the use of parachutes or reversed pitch airscrews. It is not, however, proposed to deal with these alternatives in this report, which will be confined to the usual types of brake flap as fitted to the wings of an aircraft.

The main requirement of brake flaps is, of course, to provide drag for rapid deceleration, but in general it is desirable that they should have as little effect as possible on lift, trim and stability. For night fighters this is most important, but for dive bombers a small change of trim is permissible. Quick operation is also generally desirable. A further requirement is that in operation they should not induce unpleasant buffeting or vibration of the controls or of the aircraft as a whole.

Generalisations, based on existing data, of a kind that will enable a designer to predict all the important characteristics of brake flaps for any given design are impossible. The best that can be done is to discuss the relations between these characteristics and the factors that control them in a broad and mainly qualitative manner, and to refer the reader to existing summaries or collections of data (*e.g.*, Refs. 110, 111, 118) for more detailed guidance.

11.2. *Drag.*—For brake flaps we are interested in the drag increment at a constant lift rather than at a constant incidence.

The main variables of which the drag increment of a brake flap is a function are its area, geometry, chordwise position, the wing thickness and the lift coefficient. Very roughly, one can say that at small values of C_L the drag coefficient increment of a brake flap in terms of its area is about $1 \cdot 1 \sin^2 \beta$ when the flap is at the wing trailing edge, and this coefficient rises with forward movement of the flap to nearly $3 \sin^2 \beta$ when the flap is at about the wing quarter-chord point; the drag coefficient increment then falls rapidly if the flap is moved ahead of that point. At a C_L of 0·5, the drag coefficient increment of the flap on the lower surface is about $1 \cdot 5 \sin^2 \beta$ if the flap is at the trailing edge and falls slightly if the flap is moved forward; with the flap on the upper surface the increment is only about 0·2 to $0 \cdot 3 \sin^2 \beta$ when the flap is at the trailing edge but it rises rapidly with forward movement of the flap to about $4 \cdot 5 \sin^2 \beta$ when the flap is at the quarter-chord point. In Ref. 110 it is suggested that some consistency of data can be obtained by expressing the increment in terms of the area S_f', where

$$S_f' = b_f(c_f + t_1), \quad \ldots \quad (26)$$

b_f is the span of the flap, c_f is the chord of the flap, t_1 is the normal distance from the wing surface to the chord line in the plane of the flap hinge.

Some representative values of the drag coefficient increment based on S_f' and denoted by ΔC_{BD} are reproduced from Ref. 110 in Fig. 23c.* Where more than one flap is used, the drag coefficient increments can be taken as additive.

Brake flaps are frequently perforated or slotted to reduce buffeting and vibration. The estimated drag increments should be reduced in the proportion of open area to total flap area, except in the case of round perforations for which the available evidence suggests the estimated values should be reduced in the proportion of half the open area to total flap area.

11.3 *Lift.*—The lift effect of a flap aft of about 0·5c on either the upper or lower surface of a wing can be estimated with fair accuracy from the curves of Figs. 5, 6, using the concept of reduced chord.† Alternatively, the detailed results collected in Refs. 110 and 111 may be used for guidance. In Ref. 110 the device has been used of expressing the lift coefficient increment in terms of S_f', *i.e.*, the increment is expressed as

$$\Delta C_{BL} = \Delta C_L \frac{S}{S'_f}. \quad \ldots \quad (27)$$

Mean curves of ΔC_{BL} as a function of chordwise position of flap, deduced from a fair quantity of data, are reproduced in Fig. 23a. The scatter is fairly considerable, however, and these curves should only be used to give a rough estimate, the method suggested above is probably more accurate.

In general, the lift effects of two flaps are additive, although there is a recorded case[111] where with flaps on both surfaces the lift was even less than with the single flap on the upper surface.

11.4. *Pitching Moment.*—The pitching moment change produced by a brake flap derives from

(1) the change in the wing pitching moment due to the flap,
(2) the change in downwash produced at the tail plane.

---

* There must clearly be some lower limit to the size of flap chord for which this method of representation can apply, since the method gives a drag increment other than zero when $c_f = 0$.

† For upper surface flap $\Delta C_L'$ is negative.

Generally speaking, a lower surface flap aft of about the mid-chord point produces a nose-down change in the pitching moment of the wing, whilst if it is forward of the mid-chord point the change is nose-up. For an upper-surface flap the changes are of opposite sign. For flaps aft of about 0·5c the changes can be predicted with fair accuracy using the method described in Section 4.3.2. Alternatively, the collected data of Refs. 110, 111 can be studied for guidance. Whitby and Bigg[110] have also suggested that if the pitching moment increment is expressed in the form

$$\Delta C_{BM} = \Delta C_m \frac{\bar{c}}{c} \sqrt{\left(\frac{S}{S_f'}\right)} \quad \ldots \quad (28)$$

then a rough guide can be obtained to ΔC_{BM} using the figure reproduced in Fig. 23b.

The changes in downwash at the tail plane produced by brake flaps result from the accompanying changes in wing loading distribution. Broadly speaking, inboard flaps produce an increase in downwash, and hence a nose-up moment, and outboard flaps produce a small upwash, and hence a nose-down moment. Fig. 23d is reproduced from Ref. 110 and shows some typical curves illustrating the variation with y_i/s_T of the quantity

$$\Delta C_{B\varepsilon} = \frac{\Delta \varepsilon}{\Delta C_L} \frac{b_f}{b} \quad \ldots \quad (29)$$

where ε is the downwash at the tail, y_i is the distance of the inboard end of the flap from the centre-line of the aircraft, and s_T is the tail semi-span.

Generalisation is, however, impossible, the variables are too many and the data too haphazard and unsystematic. All that can be noted here is that in any given case it is not impossible to choose a position of the flaps so as to have the total change in pitching moment of the aeroplane zero at a given lift coefficient or at a given incidence.

We may note, in passing, the use of a slotted flap, set at a negative angle to the wing chord line near the trailing edge, which can be arranged to produce a large drag with practically no change of trim or lift (*see*, for example, the Youngman flap, Refs. 111, 118).

12. *Dive-Recovery Flaps.*—It has been observed that various types of aircraft have shown considerable reluctance to recover from high-speed dives. In such cases, when beginning the recovery, little response is experienced to quite a large stick movement and stick force, and the normal acceleration is small. This phenomenon has been attributed in part to the development of a shock-stall spreading from the wing root section outwards, and in consequence the downwash at the tail is reduced and the capacity of the wings to develop lift is reduced. A method of coping with this difficulty which has been widely adopted is the fitting of dive-recovery flaps. These are small under-wing flaps situated about one third of the chord back from the leading edge fairly near the root section.

Their effect in helping the recovery is a multiple one. They increase the pitching moment of the wing in the nose-up direction and, further, they increase the lift of the wing and hence the normal acceleration. Since this lift helps to restore the circulation over the centre section, where it had been reduced by the shock-stall, the downwash at the tailplane is consequently increased and hence the nose-up pitching moment is still further increased. The net effect is that the aeroplane with dive-recovery flaps recovers steadily at an appreciably higher lift coefficient, and therefore, higher normal acceleration, than without the flaps.

It is shown in Refs, 120, 121 that in the recovery from a dive the pitching moment C_m rapidly settles down to a small value, which may be neglected for the purpose of predicting the recovery, if the derivative $\left(\frac{\partial C_m}{\partial C_L}\right)_M$ is large. This derivative is the rate of change of pitching moment coefficient with lift coefficient at constant Mach number, and its value will be large under the same conditions that make the recovery of an aeroplane from a high-speed dive sluggish and difficult, *viz.*, if there is a reduction of downwash at the tailplane and a reduction of lift-curve slope of the wing. Hence, if we know the change of lift coefficient at zero C_m produced by a dive-recovery flap we can assess the change in normal acceleration produced by it and the consequent speeding up of the recovery from a high-speed dive.

A summary of the available data on dive-recovery flaps has been compiled by Bridgland[125]. It is clear from this summary that the data are much too scanty to permit of the development of any reliable method of prediction of the characteristics of these flaps. The problem is a very complex one, since we require to be able to predict the wing lift and pitching moment increments due to the flaps and the accompanying changes in downwash at the tail plane at Mach numbers at which the wing is shock-stalled. Bridgland suggests that, in the absence of wind-tunnel tests, the low-speed increments in lift, pitching moment and downwash can be roughly estimated from the curves of Fig. 23, derived by Whitby and Bigg[110] from brake-flap data, and empirical corrections should then be made, based on high-speed tunnel tests on models of a Tempest and of a Lightning[122, 199]. Where possible, however, it is advisable to do model tests in a high-speed tunnel.

Bridgland concludes that a flap area of about 0·01 of the wing area is generally required, if the flap is well inboard. If the flap is so far outboard, as to have little effect on the downwash at the tailplane (or in the case of tailless aircraft), the flap areas will then need to be some three or four times this amount.

Dive-recovery flaps very readily cause buffeting of the wing and tailplane and to avoid this it is generally necessary to confine the flap angle to about 20 or 30 deg.

13. *Flaps on Swept-Back Wings.*—13.1. *General.*—As a result of German research demonstrating the appreciable increase in the shock stalling Mach number of a wing to be gained by sweep-back, the use of sweep-back is becoming common for high-speed designs. In addition, sweep-back is of importance for tailless designs. The use of sweep-back, however, carries with it certain disadvantages ; in particular, the maximum lift coefficient of a wing, especially when flapped, decreases with sweep-back. As mentioned in section 1, it is desirable, therefore, that this report should include some remarks on the characteristics of flaps on swept-back wings. Unfortunately, the available data are far from comprehensive or completely reliable. British research on swept-back wings has, in the main, been of an *ad hoc* character ; German work has perhaps been more systematic, but the bulk of it has been done at low Reynolds numbers (of the order of $0{\cdot}5 \times 10^6$). As a result there is a considerable scatter in the results analysed, and the broad generalisations inferred should be accepted as an interim guide pending more comprehensive and reliable tests.

13.2. *Lift Coefficient Increments.*—A number of German and British reports have been analysed [126 to 138] ; the data cover angles of sweep-back varying from —10 to 45 deg, taper ratios from 1:1 to 4·29:1, aspect ratios from 4·8 to 6·5, Reynolds numbers from $2{\cdot}5 \times 10^5$ to $5{\cdot}4 \times 10^6$, split and slotted flaps, and flap spans varying up to full span. The lift coefficient increments have been extracted from the data and each has been divided by the corresponding increment for a wing with zero sweep-back. Where measurements of the latter were not available an estimate has been made. Values of the resulting ratio (written $\Delta C_L/\Delta C_L(\gamma = 0)$) are shown plotted in Fig. 24b as a function of angle of sweep-back (γ). The scatter is clearly very large, and it is impossible to extract from the data any consistent variation associated with scale effect or taper ratio. A mean curve has been drawn through the points as a tentative guide to the variation of the lift increment with sweep-back. If we accept this curve, we see that for small angles of sweep-back the lift increment increases slightly, and reaches a maximum for about 10 deg of sweep. Beyond that angle it falls slowly, for 40 deg of sweep-back the curve suggests a reduction of the lift increment of about 15 per cent.

For flaps on the unswept centre portions of U wings, the analysis suggests that a reasonable estimate of the lift increment can be obtained if the sweep-back is neglected. For flaps set forward of the trailing edge, however, the evidence indicates that the fall in lift increment with position forward of the trailing edge is about half as great as the estimated fall but the evidence is very sketchy.

13.3. *Maximum Lift Coefficient Increments.*—Because of the marked effect of sweep-back in reducing the stalling angle of a flapped wing, it was thought desirable to examine the variation of the ratio $\Delta C_{L\,max}/\Delta C_{L\,max}$ $(\gamma = 0)$. The values of this ratio are shown plotted in Fig. 24a against sweep-back angle. The effect of sweep-back on $\Delta C_{L\,max}$ is clearly very appreciable and a mean curve has been drawn through the plotted points. The curve is actually the function $\cos^3 \gamma$; there is no theoretical reason for choosing this function, but it provides a convenient mean for the points. It is important to note that for aspect ratios not covered in the tests analysed, the variation of $\Delta C_{L\,max}$ with γ may be different.

The reduction in stalling incidence due to sweep-back is presumably associated with the lateral pressure gradients, which encourage the boundary layer near the wing trailing edge to drift towards the tips and hence produce an early tip stall. Therefore, we might expect scale effect to play an important part in controlling the reduction of $C_{L\,max}$ but no consistent scale effect was to be noted in the data examined.

13.4. *Drag Coefficient Increments.*—The ratio $\dfrac{\Delta C_{D0}}{(\Delta C_{D0})\ \ \gamma = 0}$ was similarly determined where possible and the resulting values are shown plotted in Fig. 25. Again we may note a considerable scatter. The mean curve suggested is the function $\cos \gamma$, *i.e.*,

$$\frac{\Delta C_{D0}}{(\Delta C_{D0})\ \gamma = 0} = \cos \gamma . \qquad (30)$$

This curve gives a reduction in the drag increment of about 23 per cent for a sweep-back angle of 40 deg.

13.5. *Pitching Moment Coefficient Increments.*—The pitching moment increment due to a flap on a swept-back wing can be split up into two parts. The first part derives from the change in pitching moment about the local aerodynamic centre of each spanwise element of the flapped part of the wing ; on an unswept wing this provides the total change in pitching moment due to a flap. The second part derives from the change in spanwise lift distribution over the wing produced by the flap and located on the spanwise locus of aerodynamic centres. In general, the first part is negative in sign, whilst the second part is positive, and to avoid large changes of trim when flaps are set down it is desirable to keep the net increment small.

An accurate yet speedy method for estimating the loading distribution on a swept-back wing with flaps has yet to be developed. However, an approximate method has been developed by Dent and Curtis[132], which in the absence of anything more reliable, is acceptable for providing a preliminary design estimate.

If we assume C_m varies linearly with C_L, then we can write

$$C_m = C_{m0} + \left(\frac{dC_m}{dC_L}\right) C_L \qquad (31)$$

where C_{m0} is the pitching moment coefficient at zero lift. Hence, if we can estimate the changes in C_{m0} and dC_m/dC_L (*i.e.*, ΔC_{m0} and $\Delta(dC_m/dC_L)$ respectively) due to flaps, we can estimate the total change in C_m at a given C_L. To calculate these changes Dent and Curtis took the spanwise loading on a swept-back wing to be given by the Schrenk-Thorpe approximation[20], which assumes that the lift distribution is the mean of a lift distribution proportional to the local chord and incidence (measured from the local no-lift angle) and the ideal (or elliptic) lift distribution. At zero lift the latter is zero over the whole span. The flap is assumed to produce a local change in C_{m0}, given by its two-dimensional characteristics, and a local twist or change in effective incidence. The change in lift distribution to this twist is assumed to be located on the quarter-chord line. If the flap is in the normal trailing edge position, the twist produced by it is given by

$$\delta_f = \frac{\Delta C_{Lf}}{a_6} \qquad (32)$$

where ΔC_{Lf} is the standard lift coefficient increment (as defined in section 3.5) due to the flap when full span on an unswept wing of aspect ratio equal to 6. If the flap is not in the trailing edge position then the corresponding change in twist near zero lift is given approximately by

$$\delta = \delta_f \frac{c'}{c} = \frac{\Delta C_{Lf}}{a_6} \frac{c'}{c} \quad \ldots \quad (33)$$

where c' is the effective chord.

On the basis of these assumptions Dent and Curtis have calculated the increment ΔC_{m0} for flaps of various spans and at various chordwise positions on wings of various taper ratios. Their final formula for ΔC_{m0} takes the form

$$\Delta C_{m0} = \mu_2 \Delta C_{mr} + \frac{a_0}{2} A \delta_f \Gamma \mu_3 \quad \ldots \quad (34)$$

where ΔC_{mr} is the full-span pitching moment increment as defined in section 3.3 on an unswept wing,

- μ_2 is the conversion factor for part-span flaps, already discussed in sections 3.5.2.2 and 4.3.2, and shown in Fig. 14,
- a_0 is the two-dimensional lift-curve slope of the mean wing section,
- $\Gamma = \tan \gamma$ (γ = angle of sweep-back),
- μ_3 function of wing taper ratio, flap span and flap chordwise position, shown in Figs. 27a, b, c.

The first term on the right-hand side of equation (40) represents the contribution due to the local change of C_{m0} on each spanwise element of the flapped part of the wing, the second term represents the contribution due to the change in spanwise loading at zero lift caused by the flap. For an unswept wing the latter term is zero.

From equation (38) we can write

$$\Delta C_{m0} = \mu_2 \Delta C_{mr} + \frac{a_0 A}{2a_6} \Delta C_{Lf} \Gamma \mu_3 \quad \ldots \quad (35)$$

and using the ordinary lifting-line theory for elliptic loading, we have

$$\frac{a_0}{2a_6} \simeq \frac{1}{1{\cdot}5}.$$

Hence, we can write

$$\Delta C_{m0} = \mu_2 \Delta C_{mr} + \frac{A}{1{\cdot}5} \Gamma \mu_3 \Delta C_{Lf} \quad \ldots \quad (36)$$

From sections 4, 5, ΔC_{Lf} is given by

$$\Delta C_{Lf} = \lambda_1(c_f/c)\, \lambda_2(\beta),$$

where $\lambda_1(c_f/c)$ is given in Fig. 5, and $\lambda_2(\beta)$ is given in Fig. 6 for split and plain flaps and Fig. 7 for slotted flaps.

For flaps in the normal trailing edge position (*see*, for example, section 4.3)

$$-\Delta C_{mr} = \mu_1 \Delta C_{Lf},$$

where μ_1 is given in Fig. 13 for split and plain flaps ; for slotted flaps *see* section 5.3.

For flaps not at the trailing edge we must calculate $\Delta C_L{}'_f$ (*see* equation (16), section 4.1.1) and hence $\Delta C_m{}'_r$ and finally apply equation (12) of section 3.5.2.1 to determine ΔC_{mr}.*

Dent and Curtis[132] have compared the results of their formula with some experimental results, and they conclude that the formula provides an acceptable guide to the magnitude of the pitching moment change at zero lift for preliminary design purposes. A further comparison has since been made for a number of other experimental results, and it is concluded that the

* Dent and Curtis gave curves for ΔC_{mr} and δ_f, deduced from split-flap data on NACA 230 sections, for use with equation (40) ; the above procedure is, however, more in line with previous sections of this report and is more general.

formula for ΔC_{m0} is generally correct to within $\pm 0{\cdot}03$ for sweep-back angles less than about 30 deg. For larger sweep-back angles the method may become unreliable.

For the change in dC_m/dC_L due to flaps, Dent and Curtis arrived at the formula

$$\Delta\left(\frac{dC_m}{dC_L}\right) = - K_2 A \Gamma \quad \ldots \quad (37)$$

where K_2 is given as a function of flap span for various flap chordwise positions and taper ratios in Fig. 26. It is doubtful whether great reliability can be placed on this formula, but in general the overall effect is small. When the flap is in the normal trailing edge position, theory shows that $\Delta(dC_m/dC_L)$ is zero.

14. *Summary of Main Formulae and Conclusions.*—14.1. *Lift Coefficient Increments.*—14.1.1. *Full-span flaps.*—The lift coefficient increment for aspect ratio equal to 6, based on the extended chord, is given by

$$\Delta C_L' = \lambda_1(c_f/c')\, \lambda_2(\beta)$$

where $\lambda_1(c_f/c')$ is given in Fig. 5 (all flaps),

$\lambda_2(\beta)$ is given in Fig. 6 for split and plain flaps, and in Fig. 7 for slotted flaps.

For double flaps

$$\Delta C_L' = \Delta C_L{'}_1 + \Delta C_L{'}_2$$

where $\Delta C_L{'}_1 = \lambda_1(c_{f1}/c')\, \lambda_2(\beta_1)$

and $\Delta C_L{'}_2 = \lambda_1(c_{f2}/c')\, \lambda_{22}(\beta_2)$

$\lambda_{22}(\beta_2)$ is given in Fig. 8.

To obtain the lift coefficient increment based on the basic wing chord (ΔC_L) for any aspect ratio A we use the equation

$$\Delta C_L = \Delta C_L' \frac{c'}{c} \frac{F(A)}{F(6)} + C_{Lw}\left(\frac{c'}{c} - 1\right)$$

where $F(A)/F(6)$ is given in Fig. 3.

14.1.2. *Part-span flaps.*—For part-span flaps of all types we have

$$\Delta C_{L\ \text{(part span)}} = \lambda_3(b_f/b)\, \Delta C_{L\ \text{(full span)}}$$

where $\lambda_3(b_f/b)$ is given in Fig. 9.

14.2. *Drag Coefficient Increments.*—14.2.1. *Full-span flaps.*—For split, plain and slotted flap of the Handley Page or N.A.C.A. variety

$$\Delta C_{D0} = \delta_1(c_f/c)\, \delta_2(\beta)$$

where $\delta_1(c_f/c)$ and $\delta_2(\beta)$ are given in Fig. 10 for split and plain flaps and in Fig. 11 for slotted flaps. For other types of flaps, *see* Table 2 and Figs. 15, 16, 17.

14.2.2. *Part-span flaps.*—For part-span flaps of all types we have

$$\Delta C_{D0\ \text{(part span)}} = \delta_3(b_f/b)\,.\,\Delta C_{D0\ \text{(full span)}}$$

where $\delta_3(b_f/b)$ is given in Fig. 12.

14.3. *Pitching Moment Coefficient Increments.*—14.3.1. *Full-span flaps* (rectangular wing).—We have

$$\frac{\Delta C_m{'}_r}{\Delta C_L'} = \mu_1(c_f/c)$$

where $\mu_1(c_f/c')$ is given in Fig. 13 and $\Delta C_L'$ is for $A = 6$. This figure was derived from split and plain flap data but the curves for $t/c = 0{\cdot}12$ and $0{\cdot}21$ are applicable to all types of flaps.

To obtain ΔC_{mr} from $\Delta C_{m'r}$ we have the equation

$$\Delta C_{mr} = \Delta C_{m'r} \left(\frac{c'}{c}\right)^2 - \frac{C_L}{4} \frac{c'}{c}\left(\frac{c'}{c} - 1\right) + C_{mw}\left[\left(\frac{c'}{c}\right)^2 - 1\right].$$

Alternatively, we can obtain ΔC_{mr} more directly, if somewhat less accurately, by using the following relations :—

$\frac{\Delta C_{mr}}{\Delta C_L} = \mu_1(c_f/c)$, from Fig. 13, for split and plain flaps,

$= -0{\cdot}34$, for single and double N.A.C.A. slotted flaps,

$= -0{\cdot}43$, for single and double Fowler flaps,

$= -0{\cdot}27$ to $-0{\cdot}3$, for single and double Blackburn flaps and a single Blackburn flap with deflected shroud,

$= -0{\cdot}35$, for Blackburn flap with leading-edge slat,

$= -0{\cdot}3$ to $-0{\cdot}35$, for Blackburn flap with inset slots,

$= -0{\cdot}5$, for Venetian-blind flaps.

For these relations ΔC_L corresponds to $A = 6$.

14.3.2. *Part-span flaps.*—For part-span flaps of all types

$$\Delta C_{m\ \text{(part span)}} = \mu_2(b_f/b)\ \Delta C_{mr\ \text{(full span)}}$$

where $\mu_2(b_f/b)$ is given in Fig. 14.

14.4. *High-Lift flaps.*—For the other main characteristics and the geometry of the high-lift flaps considered *see* Table 2 and Fig. 1.

14.5. *Wing-body Interference.*—To allow for wing-body interference, empirical evidence suggests that for split flaps

$$\Delta C_{D0\ \text{(with interference)}} = 0{\cdot}85\Delta C_{D0\ \text{(without interference)}}$$

and for slotted flaps

$$\Delta C_{D0\ \text{(with interference)}} = 1{\cdot}4\Delta C_{D0\ \text{(without interference)}}.$$

There is no significant indication of interference effects on lift increments.

14.6. *Wing Leading-edge Slats.*—The effects of wing leading-edge slats are roughly additive to those of flaps and when full span are given by

$$\Delta C_{L\max} = 3{\cdot}3\ \frac{\text{slat chord}}{\text{wing chord}},\ \text{approx.},$$

$$\Delta C_{m\,(\text{st})} = 0{\cdot}9\ \frac{\text{slat chord}}{\text{wing chord}},\ \text{approx.}$$

$$\Delta\alpha_{(\text{st})} = 10\ \text{deg}\ (\pm\ 3\ \text{deg}),$$

$$\Delta(\partial C_m/\partial C_L)_{0{\cdot}8\,C_{L\max}} = 0{\cdot}15\ (\pm 0{\cdot}07^5)$$

14.7. *Effect of Flaps on Induced Drag.*—The induced drag of a flapped elliptic wing is given by

$$C_{Di} = \frac{C_L^2}{\pi A} + K\frac{\Delta C_L^2}{\pi A}$$

where K is a function of flap geometry and A/a_0 is given in Figs. 18, 19, 20.

14.8. *Kruger's Nose Flap.*—The characteristic of Kruger's nose flap are illustrated in Figs. 21, 22. The reduction in its effectiveness with increase of wing leading edge radius of curvature is noteworthy (*see* Fig. 21d).

14.9. *Brake Flaps.*—Rough estimates of the effects of brake flaps on lift, drag and pitching moment can be obtained from the curves of Fig. 23.

14.10 *Flaps on swept-back wings.*—On swept-back wings of moderate aspect ratio, the available evidence suggests very broadly that (*see* Figs. 24, 25) :—

$$\frac{\Delta C_{L\,\max}}{\Delta C_{L\,\max}\ (\gamma = 0)} = \cos^3 \gamma, \text{ approx.,}$$

$$\frac{\Delta C_{D0}}{\Delta C_{D0}\ (\gamma = 0)} = \cos \gamma, \text{ approx.,}$$

whilst $\dfrac{\Delta C_L}{\Delta C_L\ (\gamma = 0)}$ is given by the curve of Fig. 24b.

The change in C_{m0} due to flaps on swept-back wings is given (to within $\pm$ 0·03) by the formula

$$\Delta C_{m0} = \mu_2 C_{mr} + \frac{A\Gamma}{1 \cdot 5} \mu_3 \Delta C_{Lf},$$

where μ_2 is given in Fig. 14,
and μ_3 is given in Fig. 27,
ΔC_{mr} is the increment in C_m due to the flap when full span on a rectangular wing,
ΔC_{Lf} is the increment in C_L due to the flap when full span in the trailing edge position on an unswept wing of aspect ratio = 6,
and Γ = tan γ (γ = angle of sweep-back).

15. *Acknowledgements.*—It will be clear from the foregoing and the Bibliography that in compiling this report the author has drawn very heavily on sources of information additional to the official Establishments in this country. In particular, he would like to acknowledge the immeasurable value of the systematic research done by the N.A.C.A. on flaps of all kinds, and also of the research done by Blackburn Aircraft Ltd. on high-lift devices.

TABLE 1

Table of Flap Paths for N.A.C.A. Small Double Flap (NACA 23012)

TABLE 1(a)

β_1 deg	x_1	y_1
0	8·36	3·91
10	5·41	3·63
20	3·83	3·45
30	2·63	3·37
40	1·35	2·43
50	0·5	1·63
60	0·12	1·48

TABLE 1(b)

β_1 deg	β_2 deg	x_2	y_2
0	0	3·22	1·58
20	10	1·55	1·52
20	20	1·32	1·50
20	30	1·06	1·50
40	20	0·32	1·50
40	30	0·06	1·27
40	40	0·25	0·59

TABLE 1(c)

Table of Flap Paths for N.A.C.A. Large Double Flap

β_1		0	10 deg	20 deg	30 deg	40 deg	β_2	0	10 deg	20 deg	30 deg	40 deg	50 deg
NACA 23012	x_1	11·5	5·50	3·50	1·50	—0·50	x_2	8·36	5·50	4·00	2·50	1·50	0·50
	y_1	5·86	5·50	5·50	3·50	1·50	y_2	3·91	3·75	3·75	3·25	2·25	1·75
NACA 23021	x_1	11·5	8·50	4·50	2·50	1·50	x_2	8·33	5·00	3·50	0·50	0	0
	y_1	9·20	9·50	8·50	6·50	4·50	y_2	4·85	6·00	5·00	3·00	2·50	2·50
NACA 23030	x_1	17·5	14·5	10·5	6·50	4·50	x_2	11·66	10·50	5·50	1·50	0·50	—0·50
	y_1	14·8^5	15·0	14·0	12·0	4·00	y_2	9·90	10·00	10·00	8·00	7·00	4·00

NOTE:

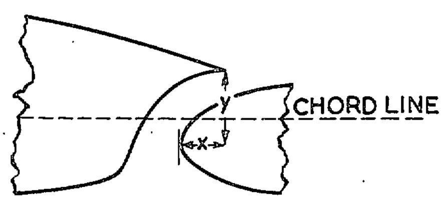

x_1 and y_1 are co-ordinates (given as a percentage of the wing chord) of the nose of the first flap relative to the first slot lip as origin and axis taken parallel and normal to the wing chord line. x_2 and y_2 are similarly co-ordinates of the nose of the second flap relative to the second slot lip as origin and axis taken parallel and normal to the first flap chord line. (*See* sketch above.)

TABLE 2

Main Characteristics of High Lift Flaps

Type of Flap, etc.	Wing Section	Flap Chords c_{f1}/c, c_{f2}/c	Flap Angles β_1, β_2 deg	Extended Chord c'/c	ΔC_L ($\alpha = \alpha_0 + 10$ deg) $A = 6$	ΔC_{D0} ($\alpha = \alpha_0 + 6$ deg) $A = 6$	ΔC_{mr} ($\alpha = \alpha_0 + 10$ deg) $A = 6$	$\Delta C_{L\,max}$	$\Delta\left(\frac{dC_m}{dC_L}\right)$ ($C_L = 0{\cdot}8\, C_{L\,max}$)	$\Delta C_L'$ (Measured)	$\Delta C_{m'r}$ (Measured)	$\Delta C_L'$ (Estimated)	$\frac{\Delta C_{mr}}{\Delta C_L}$ (Measured)	$\frac{\Delta C_{m'r}}{\Delta C_L'}$ (Measured)	Remarks	Ref.
Fowler	Clark Y	0·2	15	1·085	0·44^{5}	0·015	—0·169	0·48^{5}	—0·063	0·35	—0·109	0·35	0·38	0·31	$\Delta C_L'$ Estimated as for Split Flap	74
,,	(t/c=0·117)	0·2	30	1·185	1·05^{5}	0·036	—0·443	1·13^{5}	—0·089	0·78	—0·236	0·79	0·42	0·30		74
,,	(t/c=0·117)	0·3	20	1·181	0·69^{5}	0·033	—0·268	0·718	—0·078	0·48	—0·129	0·48	0·39	0·27	$\Delta C_L'$ Estimated as for Split Flap	74
,,	(t/c=0·117)	0·3	30		1·36^{5}	0·048	—0·610	1·44	—0·101				0·45			74
,,	(t/c=0·117)	0·3	40	1·280	1·54^{5}	0·085	—0·691	1·52	—0·067	1·08	—0·293	1·02	0·45	0·27	N.A.C.A. Tests	74
,,	(t/c=0·117)	0·4	20	1·265	0·86	0·039	—0·354	0·74	—0·058	0·49	—0·123	0·50	0·41	0·25	$\Delta C_L'$ Estimated as for Split Flap	74
,,	(t/c=0·117)	0·4	25	1·365	1·26	0·043	—0·605	1·45	—0·170	0·73	— 186	0·84	0·48	0·25		74
,,	(t/c=0·117)	0·4	40	1·365	1·77^{5}	0·099	—0·85	1·78^{5}	—0·088	1·13	—0·304	1·11	0·48	0·27		74
,,	H.P. 51 (t/c=0·16)	0·4	40·7	1·365	2·02	0·042	—0·82	1·82	—0·113	1·27	—0·291	1·13	0·41	0·23		76
Fowler + Split Flap	(t/c=0·16)	0·4, 0·1,	34·8, 45	1·365	2·38	0·052	—1·00	2·10	—0·049	1·53	—0·371	1·45	0·42	0·24	R.A.E. Tests	76
Double Fowler	(t/c=0·16)	0·4, 0·4,	13, 41·7	1·41	2·65	0·100	—1·07^{5}	2·45	—0·037	1·57^{5}	—0·346	1·49	0·41	0·22		76
N.A.C.A.	N.A.C.A.	0·1	20	1·018	0·42	0·004	—0·135	0·44	—0·007	0·40	—0·124	0·45	0·32	0·31		58
Slotted	23012	0·1	50	1·030	0·75	0·024	—0·202	0·64	—0·007	0·71	—0·179	0·69	0·27	0·25		58
,,	23012	0·26	20	1·045	0·68	0·007	—0·221	0·65	0·008	0·62	—0·186	0·69	0·33	0·30		54, 58
,,	23012	0·26	40	1·070	1·15	0·057	—0·387	1·02	0·041	1·02	—0·299	1·02	0·34	0·29		54, 58
,,	23012	0·4	20	1·076	1·00^{5}	0·014	—0·304	0·97	—0·017	0·87^{5}	—0·234	0·82^{5}	0·30	0·27		62, 56
,,	23012	0·4	30	1·100	1·38	0·026^{5}	—0·416	1·28		1·18	—0·297	1·06^{5}	0·30	0·25		62, 56
,,	23012	0·4	40	1·120	1·30	0·113^{5}	—0·367	1·34		1·08	—0·257	1·18^{5}	0·28	0·24		62, 56
N.A.C.A.	23012	0·26, 0·1	20, 20	1·076	1·17	0·015	—0·391	1·01	0·013	1·05^{5}	—0·317	1·06	0·33	0·30		58
Double Slotted	23012	0·26, 0·1	40, 40	1·100	1·67	0·099	—0·553	1·31	0·150	1·44^{5}	—0·401	1·45	0·33	0·28		58
N.A.C.A.	23012	0·4, 0·26	20, 20	1·139	1·59	0·052	—0·54	1·50	0·03	1·32^{5}	—0·354	1·32	0·34	0·27		62
Double Slotted	23012	0·4, 0·26	30, 30	1·160	2·09^{5}	0·114	—0·71	1·73	0·025	1·70	—0·493	1·64	0·34	0·29		62
,,	N.A.C.A.	0·4, 0·26	20, 20	1·118	1·49^{5}	0·061	—0·56	1·68	0·002	1·26	—0·398	1·33	0·37	0·32		62
,,	23021	0·4, 0·26	40, 30	1·183	2·13	0·187	—0·78	1·94	0·19	1·68	—0·467	1·64	0·37	0·28		62
,,	N.A.C.A.	0·4, 0·26	20, 20	1·132	1·75	0·067	—0·86	1·96	0·05	1·48	—0·615	1·32	0·49	0·41^{5}		62
,,	23030	0·4, 0·26	40, 30	1·220	2·30	0·126	—1·40	2·35	0·125	1·78	—0·83	1·68	0·61	0·47		62
,,	23030	0·4, 0·26	40, 40	1·242	2·32	0·226^{5}	—1·38	2·41	0·125	1·79	—0·785	1·74	0·59	0·44		62
Blackburn	23018J	0·3	20	1·060	0·52	0·013	—0·131	0·49	—0·024	0·45	—0·099	0·55	0·25	0·22	$\Delta C_L'$ Estimated from H.P. Flap Curves	66
Slotted	23018J	0·3	50	1·145	1·25	0·082	—0·338	1·25	+0·010	1·00	—0·202	1·04	0·27	0·20		66
,,	23018J	0·4	20	1·055	0·62^{5}	0·034	—0·162	0·56^{5}	0	0·55	—0·128	0·62	0·26	0·23	$\Delta C_L'$ Estimated from H.P. Flap Curves	66
,,		0·4	50	1·126	1·42	0·130	—0·372	1·22^{5}	+0·020	1·17	—0·239	1·18	0·26	0·20		66
,,	23018J	0·5	20	1·065	0·66^{5}	0·046	—0·165	0·67	—0·006	0·57^{5}	—0·115	0·69	0·25	0·20	$\Delta C_L'$ Estimated from H.P. Flap Curves	66
,,		0·5	50	1·17	1·58	0·161	—0·379	1·45	—	1·31^{5}	—0·205	1·29	0·24	0·16		66
,,	0018/12 (t/c=0·15)	0·5	45	1·20^{5}	1·88^{5}	0·110	—0·522	1·57^{5}	—0·018	1·43^{5}	—0·267	1·29	0·28	0·19		
,,	N.A.C.A.	0·5	25	1·105	1·18^{5}	0·034	—0·350	1·41	—0·064	1·00^{5}	—0·249	0·79 1·005	0·29^{5}	0·25	$\Delta C_L'$ Estimated from H.P. Flap Curves $\Delta C_L'$ Estimated from N.A.C.A. Flap Curves	67 67
,,	0018	0·5	45	1·194	1·60	0·117	—0·425	1·54	—0·059	1·224	—0·224	1·26	0·27	0·18		
,,	0018	0·5	55	1·24^{5}	1·78^{5}	0·160	—0·489	1·60	—0·003	1·29^{5}	—0·230	1·28	0·27	0·18		67

H.P. is abbreviation for Handley Page

TABLE 2—*continued*

Type of Flap, etc	Wing Section	Flap Chord cf_1/c_1 cf_2/c	Flap Angle β_1, β_2 deg	Extended Chord c'/C	ΔC_L ($\alpha=\alpha_0+10$ deg) $A=6$	ΔC_{D0} ($\alpha=\alpha_0+6$ deg) $A=6$	ΔC_{mr} ($\alpha=\alpha_0+10$ deg) $A=6$	$\Delta C_{L\,max}$	$\Delta\left(\frac{\partial C_m}{\partial C_L}\right)$ ($C_L=0{\cdot}8\ C_{L\,max}$)	$\Delta C_L'$ (Measured)	$\Delta C_{m'r}$ (Measured)	$\Delta C_L'$ (Estimated)	$-\frac{\Delta C_{mr}}{\Delta C_L}$ (Measured)	$-\frac{\Delta C_{m'r}}{\Delta C_L'}$ (Measured)	Remarks	Ref.
Blackburn Split & Slotted	N.A.C.A. 0018	0·5, 0·5	25, 20	1·105	2·07	0·104	—0·609	2·10	—0·044	1·79	—0·440	1·73	0·29	0·25		68
		0·5, 0·5	30, 35	1·185	2·41^5	0·189	—0·679	2·17	—0·045	2·10	—0·522	1·97	0·28	0·25		68
	R.A.E. High Speed t/c=	0·5, 0·5	35, 25	1·156	2·31	0·193	—0·664	2·09	—0·049	1·94	—0·429	1·97	0·29	0·22		68
		0·5, 0·5	35, 35	1·156	2·29	0·208	—0·660	2·08	—0·660	1·91	—0·432	1·90	0·29	0·23		68
Blackburn Flap with Flap Leading Edge Slat	B.A.0018/12	0·5, slat chord =0·086c	50	1·1335	2·28	0·143	—0·780	1·93	0	1·52	—0·293	1·35	0·34	0·19	$\Delta C_L'$ Estimated as for Single-slotted Flap of 0·57c chord at 50 deg	69
	Composite section (t/c=0·18)	0·4, slat chord 0·19c	40	1·24	1·631	0·097	—0·569	1·72	—	1·17	—0·283	1·23	0·35	0·24	$\Delta C_L'$ Estimated as for Single-slotted Flap of 0·5c chord at 40 deg	70
Blackburn Flap with Inset Slot	B.A.0018/12	0·5, 2 inset slots	50	1·285	2·33	0·117	—0·820	2·06	0	1·63	—0·360	1·28	0·35	0·22		69
	Composite section (t/c=0·18)	0·4, 1 inset slot	40	1·09	1·60	0·052	—0·467	1·55	—	1·42	—0·351	1·19	0·29	0·25		70
	Composite section (t/c=0·12)	0·4, 1 inset slot	40	1·12	2·05	0·048	—0·602	1·60	—	1·75	—0·418	1·20	0·29	0·24		70
Blackburn Flap with Shroud Deflected	B.A.0018/12	0·5, Shroud deflected =0·08c	Flap Angle =50 Shroud Angle=17	1·27	2·26	0·122	—0·675	1·78	0	1·62	—0·299	1·63 1·42	0·30	0·18	$\Delta C_L'$ Estimated as for Double-slotted Flaps $\Delta C_L'$ Estimated for Plain Front Flap and Rear Slotted Flap	69
Venetian Blind Flap	N.A.C.A. 23012	0·4c Flap made up of 4 slats (Clark Y section) 0·1c each	β_c=30 $\beta_1=\beta_2=\beta_3=\beta_4$=30	1·37	1·26^5	0·021	—0·61	1·46	—0·043	0·72	—0·222	0·96	0·48	0·31	$\Delta C_L'$ Estimated for Single-slotted Flap at 30 deg	77
			β_c=60 $\beta_1=\beta_2=\beta_3=\beta_4$=40	1·37	1·87^5	0·037	—0·96	1·93	—0·060	1·16	—0·329	1·13	0·51	0·28	$\Delta C_L'$ Estimated for Single-slotted Flap at 60 deg	77
			β_c=60 β_1=40 β_2=60 β_3=50 β_4=70	1·37	1·92^5	0·133	—0·96	2·11	—0·060	1·20	—0·327	1·13	0·50	0·27	$\Delta C_L'$ Estimated for Single-slotted Flap at 60 deg	77

BIBLIOGRAPHY

A. *General Reviews*

No.	Name	Title, etc.
1	Alston	Wing Flaps and other Devices as Aids to Landing. *J.R.Ae.S.*, Vol. 39, p. 637. 1935.
2	Irving	Wing Brake Flaps. A Review of Their Properties and the Means for Their Operation. *Aircraft Engineering*, Vol. 7, p. 189. Aug. 1935.
3	Young	A Further Comparison of High Lift Devices. A.R.C. 5089. 1941. (Unpublished.)
4	Young and Hufton	Note on the Lift and Profile Drag Effects of Split and Slotted Flaps. A.R.C. 5472. 1941. (To be published.)
5	Weyl	High Lift Devices and Tailless Aeroplanes. *Aircraft Engineering*, Vol. 17, p. 292. October, 1945.

See also Refs. 29, 39, 60, 61, 111, 125.

B. *Papers of Historical Interest*

No.	Name	Title, etc.
6	Nayler, Stedman, Stern, Bryant	Experiments on Models of Aeroplane Wings at the National Physical Laboratory. R. & M. 110. Parts IV and V. 1914.
7	Harris and Bradfield	Model Experiments with Variable Camber Wings. R. & M. 677. 1920.
8	Glauert	The Handley Page Slotted Wing. R. & M. 834. 1922.
9	Bradfield	Tests of Four Slotted Aerofoils Supplied by Messrs. Handley Page Ltd. R. & M. 835. 1922.
10	Le Page	Further Experiments on Tandem Aerofoils. R. & M. 886. 1923.
11	Schrenk and Gruschwitz	A Simple Method of Increasing the Lift of a Wing. *Z.F.M.*, p. 597. 1932.

See also Refs. 5, 32.

C. *Theoretical Papers*

No.	Name	Title, etc.
12	Glauert	*Aerofoil and Airscrew Theory*. Cambridge University Press. 1926.
13	Glauert	Theoretical Relationships for an Aerofoil with a Hinged Flap. R. & M. 1095. 1927.
14	Perring	The Theoretical Relationships for an Aerofoil with a Multiply Hinged Flap System. R. & M. 1171. 1928.
15	Keune	Auftrieb einer geknickten ebenen Platte. *Luftfahrtforschung*, Vol. XIII, p. 85. 1936. Momente und Ruderauftrieb einer geknickten ebenen Platte. *Luftfahrtforschung*, Vol. XIV, p. 558. 1937.
16	Hollingdale	Aerodynamic Characteristics of Tapered Wings with Flaps and Slots. R. & M. 1774. 1937.
17	Pearson	Span Load Distribution for Tapered Wings with Partial Span Flaps. N.A.C.A. Report No. 585. 1937.
18	Pearson and Jones	Theoretical Stability and Control Characteristics of Wings with Various Amounts of Taper and Twist. N.A.C.A. Report No. 635. 1938.
19	Pearson and Anderson	Calculation of the Aerodynamic Characteristics of Tapered Wings with Partial Span Flaps. N.A.C.A. Report No. 665. 1939.
20	Schrenk	A Simple Approximation Method for Obtaining the Spanwise Lift Distribution. N.A.C.A. Tech. Memo 948. *J.R.Ae.S.* October, 1941.

See also Refs. 93, 94, 96, 132.

D. *Loading and Pressure Distributions on Flapped Wings*

No.	*Name*	*Title, etc.*
21	Wenzinger	Wind Tunnel Measurements of Air Leads on Split Flaps. N.A.C.A. Tech. Note No. 498. 1934.
22	Wenzinger	Pressure Distribution over an Aerofoil Section with a Flap and Tab. N.A.C.A. Report No. 574. 1936.
23	Wenzinger	Pressure Distribution over a Rectangular Airfoil with a Partial Span Split Flap. N.A.C.A. Report No. 571. 1936.
24	Wenzinger	Pressure Distribution over an NACA 23012 Airfoil with an NACA 23012 External Airfoil Flap. N.A.C.A. Report No. 614. 1938.
25	Wenzinger and Anderson	Pressure Distribution over Airfoils with Fowler Flaps. N.A.C.A. Report No. 620. 1938.
26	Jacobs and Rhode	Airfoil Section Characteristics as Applied to the Prediction of Air Forces and Their Distribution on Wings. N.A.C.A. Report No. 631. 1938.
27	Wenzinger and Delano	Pressure Distribution over an NACA 23012 Airfoil with a Slotted and a Plain Flap. N.A.C.A. Report No. 633. 1938.
28	Allen	Calculation of the Chordwise Load Distribution over Airfoil Sections with Plain, Split or Serially Hinged Trailing Edge Flaps. N.A.C.A. Report No. 634. 1938.
29	Wenzinger and Rogallo	Resumé of Air Load Data on Slats and Flaps. N.A.C.A. Tech. Note No. 690. 1939.
		See also Ref. 74.

E. *Split and Plain Flap Data*

30	Weick and Harris	The Aerodynamic Characteristics of a Model Wing having a Split Flap Deflected Downwards and Moved to the Rear. N.A.C.A. Tech. Note No. 222. 1932.
31	Wenzinger	The Effect of Partial Span Split Flaps on the Aerodynamic Characteristics of a Clark Y Wing. N.A.C.A. Tech. Note No. 472. 1933.
32	Joyce	Zap Flaps and Ailerons. Supplement to *Flight*, July 27 and Aug. 31, 1933.
33	Wenzinger	The Effect of Full Span and Partial Span Split Flaps on the Aerodynamic Characteristics of a Tapered Wing. N.A.C.A. Tech. Note No. 505. 1934.
34	Jones, Bell and Smyth	Tests on Aerofoil Flaps in the Compressed Air Tunnel. R. & M. 1636. 1934.
35	Clark and Kirby	Wind Tunnel Tests of the Characteristics of Wing Flaps and their Wakes. R. & M. 1698. 1936.
36	Wallace	Investigation of Full Scale Split Trailing Edge Wing Flaps with Various Chord and Hinge Locations. N.A.C.A. Report No. 539. 1935.
37	Wenzinger	Wind Tunnel Investigations of Ordinary and Split Flaps on Airfoils of Different Profiles. N.A.C.A. Report No. 554. 1936.
38	Williams, Brown and Smyth	Tests of Airfoils RAF 69 and RAF 89 With and Without Split Flaps in the Compressed Air Tunnel. R. & M. 1717. 1936.
39	Pearson	A Method of Estimating the Aerodynamic Effects of Ordinary and Split Flaps of Airfoils Similar to the Clark Y. N.A.C.A. Tech. Note No. 571. 1936.
40	Irving, Warsap, Batson and Gummer	Some Aerodynamic Characteristics of Tapered Wings Fitted with Flaps of Various Spans. R. & M. 1796. 1936.
41	Wenzinger	Wind Tunnel Investigation of Tapered Wings With Ordinary Ailerons and Partial Span Split Flaps. N.A.C.A. Report No. 611. 1937.

No.	*Name*	*Title, etc.*
42	Dearborn and Soulé	Full Scale Wind Tunnel and Flight Tests of a Fairchild 22 Aeroplane Equipped with a Zap Flap and Zap Ailerons. N.A.C.A. Tech. Note 596. 1937.
43	Wenzinger and Ames	Wind Tunnel Investigation of Rectangular and Tapered NACA 23012 Wings with Plain Aileron and Full Span Split Flaps. N.A.C.A. Tech. Note No. 661. 1938.
44	House	The Effects of Partial Span Plain Flaps on the Aerodynamic Characteristics of a Rectangular and a Tapered Clark Y wing. N.A.C.A. Tech. Note No. 663. 1938.
45	Abbott and Greenberg	Tests in the Variable Density Wind Tunnel of the NACA 23012 Airfoil with Plain and Split Flaps. N.A.C.A. Report No. 661. 1939.
46	Wenzinger and Harris	Wind Tunnel Investigation of NACA 23012, 23021 and 23030 Airfoils with Various Sizes of Split Flaps. N.A.C.A. Report No. 668. 1939.
47	Williams and Brown	Tests on the Aerofoil EQ. 1250/1050 With and Without Flap in the Compressed Air Tunnel. A.R.C. 5517. December, 1941. (Unpublished.)
48	Williams and Brown	Tests on the Aerofoil EQ. 0950/1050 With and Without Flap in the Compressed Air Tunnel. A.R.C. Report No. 5547. 1941. (Unpublished.)
49	Muse and Neely	Wind Tunnel Investigation of an NACA 66—2.216 Low Drag Wing with Split Flaps of Various Sizes. A.R.C. Report No. 5604. 1942. (Unpublished.)

See also Refs. 4, 6, 11, 13, 15, 16, 21, 23, 27, 28, 29, 65, 79, 80, 81, 82, 83, 87, 90, 92.

F. *Slotted-flap Data* (*Handley Page, and NACA Single and Double-slotted Flaps*)

50	Clark and Callen	Wind Tunnel Tests of a Handley Page Aerofoil with Slotted Flap. A.R.C. 1368. 1934. (Unpublished.)
51	Lees	Tests on an Aerofoil with 30 per cent Handley Page Slotted Flap. R.A.E. Report No. BA 1233 (and addendum). A.R.C. 2082a. 1936. (Unpublished.)
52	Williams, Bell and Smyth	Tests on a Handley Page Aerofoil with 20 per cent Slotted Flap in the Compressed Air Tunnel. A.R.C. Report No. 3574. 1938. (Unpublished.)
53	—	Wind Tunnel Investigation of a Handley Page 15 per cent Slotted Flap. A.R.C. 3605. 1938. (Unpublished.)
54	Wenzinger and Harris	Wind Tunnel Investigations of an NACA 23021 Airfoil with Various Arrangements of Slotted Flaps. N.A.C.A. Report No. 664. 1939.
55	Wenzinger and Harris	Wind Tunnel Investigation of an NACA 23021 Airfoil with Various Arrangements of Slotted Flaps. N.A.C.A. Report No. 677. 1939.
56	Harris	Wind Tunnel Investigation of an NACA 23012 Airfoil with Two Arrangements of a Wide Chord Slotted Flap. N.A.C.A. Tech. Note No. 715. 1939.
57	Duschik	Wind Tunnel Investigation of an NACA 23021 Airfoil with Two Arrangements of a 40 per cent Chord Slotted Flap. N.A.C.A. Tech. Note No. 728. 1939.
58	Wenzinger and Gauvain	Wind Tunnel Investigation of an NACA 23012 Airfoil with a Slotted Flap and three types of Auxiliary Flap. N.A.C.A. Report No. 679. 1939.
59	Williams and Brown	Experiments on an NACA 23021 Aerofoil with a 15 per cent Handley Page Slotted Flap in the Compressed Air Tunnel. R. & M. 2305. October, 1939.
60	Lyon and Pindar	A Comparison Between Different Types of Slotted Flaps. A.R.C. 4635. 1940. (Unpublished.)

c

No.	*Name*	*Title, etc.*
61	Blackburn Aircraft Research Dept. ..	A Study of the Slotted Flap. Blackburn Report No. WT.49/40. 1940.
62	Harris and Recant	Wind Tunnel Investigation of Three Airfoils Equipped with 40 per cent Double Flaps. N.A.C.A. Advance Report. A.R.C. Report No. 4834. 1940.
63	Lowry	Wind Tunnel Investigation of an NACA 23012 Airfoil with Several Arrangements of Slotted Flaps with Extended Lips. N.A.C.A. Tech. Note 808. A.R.C. Report No. 5192. 1941.
64	Abbott and Fullner	Wind Tunnel Investigation of NACA 63, 4—420 Airfoil with 25 per cent Chord Slotted Flap. N.A.C.A. Advance Confidential Report. A.R.C. Report No. 7523. 1943.
65	Davidson and Turner	Tests of an NACA 66, 2—216, $a = 0{\cdot}6$ Airfoil Section with a Slotted and Plain Flap. N.A.C.A. Advance Confidential Report. A.R.C. Report No. 7691. 1943.

See also Refs. 3, 4, 8, 9, 27, 29, 84, 85, 86, 89.

G. *Blackburn Flaps*

66	Wind-tunnel Staff of Blackburn Aircraft Ltd.	Test aerofoil 23018J fitted with 50 per cent chord flap (section 2) 30 per cent chord flap (section 5) 40 per cent chord flap (section 6) 60 per cent chord flap (section 7) Blackburn Report No. WT. 26/39. 1939.
67	Do.	The Comparison of Four Symmetrical Aerofoils Fitted with 50 per cent Flaps. Blackburn Report No. WT. 38/40. 1940.
68	Do.	Preliminary Tests on a New Type of High Lift Flap. Blackburn Report No. WT. 44/40. 1940.
69	Do.	Systematic Tests on Large Chord Flaps with Single and Multiple Slots. Blackburn Report No. WT. 74/41. 1941. A.R.C. 5380.
70	Do.	Wind Tunnel Tests on Moderately Large Chord Flaps with Single and Multiple Slots. Blackburn Report No. WT. 85/42 and 85/42A 1942. A.R.C. 6550, 6551.
71	Do.	Preliminary Experiments on a Combination of Large Chord Slotted and Split Flaps. Blackburn Report WT. 86/43. 1943. A.R.C. 6552.

See also Ref. 3.

H. *Fowler Flaps (Single and Double)*

72	Weick and Platt	Wind Tunnel Tests of the Fowler Variable-area Wing. N.A.C.A. Tech. Note No. 419. 1932.
73	Weick and Platt..	Wind Tunnel Tests on a Model Wing with Fowler Flap and Specially Developed Leading Edge Slot. N.A.C.A. Tech. Note No. 459. 1933.
74	Platt	Aerodynamic Characteristics of a Wing with Fowler Flaps, Including Flap Loads, Downwash and Calculated Effect on Take-off. N.A.C.A. Report No. 534. 1935.
75	Gorsley	Investigations on Flaps of the Fowler Type. A.R.C. Report No. 3905. 1939. (Unpublished.)
76	Lyon and Adamson	Wind Tunnel Tests on High Lift Devices. R. & M. 2180. December, 1939.

See also Refs. 3, 5, 29, 91.

I. *Venetian-blind Flaps*

No.	Name	Title, etc.
77	Wenzinger and Harris	Preliminary Wind Tunnel Investigation of and NACA 23012 Airfoil with Various Arrangements of Venetian-blind Flaps. N.A.C.A. Report No. 689. 1940.
78	Rogallo and Spano	Wind Tunnel Investigation of an NACA 23012 Airfoil with 30 per cent Chord Venetian-blind Flap. N.A.C.A. Report No. 742. A.R.C. Report No. 5702. 1942.
		See also Ref. 3.

J. *Flaps on Wing-body Combinations. Interference Effects*

No.	Name	Title, etc.
79	Wallace	The Effect of Split Trailing Edge Wing Flaps on the Aerodynamic Characteristics of a Parasol Monoplane. N.A.C.A. Tech. Note No. 475. 1933.
80	Serby and Hufton	Full Scale Tests of Landing Flaps on a Percival 'Gull.' R. & M. 1697. 1935.
81	Serby and Shone	Full Scale Tests of Landing Flaps on a Miles 'Hawk Major.' Report No. BA 1179. A.R.C. 1807. 1935. (Unpublished).
82	Francis	Full Scale Tests of the Effect of Flaps on Lateral Stability and Control. Part I. Tests of Falcon with Standard Planform. Part II. Tests of Falcon with High Taper Wing. R. & M. 1961. December, 1936.
83	Serby, Francis and Fortescue	Full Scale Tests of the Airspeed Envoy Type AG. 69. R. & M. 1816. 1937.
84	Ellis and Morgan	Wind Tunnel Tests on Slotted Flaps on a Low Wing Monoplane, Flap Angles, 0 deg to 90 deg. R. & M. 1735. 1936.
85	Woodward Nutt and Hufton	Full Scale Tests of the Hendy Heck. R. & M. 1719. 1936.
86	Francis	Full Scale Tests of Slotted Flaps and Ailerons on a Courier. R. & M. 1819. 1937.
87	Sherman	Interference of Wing and Fuselage from Tests of 18 Combinations in the N.A.C.A. Variable Density Tunnel. Combinations with split flaps. N.A.C.A. Tech. Note No. 640. 1938.
88	Davies, Adamson and Brown	Wind Tunnel Tests on the Bristol B1/39. A.R.C. 4797. 1940. (Unpublished.)
89	Do.	Wind Tunnel Tests on the Supermarine S24/37. R. & M. 2451. March, 1941.
90	House and Wallace	Wind Tunnel Investigation of Effect of Interference on Lateral Stability Characteristics of Four NACA 23012 Wings on an Elliptical and a Circular Fuselage and Vertical Fins. N.A.C.A. Report No. 705. 1940.
91	Morgan and Morris	Flight Tests of a Youngman Flap on the Fairey P4/34 K7555. A.R.C. 5281. 1941. (To be published.)
92	Stewart	Flight Measurements of Maximum Lift Coefficients. A.R.C. 7889. 1944. (Unpublished.)
		See also Refs. 4, 36.

K. *Flap Downwash Effects*

No.	Name	Title, etc.
93	Silverstein and Katzoff	Design Charts for Predicting Downwash Angles and Wake Characteristics Behind Plain and Flapped Wings. N.A.C.A. Report No. 648. 1939.
94	Silverstein, Katzoff and Bullivant	Downwash and Wake Behind Plain and Flapped Aerofoils. N.A.C.A. Report No. 651. 1939.
95	Blackburn Aircraft Ltd.	Investigation of the Effect of Full Span High Lift Flaps on the Flow in the Region of the Tailplane and Upon Stability and Trim. Part I. Without Slipstream. Blackburn Report WT. 88/43. A.R.C. 7115. 1943.
		See also Ref. 74.

C1

L. *Flaps and Induced Drag*

No.	*Name*	*Title, etc.*
96	Young	The Induced Drag of Flapped Elliptic Wings with Cut-out and with Flaps that Extend the Local Chord. A.R.C. 6259. 1942. (To be published.)

M. *Nose Flaps*

97	Kruger	Uber eine neue Möglichkeit der Steigerung des Höchstauftriebes von Hochgeschwindigkeits Profilen. U.M. 3049. 1943.
98	Kruger	Windkanal Untersuchungen an einen Abgeänderten Mustangsprofil mit Nasenklappe. U.M. 3153. 1944.
99	Lemme	Kraftmessungen und Druckverteilungmessungen an einem Flügel mit Kricknas, Vorflügel, Wolbungs-und Spreizklappe. F.B. 1676.
100	Kruger	Systematische Windkanalmessungen an einem Laminarflügel mit Nasenklappen. F.B. 1948.
101	Staff of AVA	A Summary of the More Important Work of Recent Years at the AVA, Göttingen (translated by Young and Hufton). R.A.E. Tech. Note No. Aero. 1736., A.R.C. 9437. 1945. (Unpublished.)

N. *Brake Flaps and Dive Recovery Flaps*

102	Fuchs	Wind Tunnel Experiments on Brake Flaps. A.R.C. 3520. 1938.
103	Irving, Sornton and Gummer	Experiments on a Model of a Low Wing Monoplane fitted with Upper and Lower Surface Split Flaps and Reversible Thrust Airscrews. A.R.C. 3467. 1938.
104	Jacob and Wanner	D.F.S. Dive Control Brakes for Gliders and Power-aircraft. *Jahrbuch der Deutschen Luftfahrtforschung,* Vol. 1. 1938. R.T.P. Translation No. 1104.
105	Barnes and Lyon	Some Wind Tunnel Tests on Brake Flaps. A.R.C. 4273. 1939. (Unpublished.)
106	Irving and McMillan	Some Experiments on the Balancing of Wing Brake Flaps. R. & M. 1864. 1939.
107	Piper and Thom	An Investigation of the Optimum Position of Dive Brakes on the Spitfire. A.R.C. 5290. 1941. (Unpublished.)
108	Purser and Turner	Wind Tunnel Investigation of Perforated Split Flaps for use as Dive Brakes on a Rectangular 23012 Airfoil. N.A.C.A. Advance Restricted Report. A.R.C. Report No. 5334. 1941.
109	Davies and Bigg	Wind Tunnel Tests on Double Trailing Edge Brake Flaps for the Spitfire. R.A.E. Report No. Aero. 1722. A.R.C. 5666. 1941. (Unpublished.)
110	Whitby and Bigg	Wind Tunnel Tests on the Effect of Brake Flaps on Lift and Trim. A.R.C. 5860. 1942. (Unpublished.)
111	Davies and Kirk	A Resumé of Aerodynamic Data on Brake Flaps. A.R.C. 5979. 1942. (To be published.)
112	Purser and Turner	Wind Tunnel Investigation of Perforated Split Flaps for use as Dive Brakes on a Tapered Airfoil. N.A.C.A. Advance Restricted Report. A.R.C. Report No. 5711. 1942.
113	Knowler and Pruden	Measurements on the Effect of Brake Flaps on an Aerofoil at High Speeds. R. & M. 2211. December, 1942.
114	Pruden	Further Wind Tunnel Tests of Brake Flaps at High Speeds. R. & M. 2211. December, 1942.
115	Warden and Nixon	Some Tests on Dive Brakes. A.R.C. 5809. 1942. (Unpublished.)
116	Purser	A Study of the Application of Data on Various Types of Flap to the Design of Fighter Brakes. N.A.C.A. Advance Confidential Report. A.R.C. Report No. 6020. 1943. (Unpublished.)

No.	Name	Title, etc.
117	Purser and Turner	Wind Tunnel Investigation of Perforated Double Split Flaps for use as Dive Brakes on a Rectangular NACA 23012 airfoil. N.A.C.A. Advance Restricted Report. A.R.C. Report No. 6961. 1943. (Unpublished.)
118	Davis	Aerodynamic Brakes. N.A.C.A. Advance Confidential Report. A.R.C. Report No. 7294. 1943. (Unpublished.)
119	Erickson	Wind Tunnel Investigations of Devices for Improving the Diving Characteristics of P38 Airplanes. N.A.C.A. Confidential Memorandum Report. A.R.C. Report No. 6926. 1943. (Unpublished.)
120	Neumark, Young and Miss Young	Results of a Step by Step Calculation of the Recovery of the Typhoon from a Terminal Velocity Dive. A.R.C. 7422. 1944. (Unpublished.)
121	Neumark and Young	A Simplified Approach to the Recovery of an Aeroplane from a High Speed Dive with Constant Elevator Angle. A.R.C. 7423. 1944. (Unpublished.)
122	Britland	High Speed Tunnel Tests of Dive Recovery Flaps for a Single Engined Fighter (Tempest V). A.R.C. 9253. 1925. (Unpublished.)
123	Bridgland	Flight Tests of Dive Recovery Flaps on a Twin Engine Fighter Aircraft (Lightning). A.R.C. 9251. 1945. (Unpublished.)
124	Bridgland	Flight Tests of Dive Recovery Flaps on a Single Engine Low Wing Monoplane (Thunderbolt.) R.A.E. Tech. Note No. Aero. 1704. 1945.
125	Bridgland	A Collection of Data on Dive Recovery Flaps. A.R.C. 9252. 1945. (Unpublished.)

O. *Flaps on Sweptback Wings*

No.	Name	Title, etc.
126	Hansen	Drei-Komponentenmessungen an Pfeilflügeln mit Spreizklappen. F.B. 1626.
127	Puffert	Drei-Komponenten Windkanalmessungen an gepfeilten Flügeln und an einen Pfeilflügel-Gesamtmodell. F.B. 1726. 1942.
128	Gosnill, Packer and Levy	Wind Tunnel Tests on a Pterodactyl model. Report No. M.A. 115. Ottawa 1942.
129	Squire, Robertson and Brown	Wind-tunnel Tests on the Baynes Carrier Wing. Part I. Low Speed Model Tests on the Baynes Glider. R. & M. 2487. July, 1945.
130	Lemme	Untersuchungen an einem Pfeilflügel, einem abgestumpften Pfeilflügel und einem M Flügel. F.B. 1739/2. 1943.
131	Brennecke	Auftriebsteigerung beim Pfeilflügel. F.B. 1876. 1943.
132	Dent and Curtis	A Method of Estimating the Effect of Flaps on Pitching Moment and Lift of Tailless Aircraft. A.R.C. 7270. 1943. (Unpublished.)
133	Theil and Weissinger	6-Komponentenmessungen an einem geraden und an einem 35 deg rückgepfeilten Trapezflügel ohne und mit Spreizklappenn. U.M. 1278. 1944.
134	Trouncer, Becker and Wright	Wind Tunnel Tests on the Stability of Tailless Gliders. Part I. 'V' wing planform. R. & M. 2364. December, 1947.
135	Brennecke	Untersuchungen an Pfeilflügel mit Landehilfe. U.M. 3173. 1944.
136	Trouncer and Moss	Wind Tunnel Tests on the Stability of a 'V' Wing Tailless Glider. R. & M. 2295. July, 1945.
137	Evans and Britland	High Speed Tunnel Tests on a Tailless Aircraft (AW. 529). A.R.C. 8773. 1945. (Unpublished.)
138	Williams, Brown and Miles	Tests on Some 'General Aircraft' Wings With and Without Sweepback in the Compressed Air Tunnel. A.R.C. 9321. 1946. (Unpublished.)

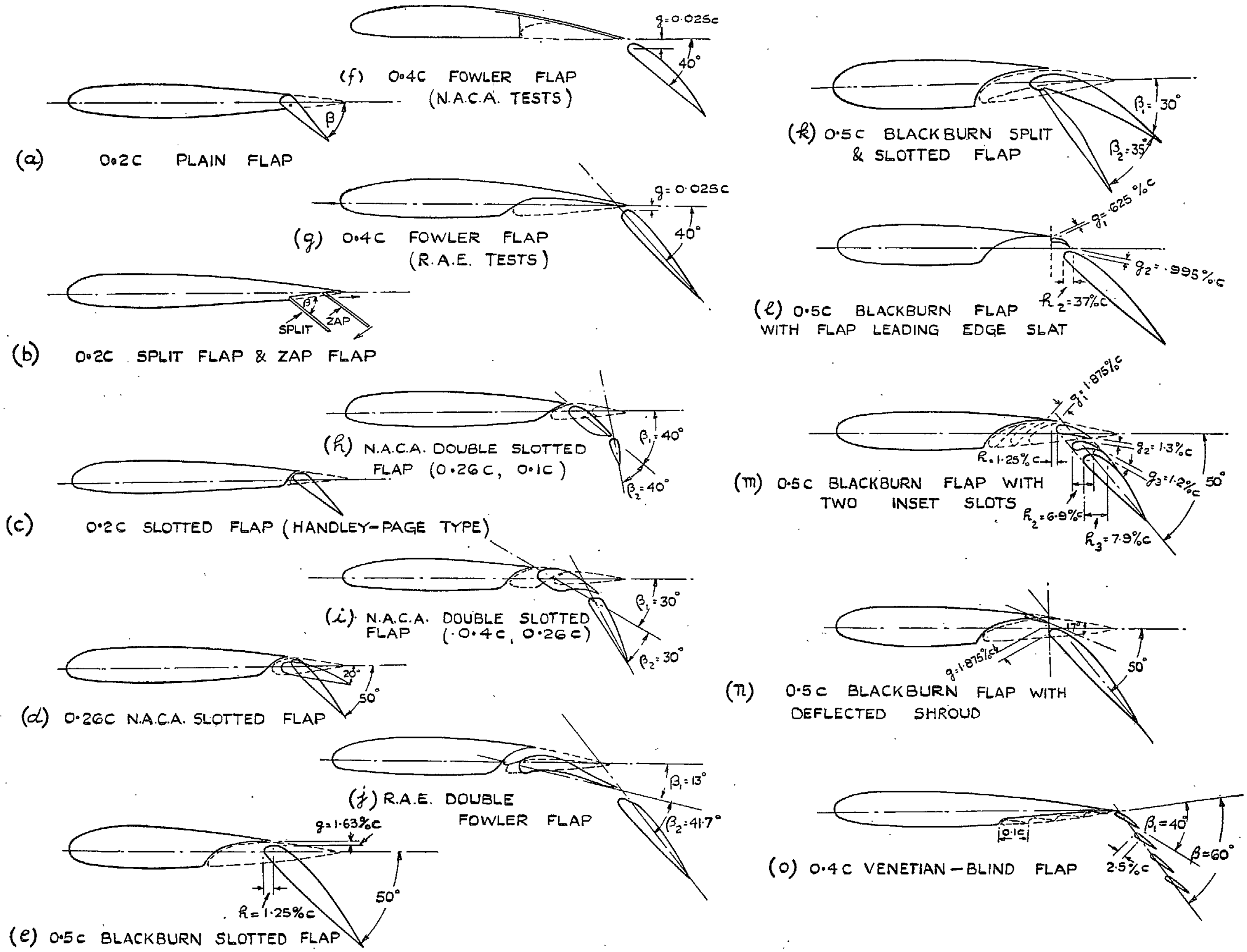

FIG. 1. Illustrations of flaps considered.

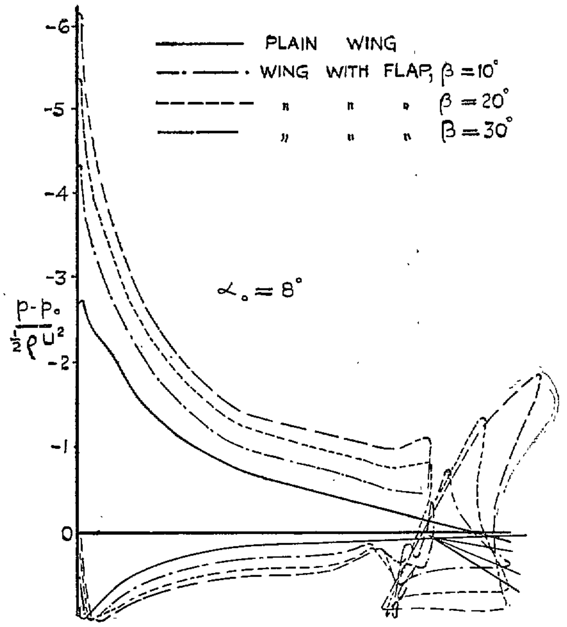

(a) NACA 23012 section and 0·26c slotted flap.

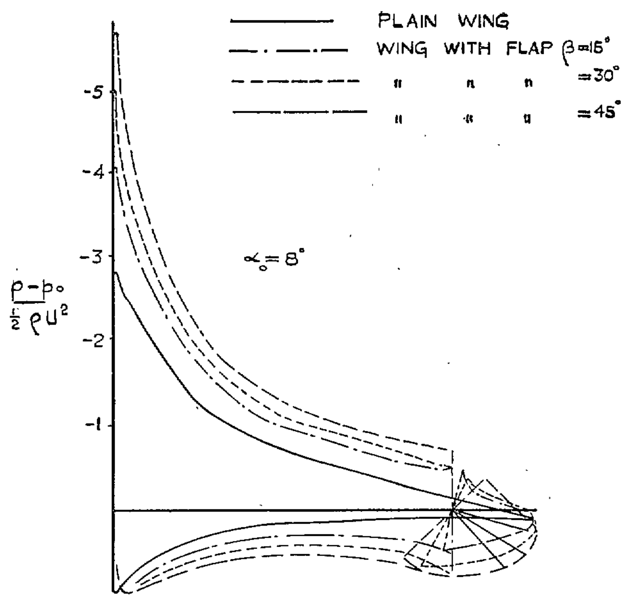

(b) NACA 23012 section and 0·2c plain flap.

FIG. 2. Illustration of loading distributions on a wing with a slotted flap and a plain flap.

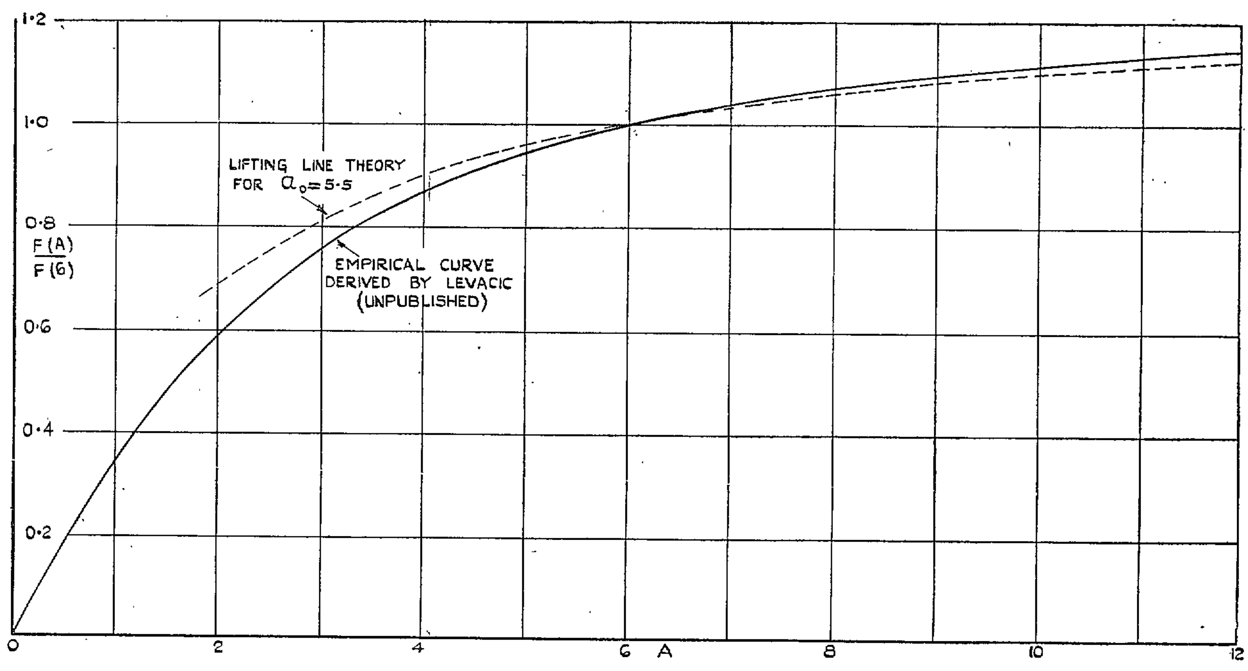

FIG. 3. Variation of lift-curve slope with aspect ratio.

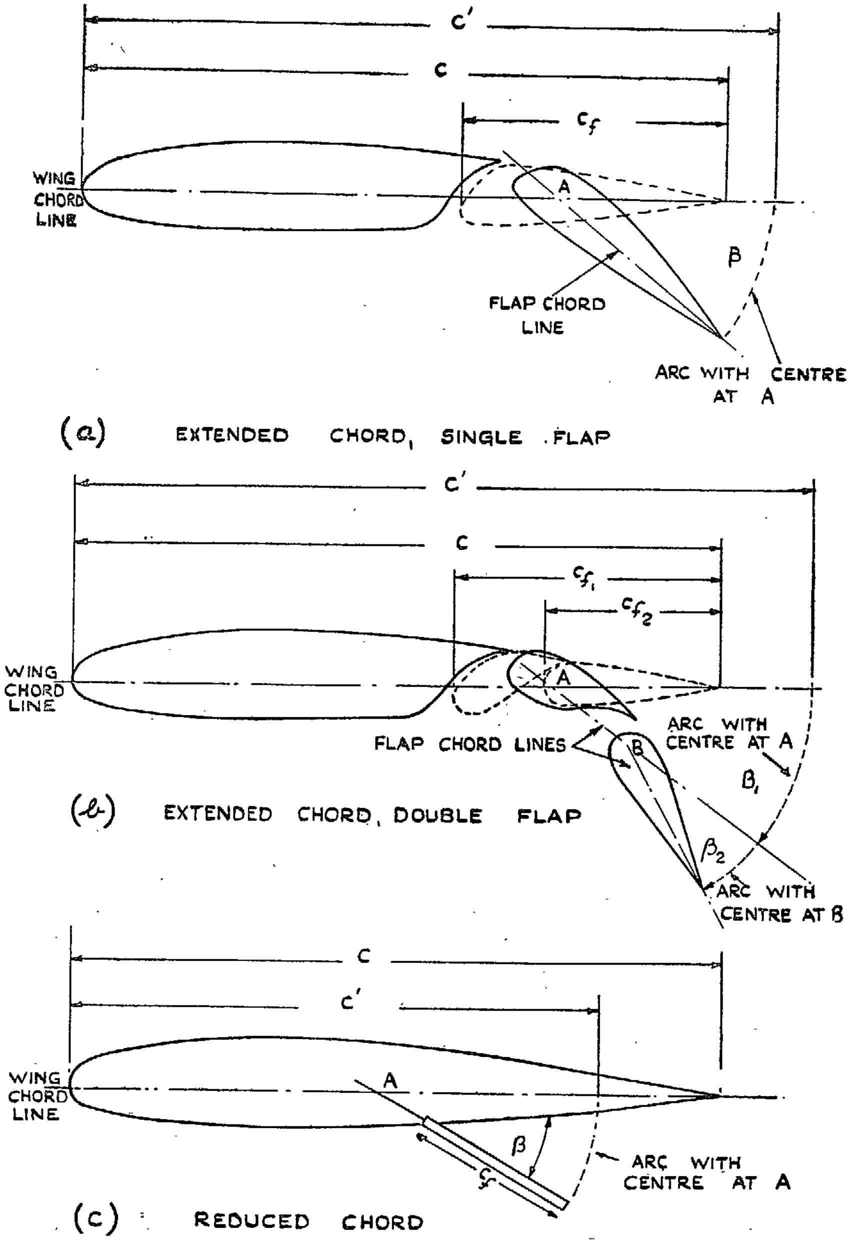

FIG. 4. Sketches illustrating derivation of effective (extended or reduced) chord.

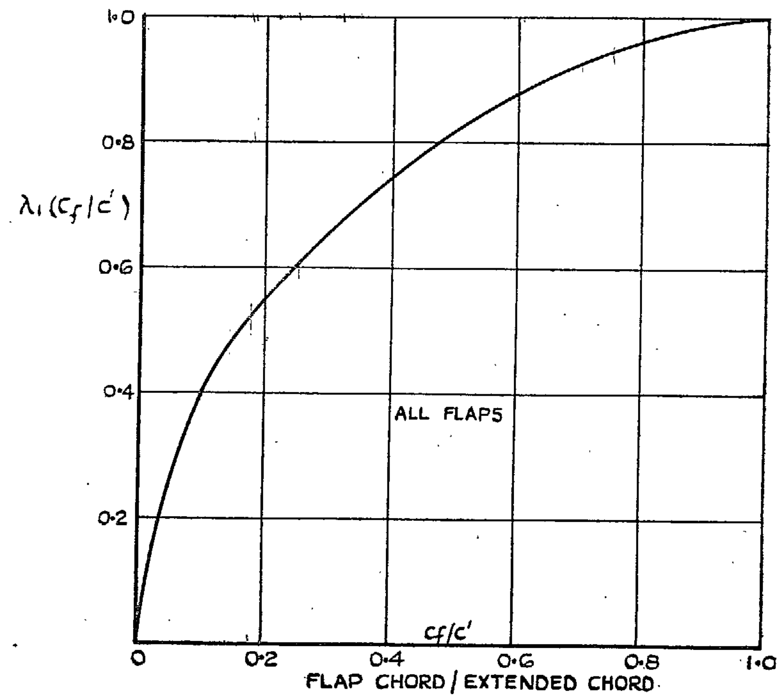

FIG. 5. The function $\lambda_1(c_f/c')$, all flaps.

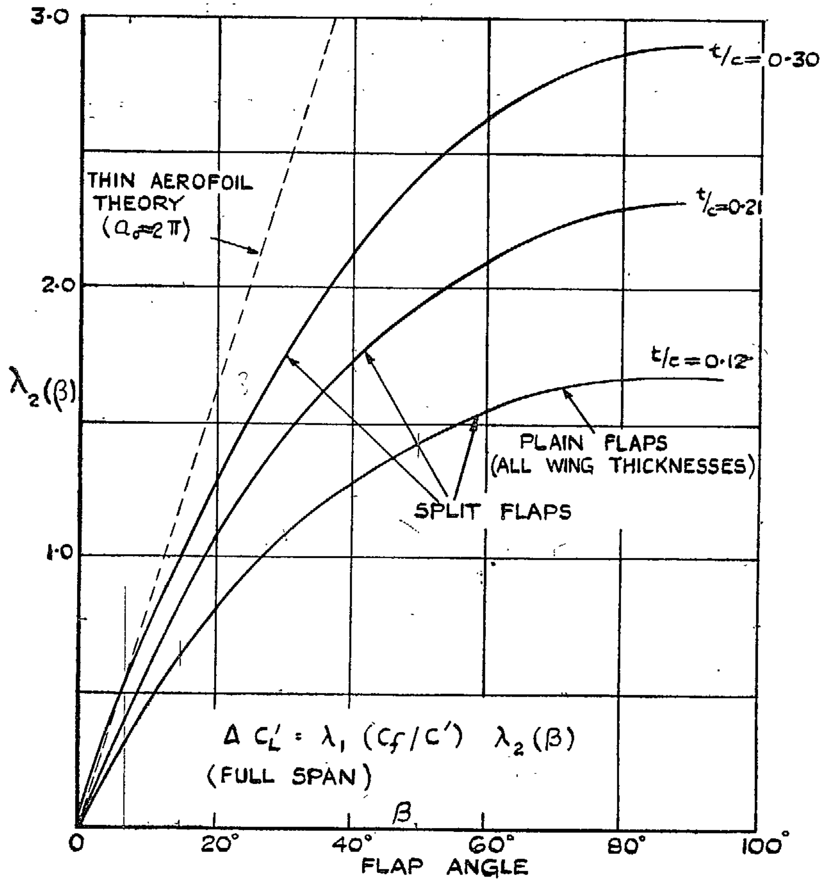

FIG. 6. The function $\lambda_2(\beta)$ for split and plain flaps.

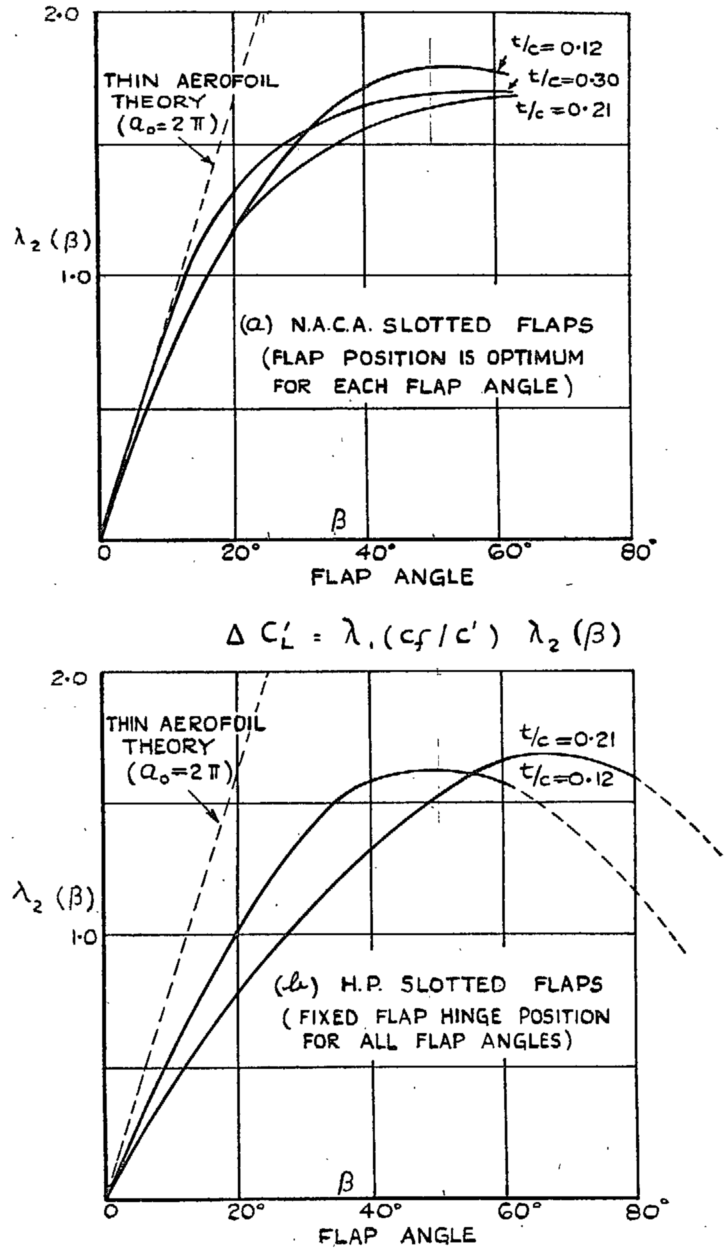

FIG. 7. The function $\lambda_2(\beta)$ for slotted flaps.

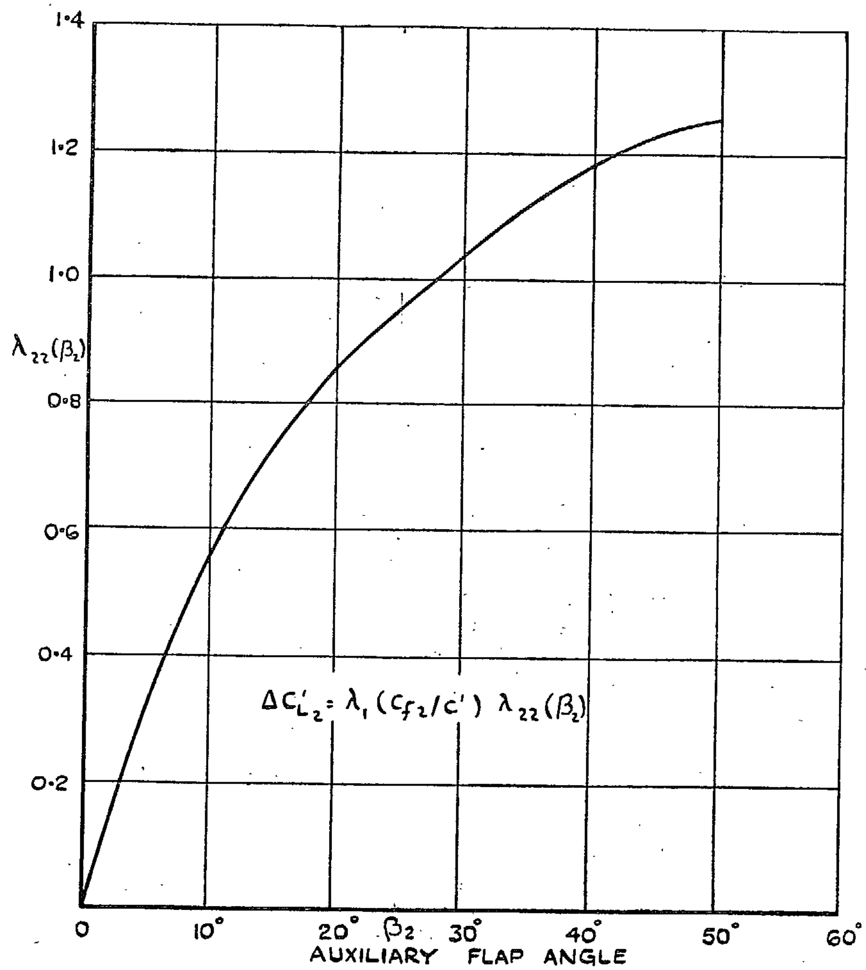

FIG. 8. The function $\lambda_{22}(\beta_2)$ for determining the lift coefficient increment of an auxiliary flap.

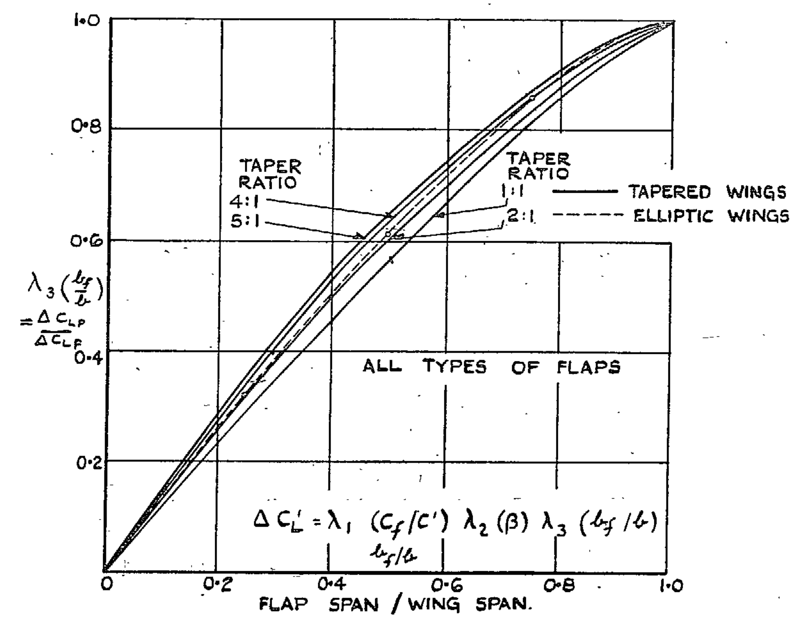

FIG. 9. The function $\lambda_3(b_f/b)$ ratio of lift increment of part-span flap to lift increment of full-span flap.

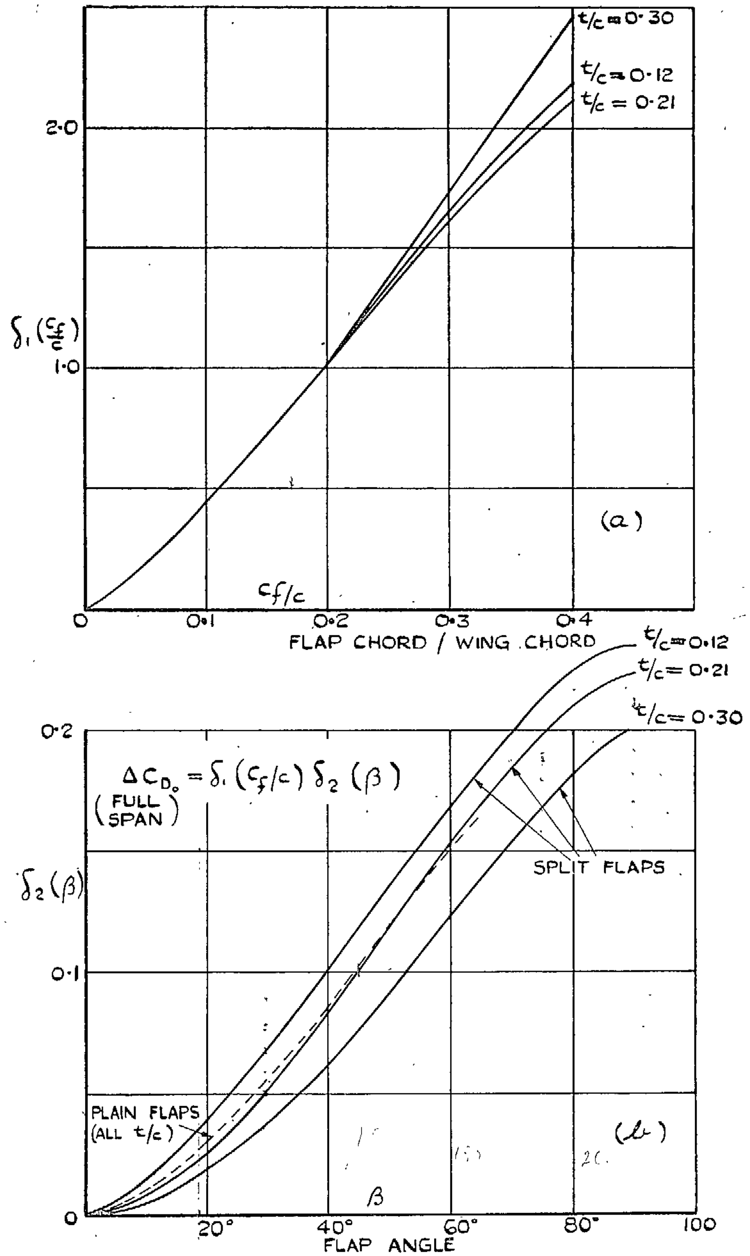

Fig. 10. The functions $\delta_1(c_f/c)$, $\delta_2(\beta)$ for split and plain flaps.

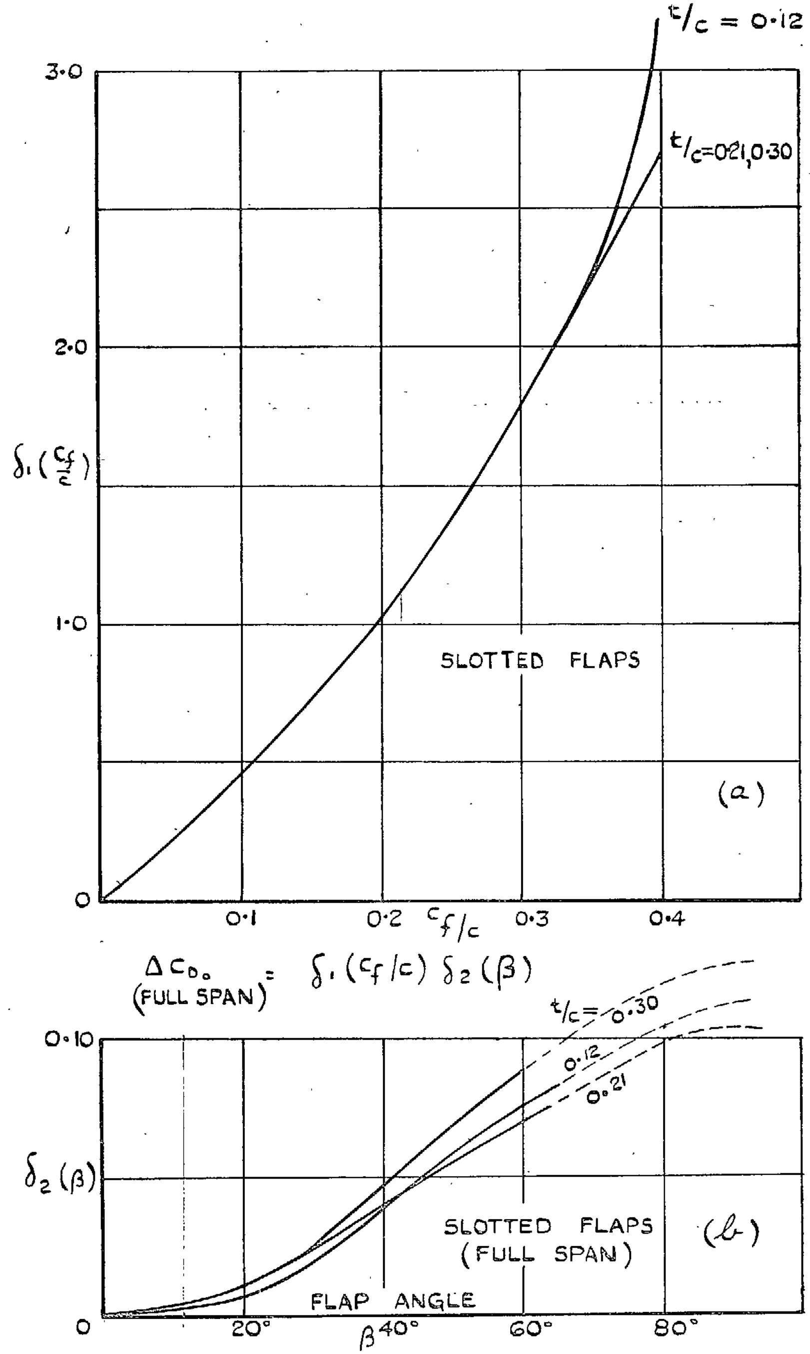

Fig. 11. The functions $\delta_1(c_f/c)$ and $\delta_2(\beta)$ for slotted flaps.

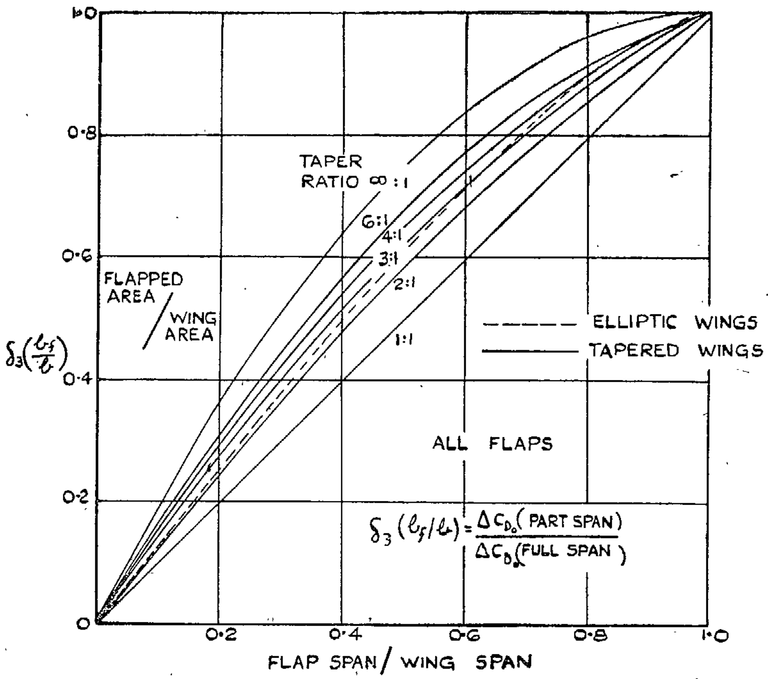

FIG. 12. The function $\delta_3(b_f/b)$ ratio of drag increment of part-span flap to drag increment of full-span flap.

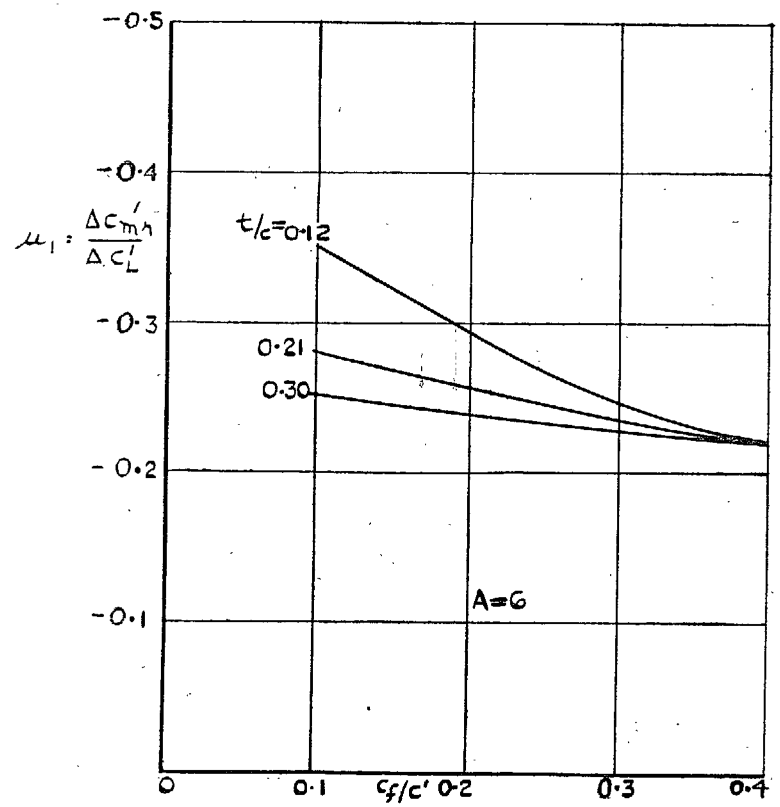

FIG. 13. The function $\mu_1(\Delta C_{m'r}/\Delta C_L')$ for split and plain flaps (applicable to all types of flaps on wings for which t/c is less than about 0·2).

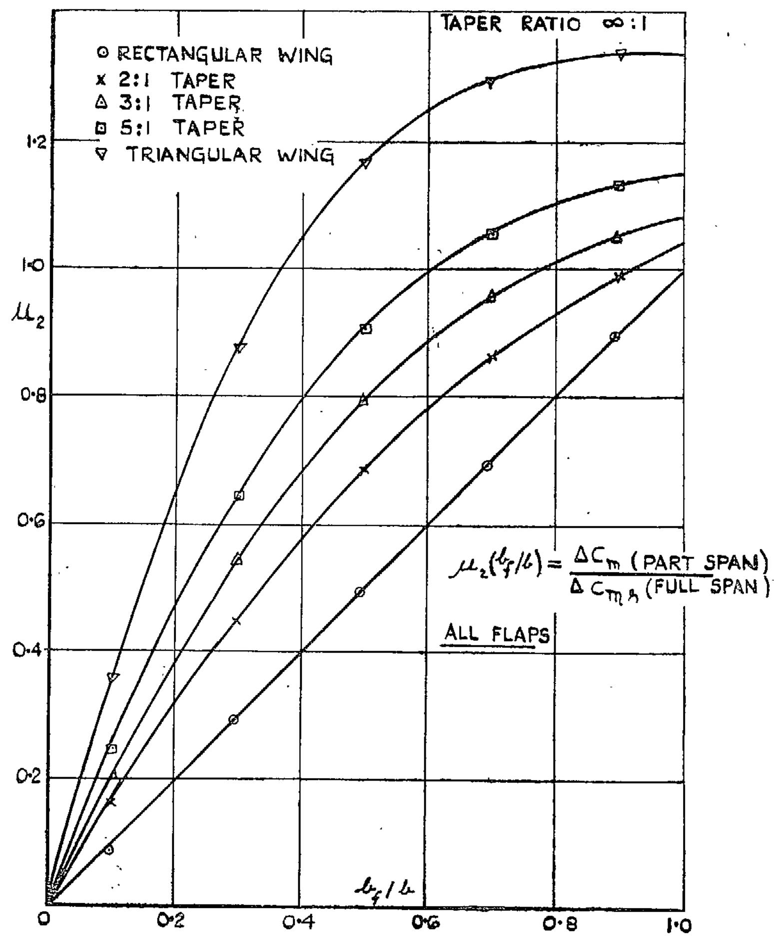

FIG. 14. The function $\mu_2(b_f/b)$ ratio of pitching moment coefficient increment of part-span flap to pitching moment coefficient of full-span flap on a rectangular wing.

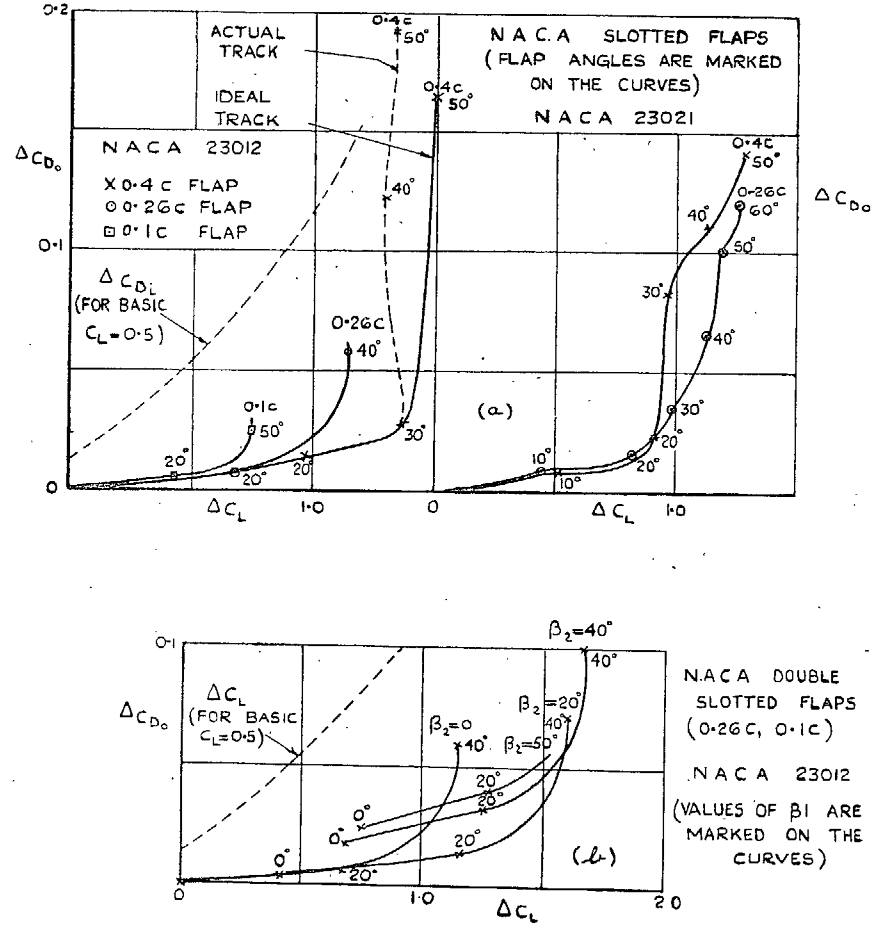

FIGS. 15a and 15b. Increments in profile drag coefficient ($\alpha = \alpha_0 + 6$ deg, $A = 6$) against increments in lift coefficient ($\alpha = \alpha_0 + 10$ deg, $A = 6$). NACA slotted flaps.

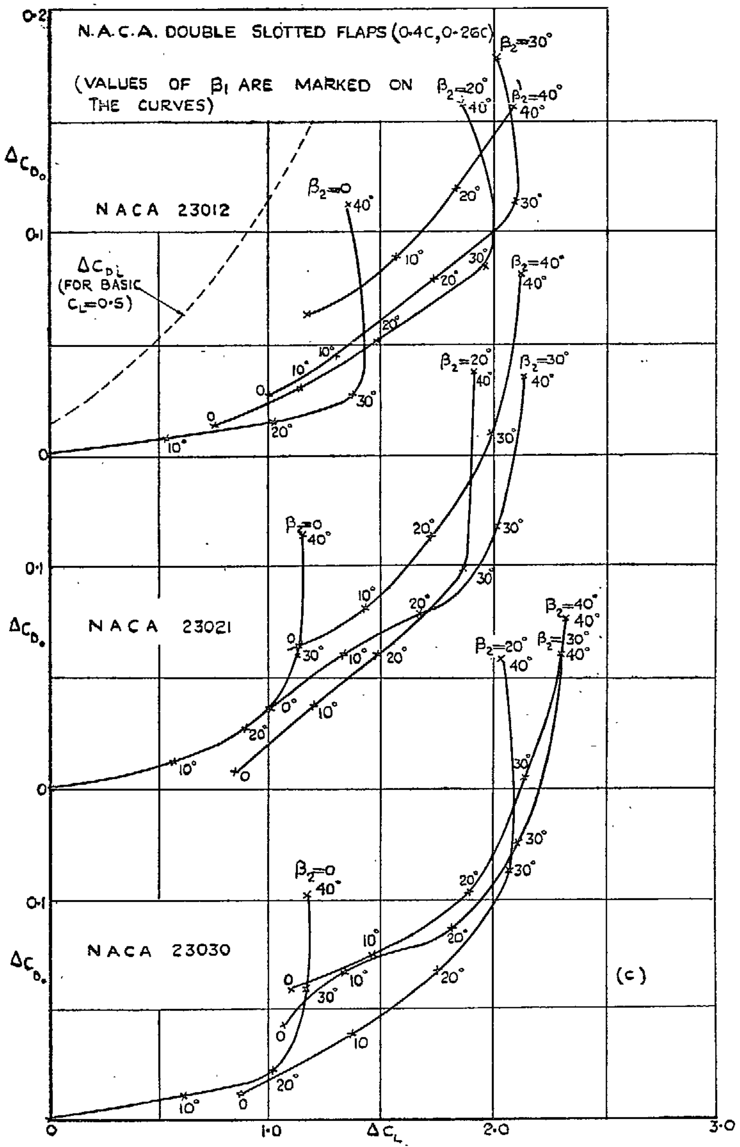

FIG. 15c. Increments in profile drag coefficient ($\alpha = \alpha_0 + 6$ deg, $A = 6$) against increments in lift coefficient ($\alpha = \alpha_0 + 10$ deg, $A = 6$). NACA slotted flaps.

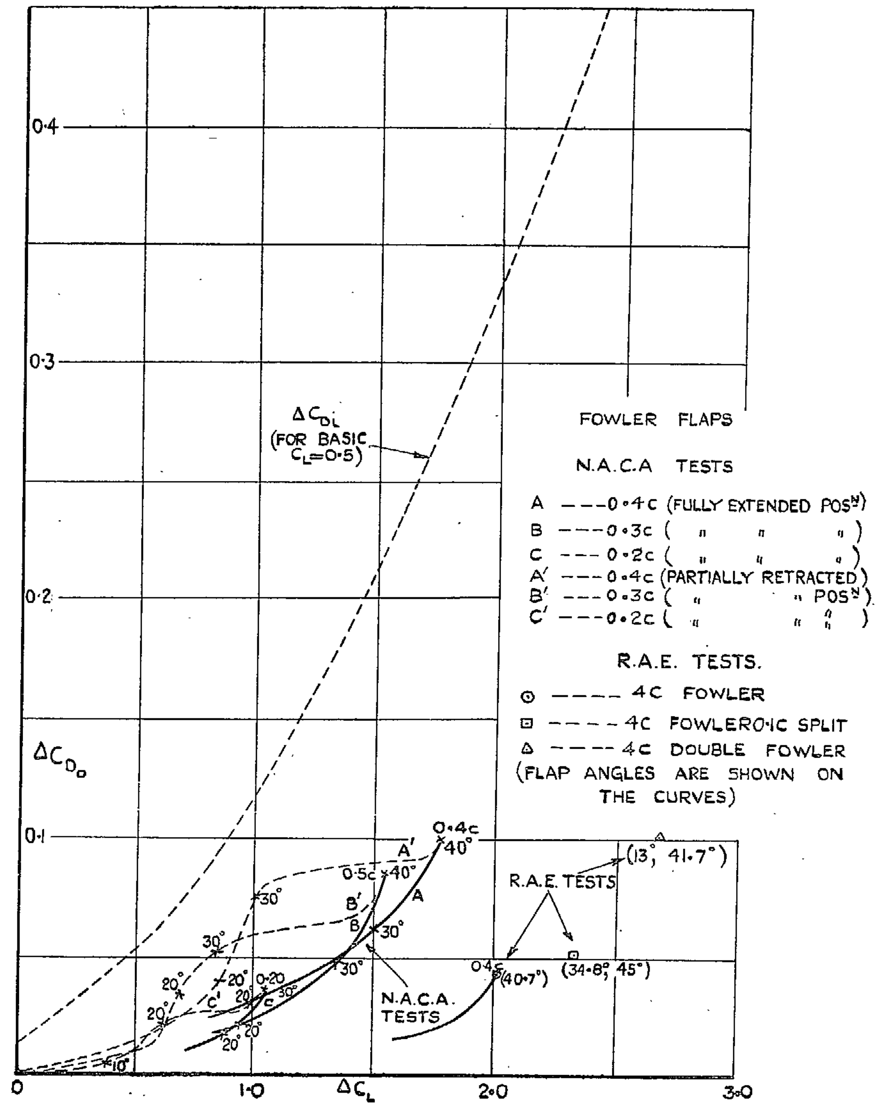

FIG. 16. Increments in profile drag coefficient ($\alpha = \alpha_0 + 6$ deg, $A = 6$) against increments in lift coefficient ($\alpha = \alpha_0 + 10$ deg, $A = 6$). Fowler flaps.

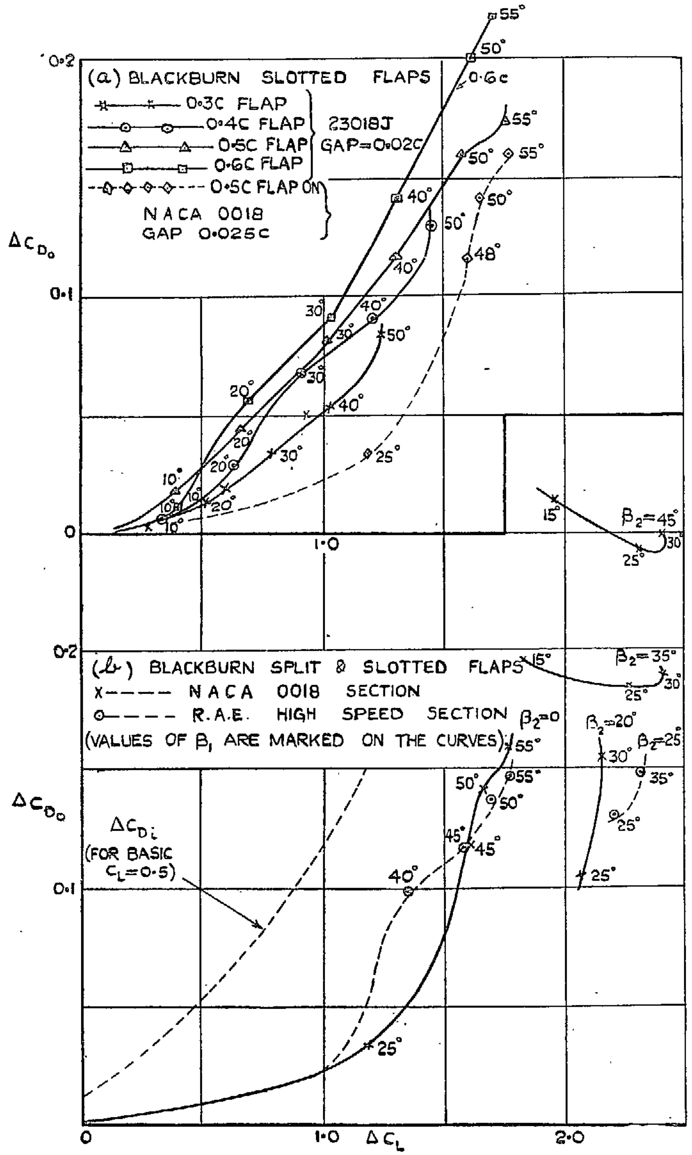

FIG. 17. Increments in profile drag coefficient ($\alpha = \alpha_0 + 6$ deg, $A = 6$) against increments in lift coefficient ($\alpha = \alpha_0 + 10$ deg, $A = 6$). Blackburn flaps.

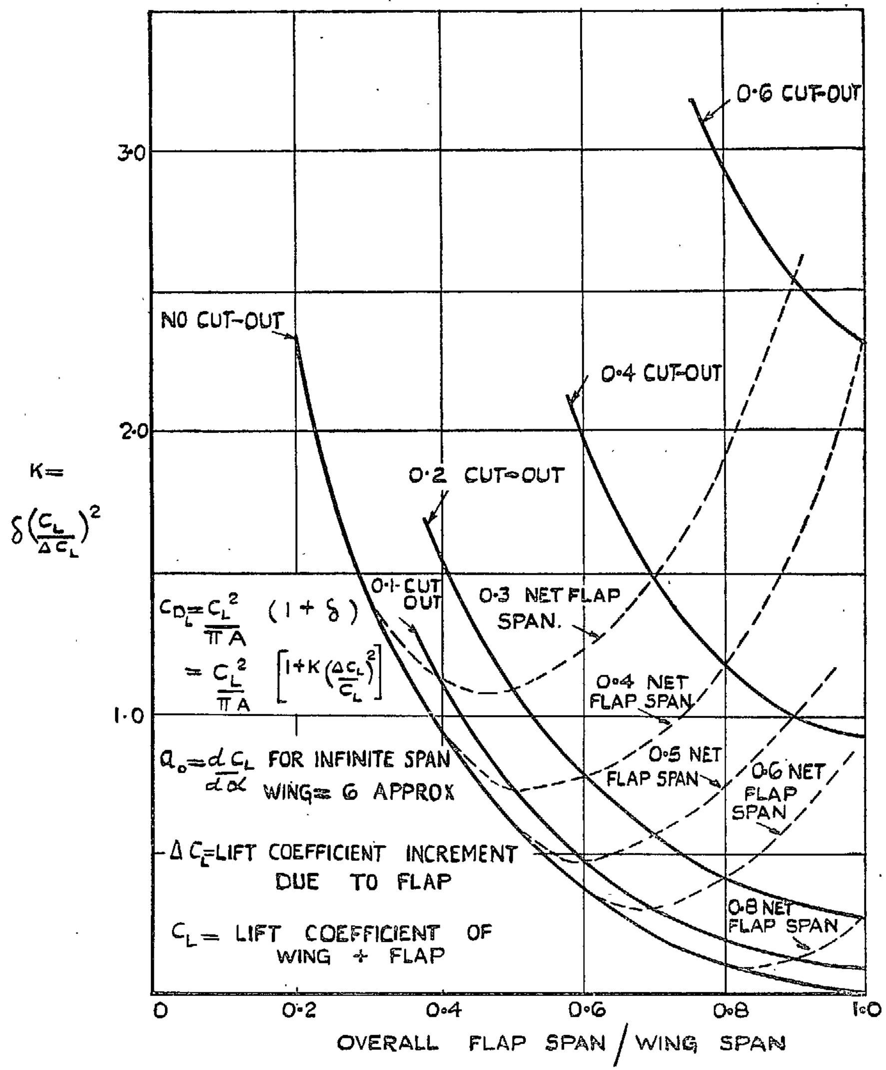

FIG. 18. Factor K for calculating induced drag of an elliptic wing with part-span flaps and cut-out. $A/a_0 = \frac{2}{3}$.

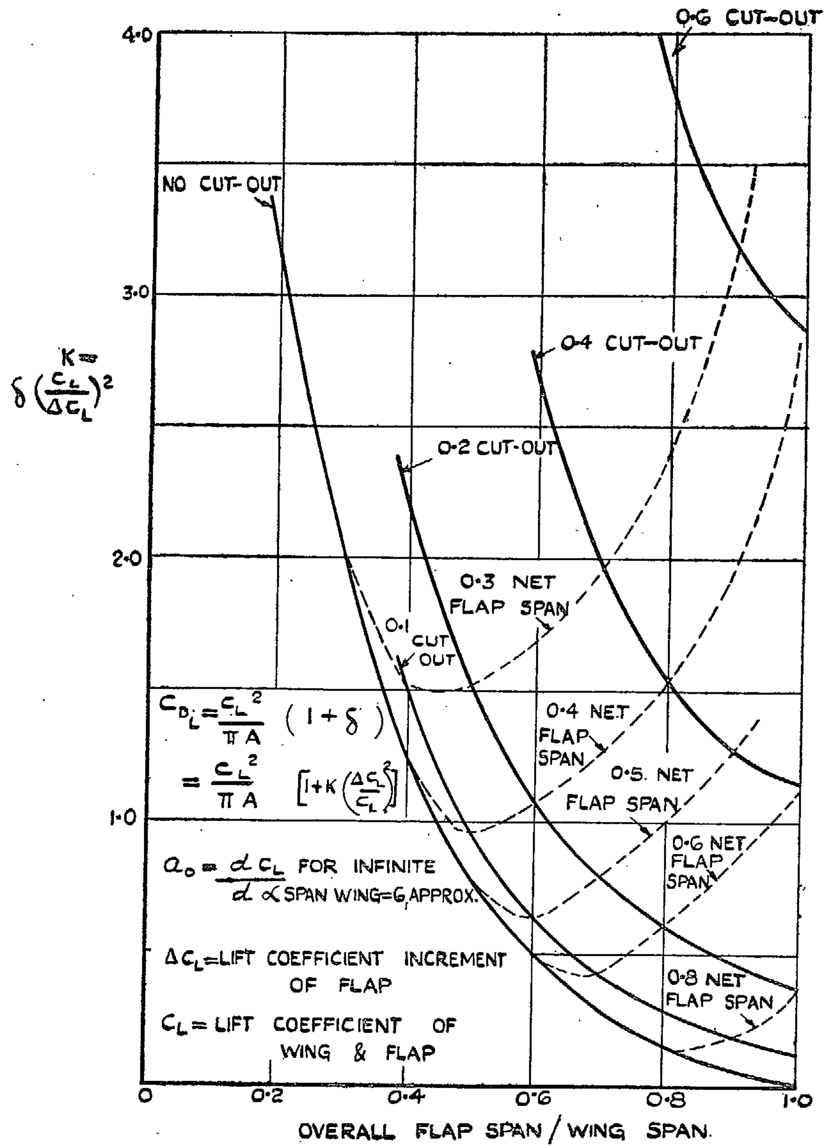

FIG. 19. Factor K for calculating induced drag of an elliptic wing with part-span flaps and cut-out. $A/a_0 = 1{\cdot}0$.

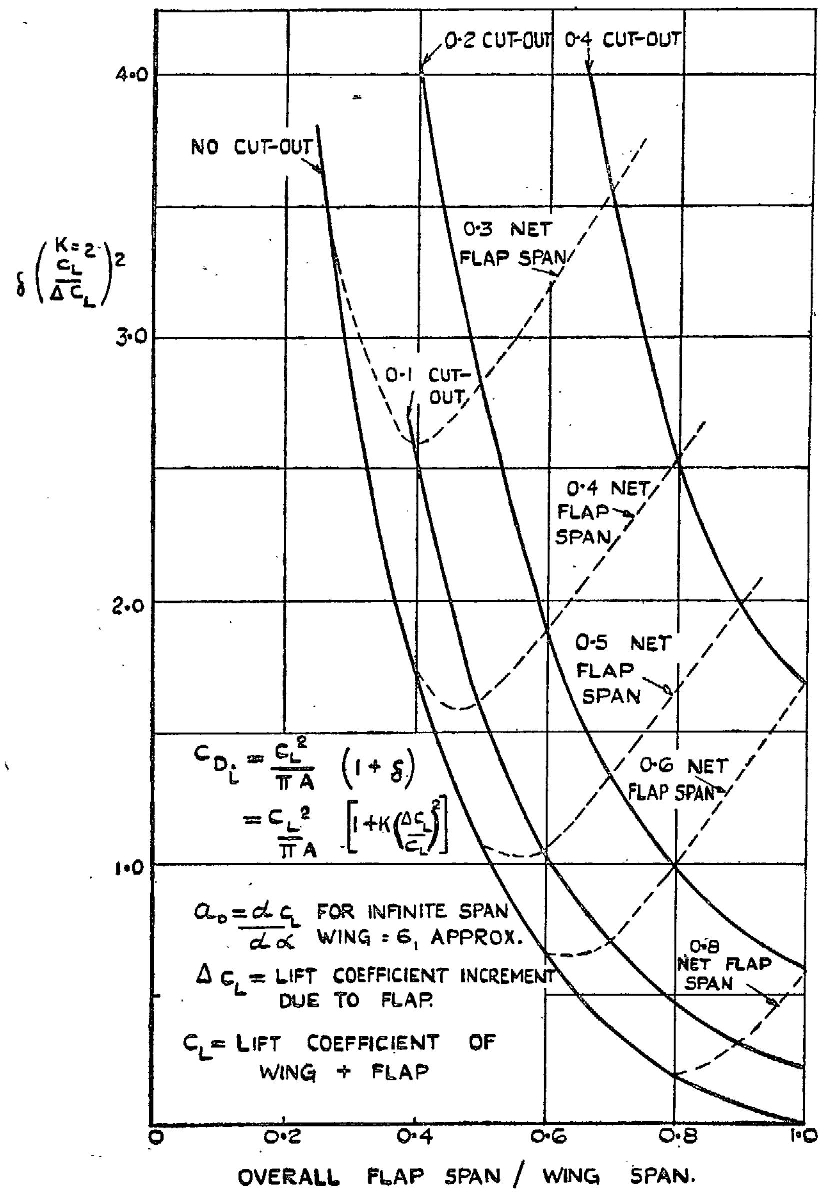

FIG. 20. Factor K for calculating induced drag of an elliptic wing with part-span flaps and cut-out. $A/a_0 = 2{\cdot}0$.

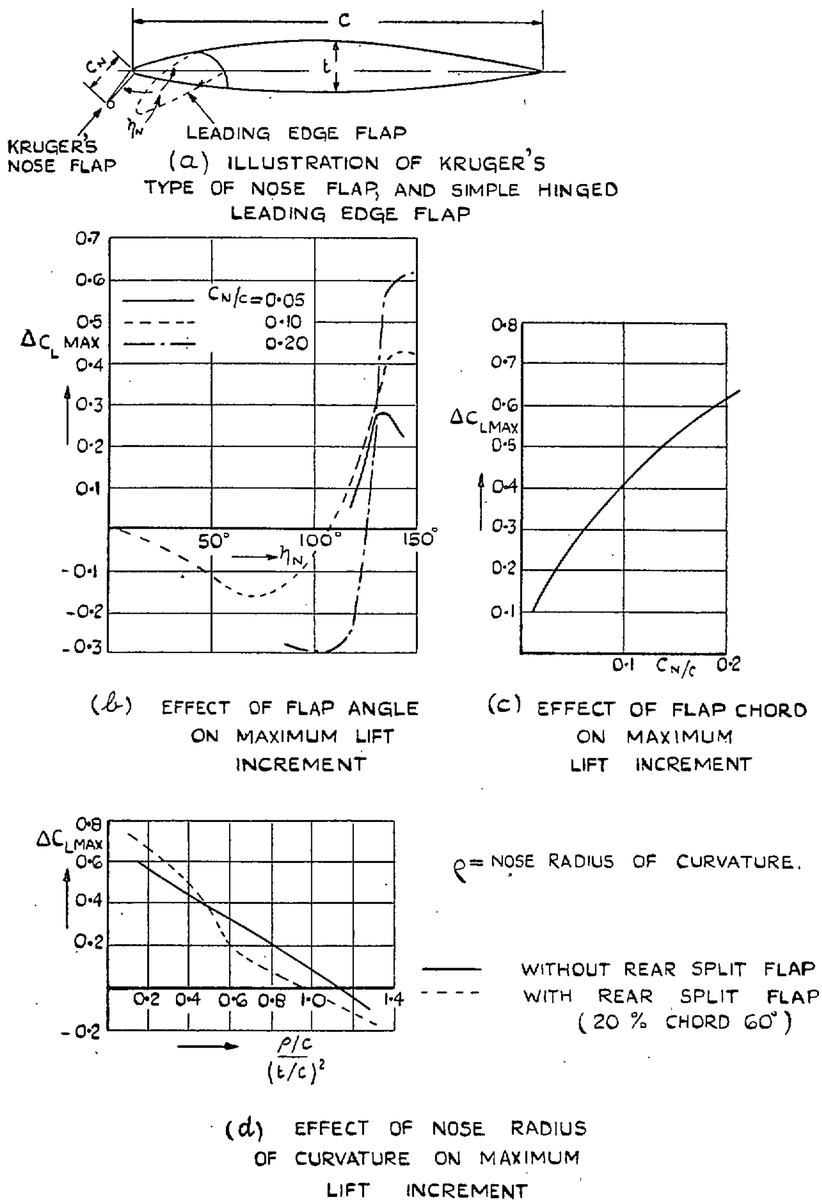

FIG. 21. Characteristics of Kruger's nose flap.

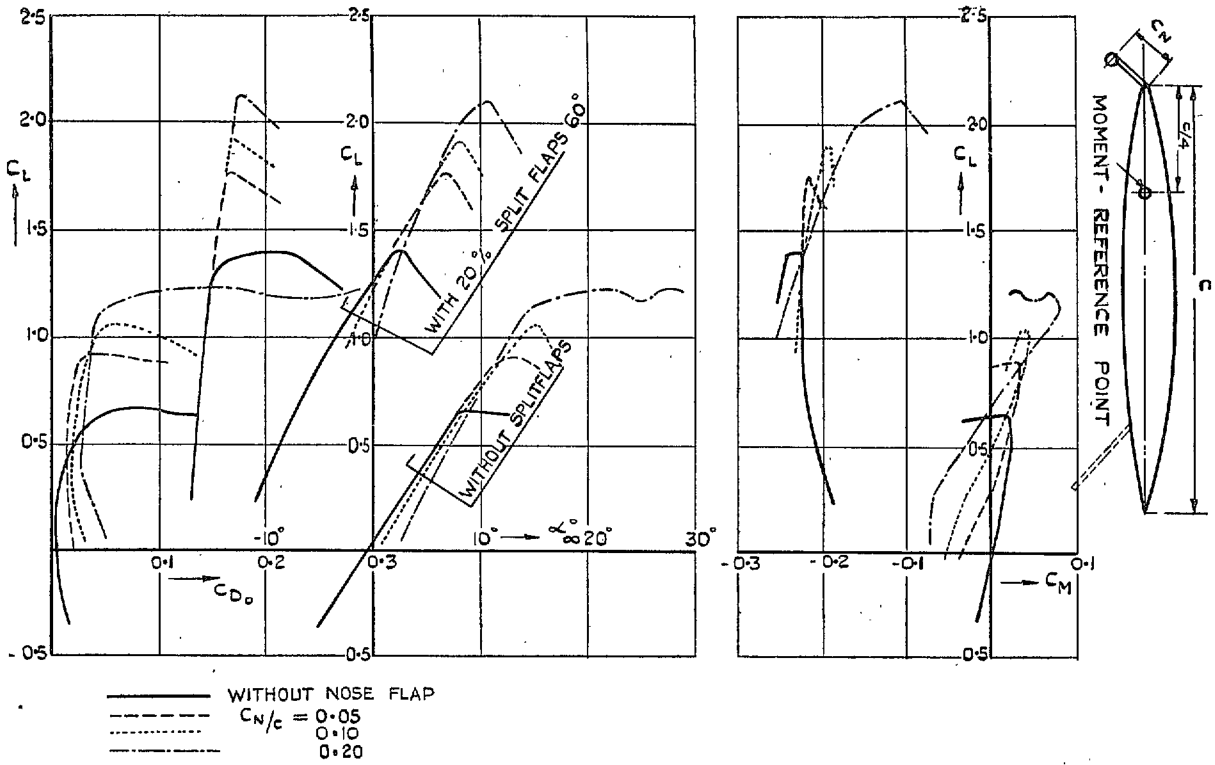

FIG. 22. Effect of Kruger's nose flap on the aerodynamic characteristics of a wing of high-speed section with and without a split flap.

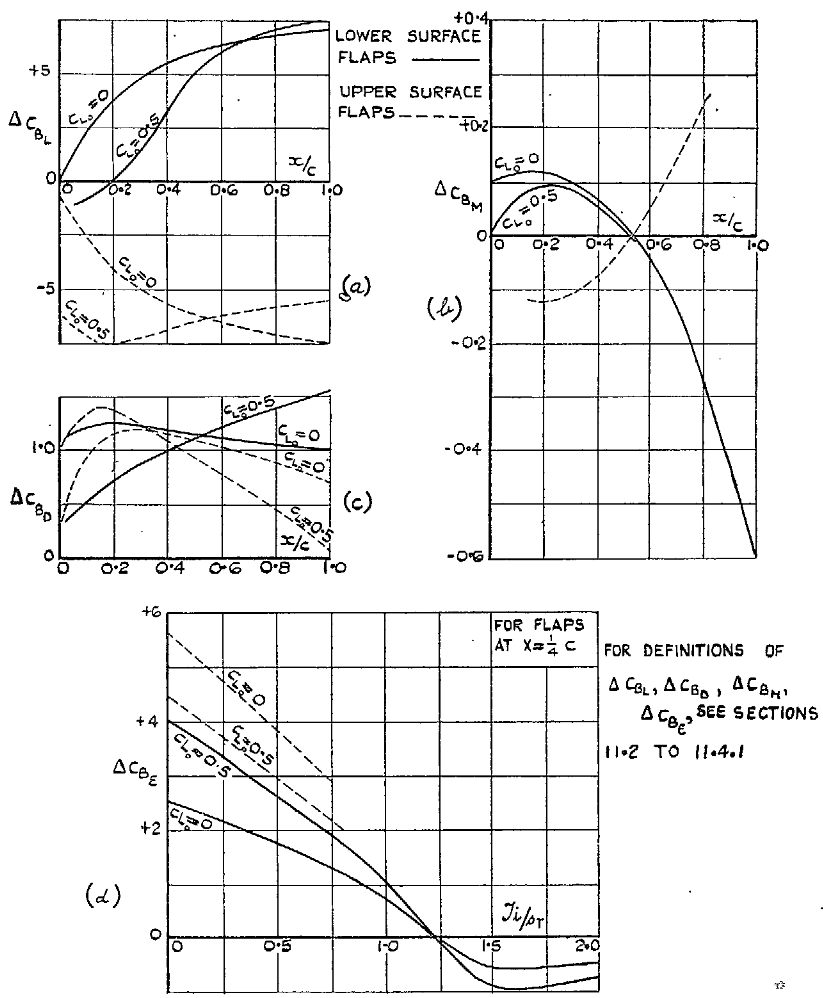

Fig. 23. Typical curves of variation of ΔC_{BL}, ΔC_{BD}, ΔC_{BM} with chordwise position and of $\Delta C_{B\varepsilon}$ with spanwise position of a brake flap.

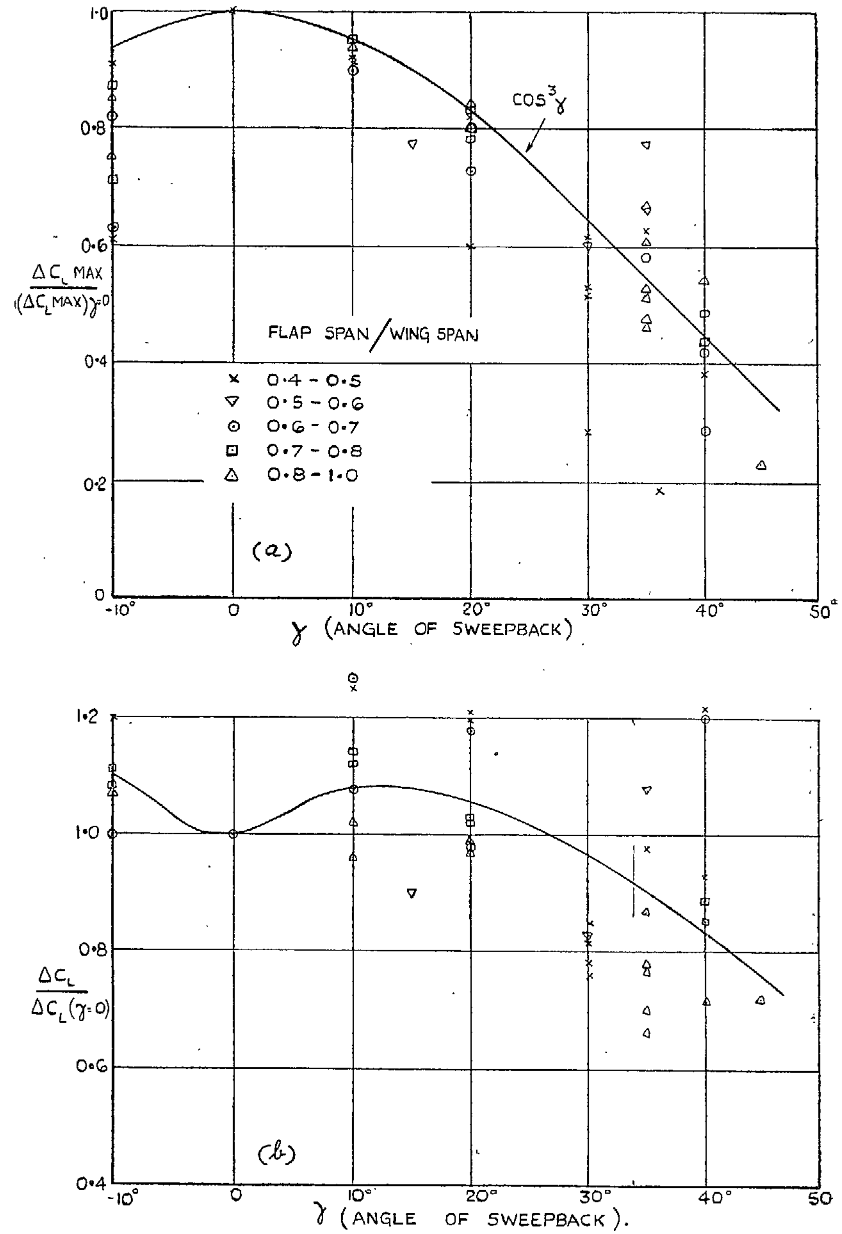

Fig. 24. Effect of sweep-back on (a) $\Delta C_{L\,max}$ (b) ΔC_L due to flaps.

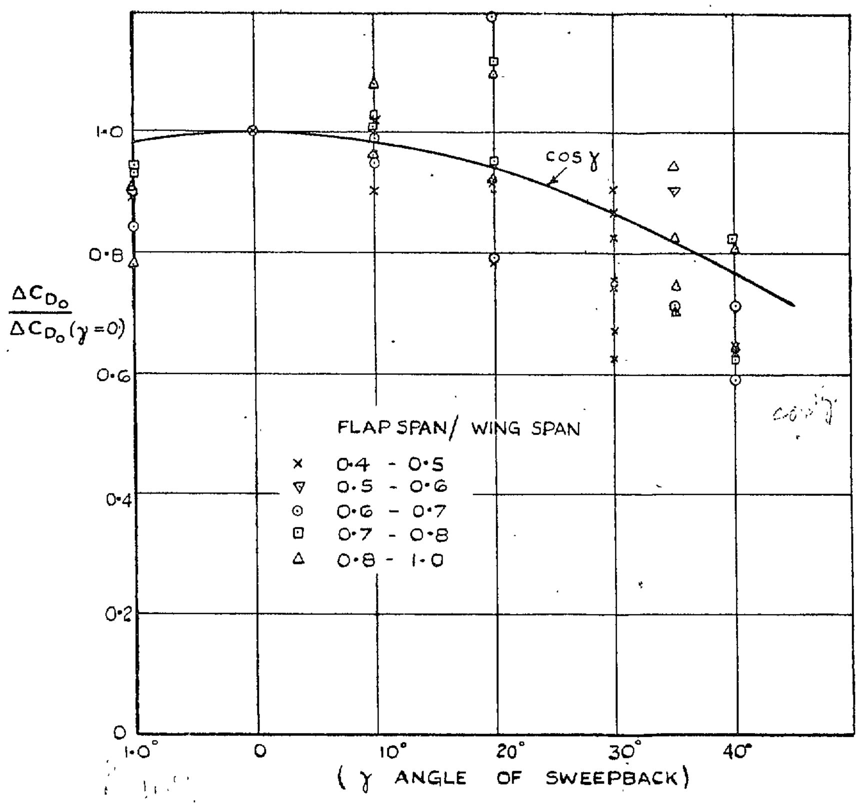

FIG. 25. Effect of sweep-back on ΔC_{D0} due to flaps.

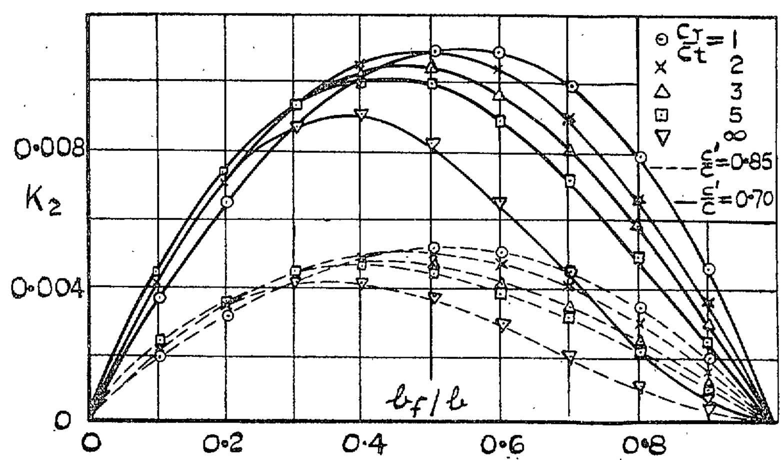

FIG. 26. Effect of flaps on swept-back wings on dC_m/dC_L.

$$\Delta\left(\frac{dC_m}{dC_L}\right) = -K_2 A \Gamma$$

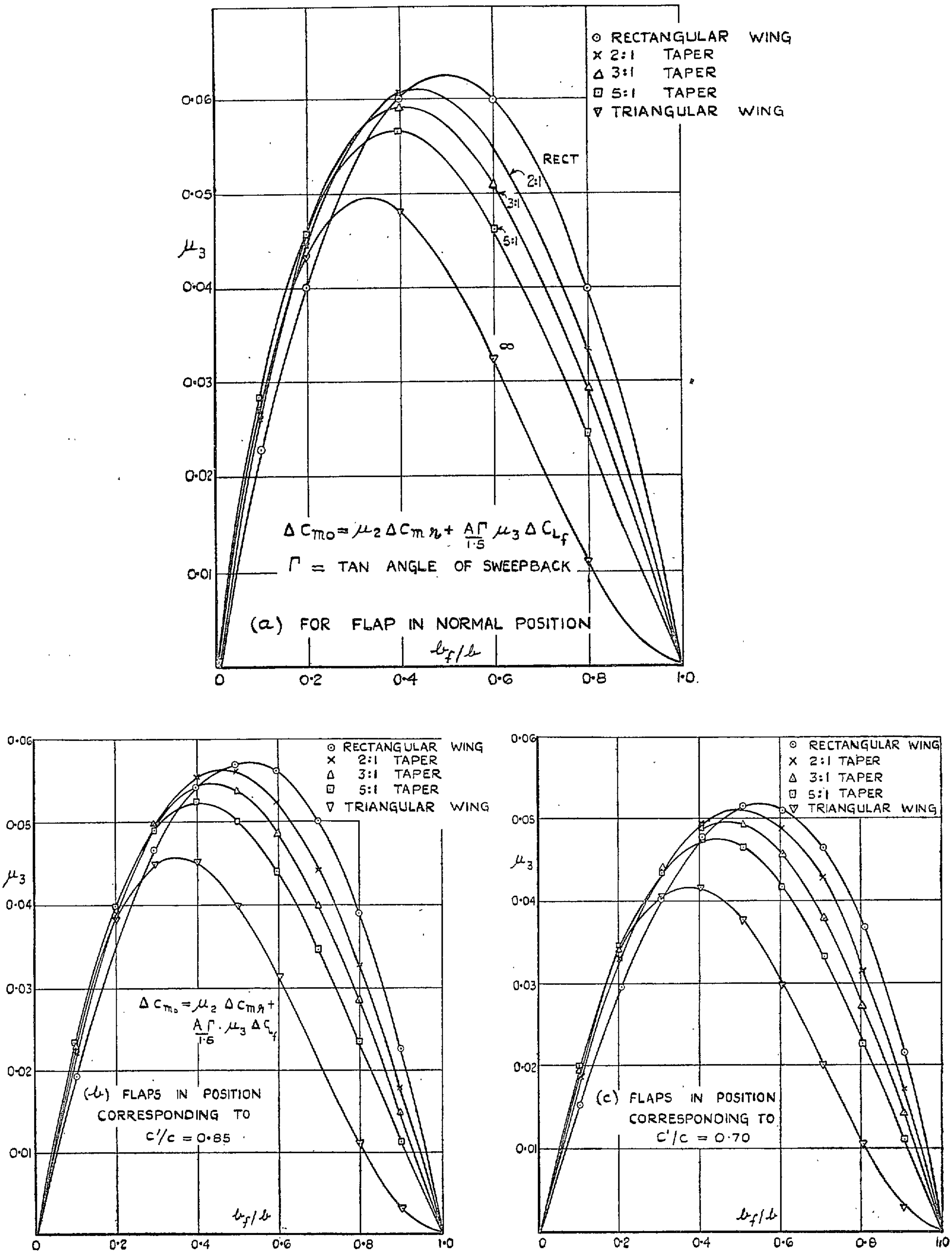

FIG. 27. The function μ_3 for determining the pitching moment increment of flaps on swept-back wings.

R. & M. No. 2622
(10,766)
A.R.C. Technical Report

Publications of the Aeronautical Research Council

ANNUAL TECHNICAL REPORTS OF THE AERONAUTICAL RESEARCH COUNCIL (BOUND VOLUMES)

1936 Vol. I. Aerodynamics General, Performance, Airscrews, Flutter and Spinning. 40s. (40s. 9d.)
Vol. II. Stability and Control, Structures, Seaplanes, Engines, etc. 50s. (50s. 10d.)

1937 Vol. I. Aerodynamics General, Performance, Airscrews, Flutter and Spinning. 40s. (40s. 10d.)
Vol. II. Stability and Control, Structures, Seaplanes, Engines, etc. 60s. (61s.)

1938 Vol. I. Aerodynamics General, Performance, Airscrews. 50s. (51s.)
Vol. II. Stability and Control, Flutter, Structures, Seaplanes, Wind Tunnels, Materials. 30s. (30s. 9d.)

1939 Vol. I. Aerodynamics General, Performance, Airscrews, Engines. 50s. (50s. 11d.)
Vol. II. Stability and Control, Flutter and Vibration, Instruments, Structures, Seaplanes, etc. 63s. (64s. 2d.)

1940 Aero and Hydrodynamics, Aerofoils, Airscrews, Engines, Flutter, Icing, Stability and Control, Structures, and a miscellaneous section. 50s. (51s.)

1941 Aero and Hydrodynamics, Aerofoils, Airscrews, Engines, Flutter, Stability and Control, Structures. 63s. (64s. 2d.)

1942 Vol. I. Aero and Hydrodynamics, Aerofoils, Airscrews, Engines. 75s. (76s. 3d.)
Vol. II. Noise, Parachutes, Stability and Control, Structures, Vibration, Wind Tunnels. 47s. 6d. (48s. 5d.)

1943 Vol. I. (*In the press.*)
Vol. II. (*In the press.*)

ANNUAL REPORTS OF THE AERONAUTICAL RESEARCH COUNCIL—

1933–34	1s. 6d. (1s. 8d.)	1937	2s. (2s. 2d.)
1934–35	1s. 6d. (1s. 8d.)	1938	1s. 6d. (1s. 8d.)
April 1, 1935 to Dec. 31, 1936.	4s. (4s. 4d.)	1939–48	3s. (3s. 2d.)

INDEX TO ALL REPORTS AND MEMORANDA PUBLISHED IN THE ANNUAL TECHNICAL REPORTS, AND SEPARATELY—

April, 1950 – – – – – R. & M. No. 2600. 2s. 6d. (2s. 7½d.)

AUTHOR INDEX TO ALL REPORTS AND MEMORANDA OF THE AERONAUTICAL RESEARCH COUNCIL—

1909–1949 – – – – – R. & M. No. 2570. 15s. (15s. 3d.)

INDEXES TO THE TECHNICAL REPORTS OF THE AERONAUTICAL RESEARCH COUNCIL—

December 1, 1936 — June 30, 1939.	R. & M. No. 1850.	1s. 3d. (1s. 4½d.)
July 1, 1939 — June 30, 1945.	R. & M. No. 1950.	1s. (1s. 1½d.)
July 1, 1945 — June 30, 1946.	R. & M. No. 2050.	1s. (1s. 1½d.)
July 1, 1946 — December 31, 1946.	R. & M. No. 2150.	1s. 3d. (1s. 4½d.)
January 1, 1947 — June 30, 1947.	R. & M. No. 2250.	1s. 3d. (1s. 4½d.)
July, 1951 – – – –	R. & M. No. 2350.	1s. 9d. (1s. 10½d.)

Prices in brackets include postage.

Obtainable from

HER MAJESTY'S STATIONERY OFFICE

York House, Kingsway, London W.C.2 ; 423 Oxford Street, London W.1 (Post Orders : P.O. Box No. 569, London S.E.1) ; 13A Castle Street, Edinburgh 2 ; 39 King Street, Manchester 2 ; 2 Edmund Street, Birmingham 3 ; 1 St. Andrew's Crescent, Cardiff ; Tower Lane, Bristol 1 ; 80 Chichester Street, Belfast OR THROUGH ANY BOOKSELLER

S.O. Code No. 23-2622